Wide Area Power System Islanding Detection, Classification and State Evaluation Algorithm

Rui Sun

Dissertation submitted to the faculty of the Virginia Polytechnic Institute and State University in partial fulfillment of the requirements for the degree of

Doctor of Philosophy

in

Electrical Engineering

Virgilio A. Centeno (Chair)

Arun G. Phadke

James S. Thorp

Jaime De La Reelopez

Sandeep Shukla

Werner E. Kohler

December 14th, 2012

Blacksburg, Virginia U.S.A

Keywords: islanding, detection & identification, state evaluation, wide area measurements, data mining, decision trees.

Wide Area Power System Islanding Detection, Classification and State Evaluation Algorithm

Rui Sun

Abstract

An islanded power system indicates a geographical and logical detach between a portion of a power system and the major grid, and often accompanies with the loss of system observability. A power system islanding contingency could be one of the most severe consequences of wide-area system failures. It might result in enormous losses to both the power utilities and the consumers. Even those relatively small and stable islanding events may largely disturb the consumers' normal operation in the island. On the other hand, the power consumption in the U.S. has been largely increasing since 1970s with the respect to the bloom of global economy and mass manufacturing, and the daily increased requirements from the modern customers. Along with the extreme weather and natural disaster factors, the century old U.S. power grid is under severely tests for potential islanding disturbances. After 1980s, the invention of synchronized phasor measurement units (PMU) has broadened the horizon for system monitoring, control and protection. Its real time feature and reliable measurements has made possible many online system schemes. The recent revolution of computers and electronic devices enables the implementation of complex methods (such as data mining methods) requiring large databases in power system analysis. The proposed method presented in this dissertation is primarily focused on two studies: one power system islanding contingency detection, identification, classification and state evaluation algorithm using a decision tree algorithm and topology approach, and its application in Dominion Virginia power system; and one optimal PMU placement strategy using a binary integral programming algorithm with the consideration of system islanding and redundancy issues.

To my parents: Ying Sun and Jin Tan

Acknowledgements

First and foremost, I would like to express my deepest appreciation to my advisor and committee chair, Dr. Virgilio Centeno, who has continually and convincingly kept a spirit in regard to the research and teaching. Dr. Centeno has taught me so much throughout many aspects of my study and life. Without his patient guidance and support I cannot finish my research and have today's achievement.

I would like to thank Dr. Arun Phadke and Dr. James Thorp for their great help and guidance in my researches. From them, I learned an attitude and spirit of research and working. My appreciation also goes to Dr. Jaime De Ree and Dr. Sandeep Shukla. They are knowledgeable and always enthusiastic to offer help. My gratitude also goes to the Dr. Werner Kholer, Dr. Yaman Evrenosoglu and Dr. Broadwater, for their genuine interest and support. I would also like to acknowledge my friends, lab-mates in the Power Lab at Virginia Tech and personals at Dominion Virginia Power. I'm honored to work with these great minds. Special thanks to Zhe, who is always standing beside me and giving me courage.

Last but not the least, I want to give my highest appreciation to my parents, Ying Sun and Jin Tan, who are always the strongest support of me and my mentors of life. No matter how far I go, they are always with me in the bottom of my heart.

Table of Contents

List of Figures

List of Tables

Chapter 1: Introduction

1.1 The History of Islanding Scenarios

An islanded power system indicates a geographical and logical detach between a portion of a power system and the rest of the system (which is called the main grid in some references). A well-defined islanding scenario satisfies the following options: 1) the isolated area includes power plants and loads; the generators are continuing to power this area after detachment, which might possibly maintain a transient or permanent stability of the islanded region. 2) After the isolation, the island and the main grid lose most of their observability of each other, judgments in stability and regulation are largely performed with an absence of knowledge of the system behavior in the other area.

A power system islanding contingency could be one of the most severe consequences of wide-area system failures. It might result in enormous losses to both the power utilities and the consumers. Even those relatively small and stable islanding events may largely disturb the consumers' normal operation in the island. The islanding duration could be as short as seconds when the system recovers from breaker reclosing or last for several days when the physical dame to the network is severe. Among the recorded historical islanding contingencies, many of them were economically and ecologically catastrophic blackouts. According to NERC (North America Electric Reliability Corporation) annually disturbance reports [1-15], since 1992, over 15 major islanding contingency disturbances have occurred and millions of customers have been affected. Temporary islanding events are also part of other types of disturbances. Although these contingencies were not severe, they apparently worsened the situation and increased the complexity of the disturbance. The research in this dissertation is motivated by these historical

cases [1-19].

1.1.1 Major Power System Disturbances involving Islanding

In this section, some major islanding scenarios in the U.S. history are analyzed. Four particular cases are introduced in details (More information about detailed islanding cases is introduced in Appendix. A). Most of these historical islanding events featured an under/over frequency oscillation and unbalanced load-generation situation. For many of them, rapid load-shedding and/or generation tripping schemes were applied to maintain the island. During this procedure, many loads were dropped and customers inside the island were affected. Most islands were successfully retained and restored to the system. However some failed to regain synchronization and finally collapsed.

Gulf Coast Area Power System Disturbance, August 7, 1973

This disturbance occurred at 7:53 A.M. on Tuesday, August 7, 1973. The islanded was generating 3745 MW and exporting 1952 MW before the event. “The upset started at a transmission substation which cleared all its lines, followed by tripping of all lines out of the island due to instability” [16]. Frequency began to raise and generator units Barry #5 and Crist #6 (Fig. 1.1), which were generating 1045 MW at the moment, were tripped off simultaneously to set the frequency at approximately 61.2 Hz under governor control. The frequency stayed at 61.2 Hz for 2 minutes then it began to fall until it reached approximately 59 Hz. The under-frequency load shedding scheme in the islanded region operated and dropped approximately 15% of its connected load. “Approximately 7 minutes, 25 seconds after the island formation, transmission lines across the island boundary were reclosed by operator action via supervisory controls. The island came into synchronism and other transmission lines across the island

boundaries were reclosed manually and by synchro-check relay action, ending the disturbance." [16]

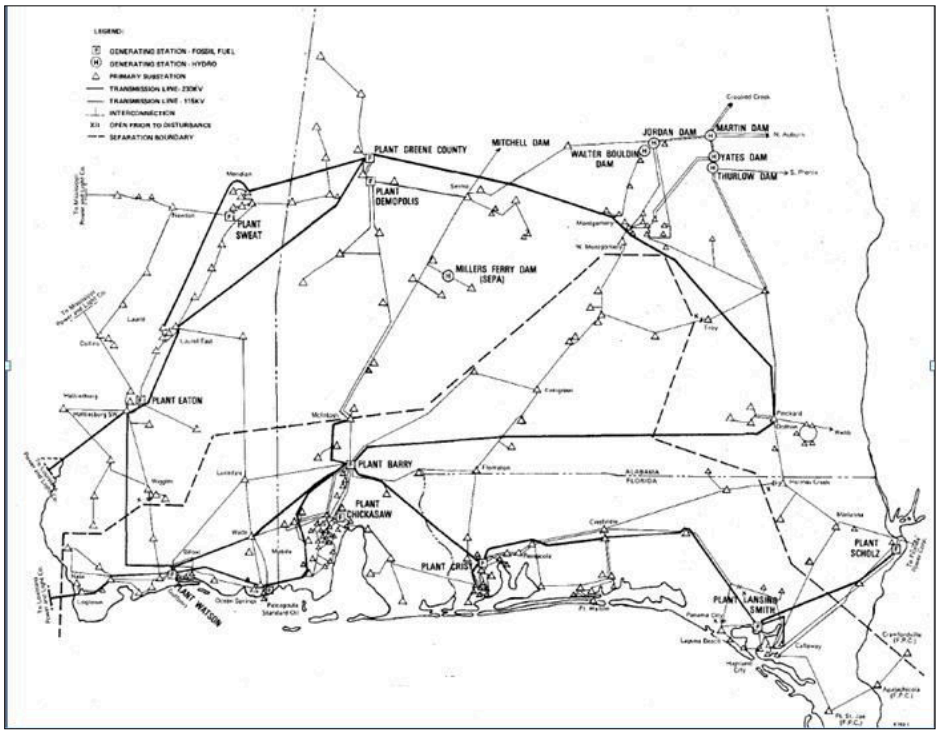

Figure 1.1: Affected areas in the Gulf Coast Area Power System Disturbance [16]

BC Hydro – Vancouver Island Outage, June 4, 1993

This disturbance started at 19:01 P.M. PST on Friday, June 4, 1993 [2]. Figure 1.2 shows the system configuration before the event. Before the event, The Vancouver Island was served by two Malaspina-Dunsmuir 500 kV AC lines, two Arnott-Vancouver Island Terminal 230 kV DC lines, and two Arnott-Vancouver Island Terminal 138 kV AC lines (one line was not in service at that time). The two 500 kV lines tripped at 19:01 within 7 cycles. A lightning storm was reported in the area at the same time and might be the cause of the tripping. The auto-reclosing of both lines were blocked and left both lines open at Malaspina end because of a parallel current supervision scheme which was used to prevent an out-of-synchronization reconnection situation for the 500 kV lines. The generation on the island could meet only 25% of the island's peak

demand and a sudden 350MW power transfer tripped the working 138 kV AC line, which was reestablished after 27 minutes. The generation-load shortage resulted in a frequency drop to 58.4 Hz. About 730 MW of demand was lost and 37,000 customers were affected.

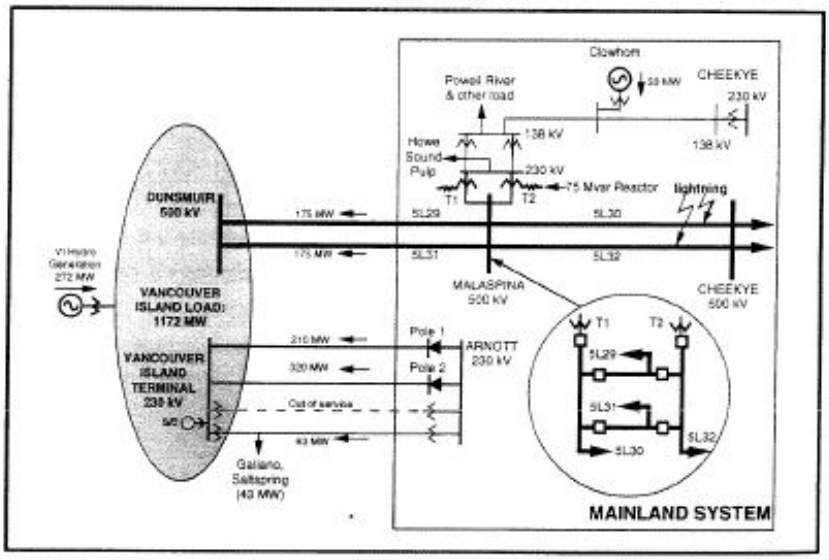

Figure 1.2: Affected areas in the BC Hydro – Vancouver Island Outage [2]

Northridge Earthquake Disturbance, January 17, 1994

This catastrophic disturbance was caused by a magnitude 6.8 earthquake in the early morning on January 17, 1994 [3]. The epicenter of the earthquake was in Northridge, California. This extensive disturbance separated the Western interconnection into five electrical regions (Fig. 1.3). Three smaller regions – the Los Angeles metropolitan area including Ventura and Santa Barbara counties in California, central Nevada and western Utah, and the southeastern Idaho and western Wyoming were physically isolated from the main grid and finally blacked out. The rest of the system separated into two regions, the north-western part – central & northern California, northern Nevada, Oregon, Washington, Montana, British Columbia and Alberta experienced low frequency (59.1 Hz) and applied load shedding. The fifth region – Southern California, Arizona, southern Nevada, New Mexico, Colorado, Utah and Wyoming experienced high frequency (60.8

Hz). The causes of the islands varied however all islands formed within 4 minutes after the earthquake struck. The earthquake caused intense ground movements that damaged transmission towers and substations, followed by multiple transmission line relay operations and transformer sudden-pressure operations, creating the first island in Southern California. The following series of cascading relay operations at 500 kV and 230 kV transmission networks opened the WSCC loop, separated the system into five pieces. Three islands finally collapsed due to huge generation-load gaps and instability conditions of the islands.

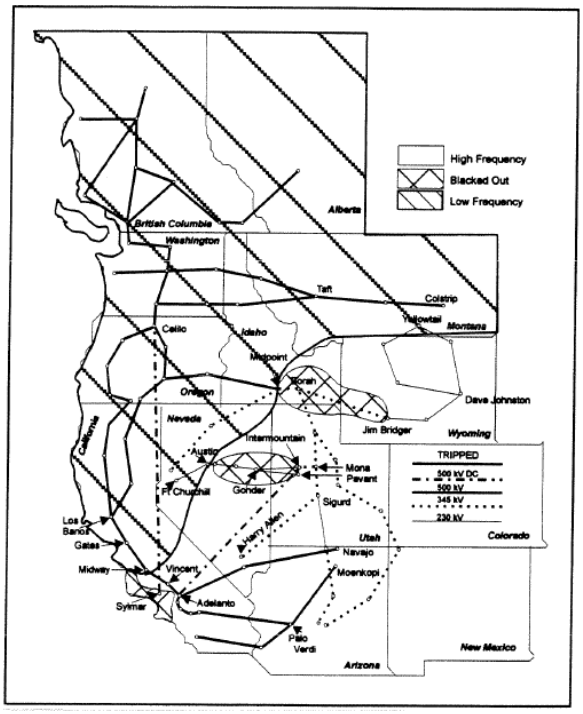

Figure 1.3: Affected areas in the Northridge Earthquake Disturbance [3]

For the whole disturbance, a total of 2.5 million customers were affected and 7,500 MW load was lost due to the separation and following load shedding. Nearly 6,400 MW of generation tripped. Power at most areas was restored within hours. However the restoration lasted for three days for areas suffering physical damage and permanent repairs to some facilities in the southern California took more than a year to be completed.

Hurricane Gustav Disturbance, September 1, 2008

This catastrophic disturbance was caused by Hurricane Gustav which made its landfall at 9:30am on January 17, 1994 close to New Orleans, Louisiana. Over 964,000 customers were affected [18, 19]. As the storm moved inland 14 transmission lines serving the Baton Rouge and metropolitan New Orleans areas tripped with a time span of several hours. This resulted in an island consisting of the metropolitan New Orleans area and a corridor along the Mississippi River between New Orleans and Baton Rouge physically disconnected from the external grid, Fig 1.4. The island contained a load of approximately 3,000 MW and the generation capacity was made up by plants Michoud, Ninemile, Waterford and Gypsy.

Unlike previous islanding disturbances, the formation of this island was monitored by PMUs installed inside and outside the islanded regions. The diverging frequency was recorded and the PMUs assisted the operators in detecting the island. Maintaining the island was successfully accomplished by adjusting governor controls and by closely monitoring the frequencies in the area using PMU measurements. The island stood for 33 hours before Entergy restored the island from both the east and the west side of the island through two pairs of 230 kV lines with the help of PMU measurements in the re-synchronization procedure.

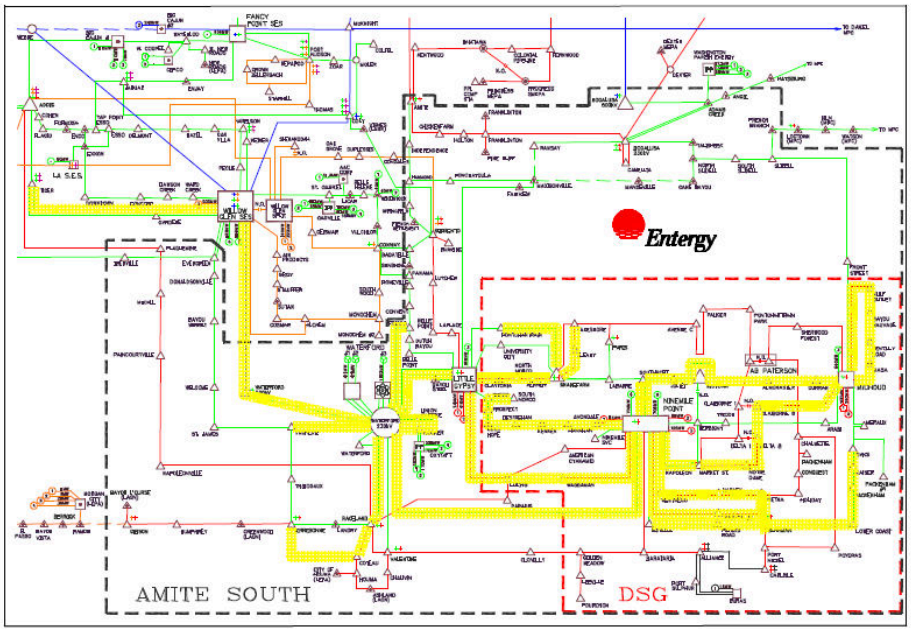

Figure 1.4: Affected areas in the Hurricane Gustav Disturbance [18]

The previous paragraphs described four historical islanding disturbances in the U.S. power system. The causes to the four cases were different and the size and duration of each island also varied. However, all cases shared one common characteristic: they all experienced one or multiple stages of under/over frequency oscillations that resulted in the inevitable shedding of loads and/or generation. Table 1 lists most of the major islanding disturbances recorded by NERC and other sources from 1992 to 2009.

TABLE 1.1: MAJOR ISLANDING DISTURBANCES IN NERC [1-19]

Case #	Case Date	Time	Region	Cause	GEN involved	Loads involved	Customers affected	Restoration
1	1973.8.7	07:53 EST	Gulf Coast Area, SCS	Cascading hidden failure (?)	3,745MW (1,045MW tripped)	1,793MW (15% shed)		7min 25sec
2	1992.1.6	15:04 PST	D.C., PEPCO	Equipment failure, S.C.		335MW dropped	18,000	Within 3 hours
3	1993.6.4	19:01 PST	Vancouver Island, BC Hydro	Weather: Lightning		730MW lost	37,000	27min
4	1994.1.7	04:31 EST	WSCC	Natural: Earthquake	5 Islands (3 collapsed) 6,400MW lost	7,500MW lost	2,500,000	3hours-3days
5	1994. 12.14	01:25 MST	WSCC	LG fault caused cascading tripping	5 Islands 11,300MW lost	9,336MW lost	1,700,000	10min-4hour
6	1996. 3.12		Peninsula Florida	Weather: Cool temperature GEN Planned outage	12,588MW (784MW dropped)	9,932MW (3,440MW dropped)		90sec
7	1996.7.2	14:24 MST	WSCC	LG fault caused cascading tripping/ faults	5 Islands 2,000MW dropped	Over 8,000MW dropped	Over 1,600,000	10min-2.5hour
8	1996. 8.10	15:48 MDT	WSCC	Weather: hot temperature	4 Islands 21,570MW dropped	28,840MW lost	7,446,000	90% within 5 hours
9	1997. 6.20	20:27 EDT	Potomac Electric Power	Equipment failure	482MW	350MW	18,000	Within 2.5 hours
10	1998. 6.25	01:34 CDT	MAPP, NPCC	LG fault Weather: Lightning	3 Islands 4,270MW removed	950MW shed	152,000	1.5hour
11	2001. 11.14	06:45 CDT	Northeastern Wisconsin/ Upper Michigan Peninsula	Natural: Tree growth; Planned line outage	742MW	1,000MW (263MW shed)		36min
12	2002. 4.29	15:50	Jacksonville Electric Authority	Equipment failure caused Chain failure	Island collapsed (load shedding failed to work)	1,729MW lost	Most of 365,000	60% in 36min-8hour
13	2002. 12.26	12:02 PST	WECC	Weather: Ice	HVDC remain (285MW Internal QF tripped)	1,567MW (950MW lost)	140,000	36min
14	2003. 3.22	6:50 PST	WECC-NWPP, BCHA	Line fault	HVDC remained		135,000	2hour 24min
15	2005. 9.21	8:33 PDT	WECC-NWPP, BCHA	Human Error	291MW tripped	no		19min
16	2006. 7.24	15:28 PDT	WECC-NWPP, BCTC	Weather: Lightning	525MW tripped	Neighboring system shed 650MW		26min
17	2007. 1.23	13:46 PST	WECC-NWPP, BCTC	Human Error	2935MW lost	1000MW lost	90,000	Till 6pm
18	2007. 11.04	9:31 EDT	NPCC-HQ	Weather: Tropical Storm Noel	Island collapsed	1039MW lost	20,000	2hour– the same day
19	2008.9.1		WECC-New Orleans	Weather: Hurricane Gustav	Over 5000MW	3000MW	964,000	33hour – 3days

The analysis to the major islanding disturbances has indicated that the causes to islanding events are variable. If we conclude, there are several major contributors: 1) Equipment failures

caused cascading line and generator tripping actions; 2) Faults or extreme weather conditions (Lightning, ice, and hot weather, etc) caused cascading line and generator tripping actions; 3) Natural disasters (hurricane, earthquake, and Tropical storm, etc); and 4) Human errors, which also include incorrect operations during the island maintaining and bad-considered determinations on planning line/generation outages.

1.1.2 Power System Disturbances involving Small Islanding Events

According to the NERC's annual disturbances report, small islanding conditions occurred in quite a number of disturbance cases. The small islanding conditions indicate the islanded area is relatively small (usually consisting of loads below 100MW) and could maintain power balance with internal generation and loads. The small islanding events mostly happened in areas surrounding certain plants. Such cases appearing in [12-15] normally experienced slight or no load loss and were restored and re-synchronized with the main grid within 2 hours after the isolation.

In the proposed research, these events are treated the in the same way as major islanding disturbances. Because they feature all the characteristics of a massive islanding event: physically disconnection from the main grid; consisting of both generations and loads; and experiencing frequency oscillations and power balance adjustments. These event are of interest for this research because: 1) these cases happen at relatively low transmission voltage levels (115kV and below) that have lower chance for the wide area measurement system (whose devices are mainly installed at 500/230kV transmission networks) to access the information in such area when they isolate from the main grid; and 2) these events occur more frequently than the major islanding disturbances.

1.1.3 The PMU's role in islanding Scenarios

The phasor measurement unit (PMU) or synchrophasor may be one of the most important inventions in the power systems area in the 20th century. The PMU was invented in 1988 by Dr. Arun G. Phadke and Dr. James S. Thorp at Virginia Tech. A PMU is a device which measures electrical signals (voltages and currents) on an electricity grid, using a common time source for synchronization. Time synchronization allows the power system operation center to utilize synchronized real-time measurements of multiple remote points on the grid [20, 21] and obtain a snapshot of the state of the system.

The PMU features such characteristics as high accuracy, fast data transmission, and wide area system observability. Conceptually the GPS-synchronized PMU measurements could achieve better than 1 microsecond in time accuracy and better than 0.1% in magnitude accuracy. The reporting rates vary from 1 to 60 times per second but 30 times per second seems to be the preferred rate by utilities. They can be used in many applications in power system generation, transmission and distribution. These applications include real-time monitoring of the system, real-time state measurements and the monitoring of disturbance, state estimation, system transient stability monitoring and wide-area protection. All PMUs follow the 2005 IEEE C37.118 standard (lately revised in 2011 as C37.118.1, 2 and published by IEEE in 2011), which deals with issues concerning the use of PMUs in electric power systems. The standard specifies the PMU measurements, the method of quantifying the measurements, testing & certification requirements for verifying accuracy, and data transmission format and protocol for real-time data communication.

In recent years, with the rapid implementation of PMUs in the major power system grids in the U.S, the wide area monitoring system (WAMS) has become possible. The WAM System

can enhance the following functions [33] under stress or emergencies conditions: a) power oscillations monitoring, which in the long run can help enhance power systems stabilizers (pss) tuning and necessary operating actions as load shedding; b) voltage stability monitoring, that can help in providing better reactive power support; and phase angle difference monitoring, that can detect possible network separation sand help in line-reclosing or system restoration.

The PMUs have already proven their contribution in islanding events. According to the reports from Energy Transmission, Inc and TEPCO [18-19, 28], the phase measurement system successfully detected the possibility of island formation and informed the danger to protection devices in several severe contingencies. In the 2008 Hurricane Gustav case, with PMUs implemented inside/outside the island, the formation of the island was detected by Entergy operators through reading of the diverging frequency. The PMUs successfully assisted the operators in maintaining the island via adjusting governor controls by offering close-up and accurate frequencies measurements. The PMU measurements also contributed in the re-synchronization procedure.

1.2 Researches on Islanding Issues

1.2.1 The Studies of Controlled Islanding

The present researches related to the power system islanding issue are divided into two major categories: controlled islanding and uncontrolled islanding [23]. Controlled islanding works as a strategy in separating a severely disturbed power system into several islands, in order to prevent an eventual collapse of the whole system. The islands are considered to be self-healing and the formation of the controlled islands is predetermined based on grouping the generators in the same island via their static and dynamic characteristics. Such grouping strategies include minimum load-generation unbalances, slow-coherent generators, etc.

The term “controlled islanding” was introduced by H. You, V. Vittal and X. Wang in [57, 58], they authors analyzed the stability margin of the power system and developed automatic islanding formation scheme based on weak connections within certain region and an analysis of slow coherent generator groups. In [58], the authors combined the controlled islanding protection scheme with the frequency decline-based load shedding in order to prevent the system from collapsing under severe stress situations.

In One study, N. Senroy and V. Vittal identify and analyze the behavior of controlled islands based on the formation of slow coherent groups of generators under an islanding contingency [23]. They have discovered that slow coherent generators tended to separate from the rest of the system in well defined and consistent groups. And each critical group of machines separating from the system corresponds to a particular mode of instability. The behaviors of different groups vary distinctly in the final stability condition. The options could be extreme stable, disturbed stable or instable.

In another research, R. Diao and V. Vittal define islanding cases using slow coherent generator grouping and minimum power imbalance on a study of the 16,100 bus Eastern power grid of North America [24]. They draw the conclusion that the controlled islanding is the last line of defense to stabilize the whole power system and provides a promising control strategy under stressed system conditions.

Another islanding method is a three-phase method using online search for splitting boundaries for large scale system based on Ordered Binary Decision Diagram [25, 26]. This method considers an interconnected power system as a graph and looks for branches that will create logical islands when tripped. The OBDD method can easily represent the balances partition problem and perform an enumeration searching at whole space of the system.

1.2.2 The Studies of Islanding Disturbances

The islanding disturbances, on the other hand, are more complex to study. It refers to the island(s) created against the utility's planning. It is a power system disturbance rather than a protection scheme. The difficulty to distinguish the islanding situation in real time is because it influences both the stability and the structure of the system, making it obscure to monitor. Furthermore, the potential locations and sizes of the islands remain unclear. In one study of cascading hidden failures, H. Wang and J. S. Thorp has examined over 170,000 blackouts by characterizing the cases as a tree-search problem and defined a random search algorithm with certain thresholds [43].

As discussed in Section 1.1.1, there are many possible reasons to cause an islanding contingency: a series of cascading hidden failures or multiple lines and generation tripping due to faults, human errors, extreme weather conditions, or natural disasters like earthquakes, tropical storms or hurricanes. It is often considered as a spontaneous phenomenon and typically starts

from the electrical centers in a power system [27] while the geographical characteristics are also of concern. Another important issue is maintaining the island stability after its formation. The situation becomes worse when the system's observability is not fully achieved. Without the certainty of the size and the location of the island, the analysis of the load-generation balance condition and the corresponding frequency bias between the main grid and the isolated area cannot be eliminated. Historically, the utilities and operators have made lots of efforts when facing islanding disturbances. Logically, for an islanded power system, the primary goal is to balance the generation and loads to decrease the chance of further loss of frequency synchronism, preventing the island from collapsing. At the same time, maintaining the maximum firm demand for the island to prevent customers' losses. Possible schemes include load shedding, capacitor and shunt switching, branch tripping and/or generation rejection. (For large natural disasters like tornado and hurricane, some actions can be done prior to prevent the loss, including set generators on hot standby or let them serve only the station load.) The under/over-frequency protection schemes have been proven to be the most efficient operation for most generation deficiency islanding situations and could effectively prevent frequency oscillation. The major drawback is that significant generation and loads have to trip during the process and permanently lost till the island is re-synchronized, even in those generation abundant conditions. In many cases, the frequency jumped back and forth between the high and low limits and caused the protection scheme trip loads and units multiple times. This is believed partially cause because the islands were detected and identified much later after their formation thus greater effort was required to drive the frequency back to nominal. In some cases, the operators were unaware of the separation till the under-frequency scheme took place. In contrast, the fast detection of the island helps the operators take correct and fast reaction to maintain the island stability. The

recent Hurricane Gustav disturbance has perfectly demonstrated that: the Entergy operators identified island formation at the first place via PMU frequency measurements. Several units were set as hot stand-by and some others tripped off the network for safety consideration. The island stood for 33 hours perfectly maintained and no additional load shedding was required [18, 19].

In the research area, the detection of islanding is of most concern. TEPCO have developed a scheme detecting power system islanding using the voltage angle differences between PMUs [22, 28]. According to their research, the frequency scheme is not as sensitive as the angle scheme [28]. The reaction time for judging an islanding case varies by different system operating conditions, the scale of the system and other aspects. In the real cases tested in TEPCO network, the phase system spent 0.27s and 0.4s to identify the islanding and a protecting action took place immediately stopping the system from islanding. [22]

In another paper published in 1994, the author presents an island AGC function to detect the island by computing the frequency bias using the generator parameters and the optimal 60Hz. This function could also apply corresponding load shedding or generator tripping scheme to maintain the island stability.

Some researchers have concentrated on the system topologies in determining the system's detaching status and thus identifying the islands. O. Mansour, A.A. Metwally, and F. Goderya has introduced a full matrix algorithm [55, 56] using the Boolean algebra computed on the system's connectivity matrix. The full matrix obtained through booleanly multiplication is filled with all 1s or remain constant, indicating the system's connectivity condition. System with islands can be distinguished by analyzing the zero conditions of the final matrix.

In [56], the authors modified the full matrix method with two successive methods. The row-sweep method applies Boolean multiplication only to the rows of the system connectivity matrix and studies the zero conditions of the final. A system is considered islanded when the final vector has zero elements. The method has reduced computation time compared to the full matrix method. The other method the authors introduced is called row-sum method which took one step further in simplifying the row multiplication by replacing the two rows with non-zero Boolean multiplication results with one row of Boolean summation of the two. It in some extent fatherly reduced computation iterations and time.

One recent research on this issue is using decision tree (DT) algorithm to apply an enumeration islanding analysis in desired islanding locations selected within the study system [29]. The author enumerated and simulated every potential islanding contingency case to form a database for the DT use.

1.2.3 The Virginia Power System

The islanding analysis method introduced in this dissertation is inspired by the historical events that happened nationwide. This research is a part of the PMU measurements application study which is sponsored by the Dominion Virginia Power (DVP) & the U.S. Department of Energy (DOE). In this project, the online system state monitoring and protection software is going to be installed on one DVP server and deal with real time synchrophasor measurements from various substations located in the DVP system. The islanding module's major task is working out an effective online scheme for islanding detection and identification. The major area this project will be implemented to is the Virginia mountain territory belonging to the Dominion Virginia Power. The DVP's transmission and distribution region is shown in Fig. 1.5.

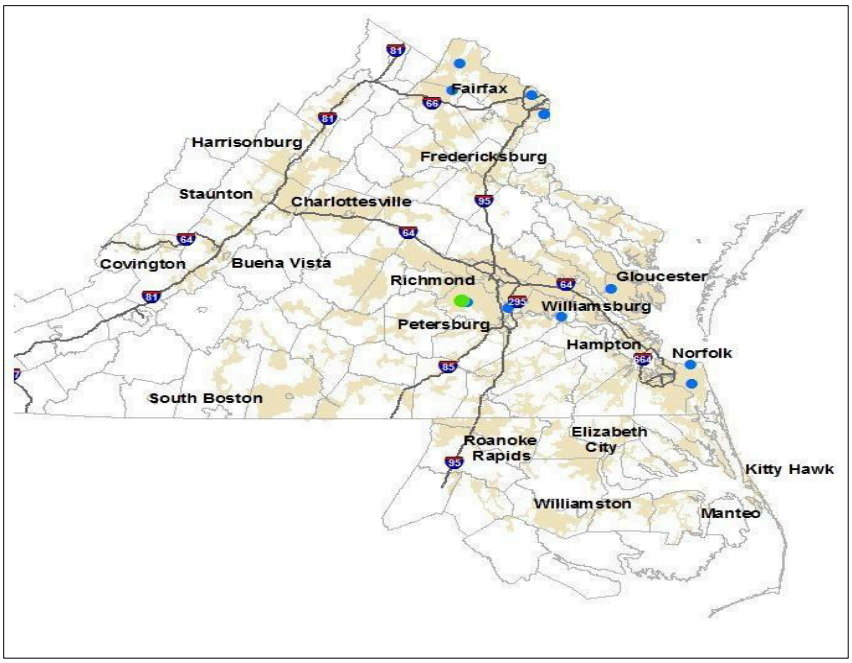

Figure 1.5: The Dominion Virginia Power Region

The Virginia Power system is geographically dispersed with several major generation and load centers, which can be seen via the area diagram. According to [17], some portions of the transmission system are more heavily loaded than others. This may become the major weak point to the system in case it splits into parts because the islanded area may face unbalance generation-load situations. At the same time, The Virginia Power system is along the east coast of the United States, and is easily disturb by hurricanes, windstorm and thunder storms. These severe weather conditions are major causes in tripping of heavily loaded transmission lines. One of the recent cases was caused by Hurricane Irene which made its landfall over Eastern North Carolina's Outer Banks on the morning of August 27, 2011. This powerful Atlantic hurricane caused one of the major 500kV transmission lines in DVP to trip. This line was carrying 250MW at the moment and the tripping lasted over 1 min.

Model simulation have shown than under certain circumstances, the two aspects may interact and result in additional cascading trips, forming island within the DVP areas. Historically no islanding disturbance has been reported in the DVP. The closest case was a

severe disturbance that happened close to the Yorktown station that caused the plant to shut down. However the engineering studies indicate that the possibility for islands formation within the Virginia Power system exists.

A detailed introduction of the DVP system is given in Chapter Four.

1.3 Overview of the Dissertation

The proposed method presented in this dissertation is primarily focused on detecting and analyzing power system islanding contingencies using online PMU measurements and related issues including islanding stability assessment and optimal PMU placement with the consideration of islanding.

Chapter One has introduced the history of wide-area islanding disturbances in the U.S. power grid, and summarized previous researches related to the islanding issue. The research works are categorized into controlled islanding protection scheme and non-controlled islanding disturbances. A discussion about the Virginia power network is also raised.

Chapter Two discussed the principles of the proposed DT based Islanding detection, classification and evaluation method. The primary method is composed of an intelligent decision tree for islanding detection and identification basing on a database of system's simulated and practical operation and contingency records, system geographical information, and a severity index. The DT is generated from the islanding contingency database to: distinguish an islanding scenario from other system events as short circuits, line-tripping or generator-tripping only basing on the state variables changes from outside the island; estimate the stability condition of the island and locate the approximate islanded area; and help in deciding the PMU placements for a better islanding detection and identification. The chosen methodology to grow DTs in the proposed method is CART (Classification and Regression Trees) [37].

Another issue touched in the proposed method is the optimal PMU placement strategy with the consideration of islanding issues and redundancies. In this chapter, some optimal PMU placement assumptions and theorems are derived and discussed and the modification in PMU placement strategy and power system bus reduction scheme is made. A fast and accurate method

using binary programming method to solve PMU placement problem with consideration of islanding conditions is introduced.

Chapter Three examines the proposed decision tree algorithm in islanding detection, estimation and classification with wide-area system model. The tests are carried out on the precision of the system islanding detecting strategy and modified depth first method, the efficiency and accuracy of the decision tree on islanding judgment, and the transient behaviors of the islanding severity index. The optimal PMU placement strategy using binary integer programming algorithm is also tested and analyzed.

Chapter Four introduces the practical utilization of the DT based islanding scheme in the Dominion Virginia Power (DVP) system. The islanding analysis is part of the PMU measurements application study which is sponsored by the Dominion Virginia Power & the U.S. Department of Energy. In this project, online system state monitoring and protection software is being installed on Dominion's server for processing real time synchrophasor measurements from various substations located in the DVP system. The islanding module adopts an efficient online scheme in detecting any potential islanding failures that may happen in the DVP system. The principle and operating procedures of this scheme are fully described and series of tests and analytics are applied.

Chapter Five summarizes the main contributions of this research work and suggests possible topics that can be explored in the future.

CHAPTER 2: METHODOLOGY

2.1 The Decision Tree Algorithm in Islanding Analysis

In this section, the utilization of the DT algorithm in islanding contingency detection and classification and an islanding behavior analysis arefully demonstrated.

A decision tree is an inductive learning data-mining algorithm that draws the underlying mechanisms and hidden relationships from the created database through the input-output paired model construction process. This is achieved through a simple yet clever way: decision rules are developed through performing a binary partitioning with the aid of series of if-else judgments. The complete instruction of the DT theory can be found in [37] and [38]. According to a recent overview on applications of data mining to power systems given by [39], the Decision Trees are used as the preferred method in 86.6% of the papers.

The DT method has been used in a wide range of areas in power systems, such as security assessment, load forecasting, state estimation, etc. The DT algorithm is already widely used in the controlled islanding studies. In [23], the DT is trained to predict the controlled island's transient stability. Generated offline, the DT is considered quickly accessible to monitor the system online performance and predict the separation. In [24], each DT is trained only for a specified critical contingency that can potentially cause cascading events and high prediction accuracy is obtained. For islanding scenarios, the DT is generated offline via the enumerated islanding contingency simulation of the study system [30], and purposed for online wide area system monitoring and detecting islanding contingencies using synchrophasor measurements.

The chosen methodology to grow DTs in the proposed method is CART (Classification and Regression Trees). It's mainly on classification trees due to the nature of the problem. CART

performs an exhaustive search over all data channels (attributes) and all possible splitting values to grow the optimal tree.

2.1.1 Overview of Decision Trees

2.1.1.1 The Formation of a DT

The Decision Tree is a carrier of inductive reasoning. The algorithm has made an investigation of the dataset, extracting the underlying mechanism given rise from the data, and deriving a model that carries the information and past experiences, which are repeatable, to satisfy certain pre-determined judgment requests on targets. The DT is tree-like, with multiple nodes, branches and terminals. Fig. 2.1 depicts the schematic structure of one example classification tree. The upmost node is called the "root" of the DT. The whole tree grows out from this node. The node contains certain quantity of the samples in the dataset. At each node $\mathbf{t}$, the samples are split into two subsets $\mathbf{t_L}$ and $\mathbf{t_R}$ (the left and right child) basing on certain judgment made upon samples' differences at certain attribute. A splitting value for this attribute at this node is obtained. The splitting process will iterate until no more split is possible. The ending node is called a "terminal" node. The final classification decision is made with the terminal nodes. In Fig. 2.1, the two colors of the terminal nodes indicate the two opposite judgment/decisions on certain attribute. In certain cases, the DT may have multi-way splits at one node. Multi-way splits tend to fragment the data too quickly which leads to a less efficient split on the next level [40].

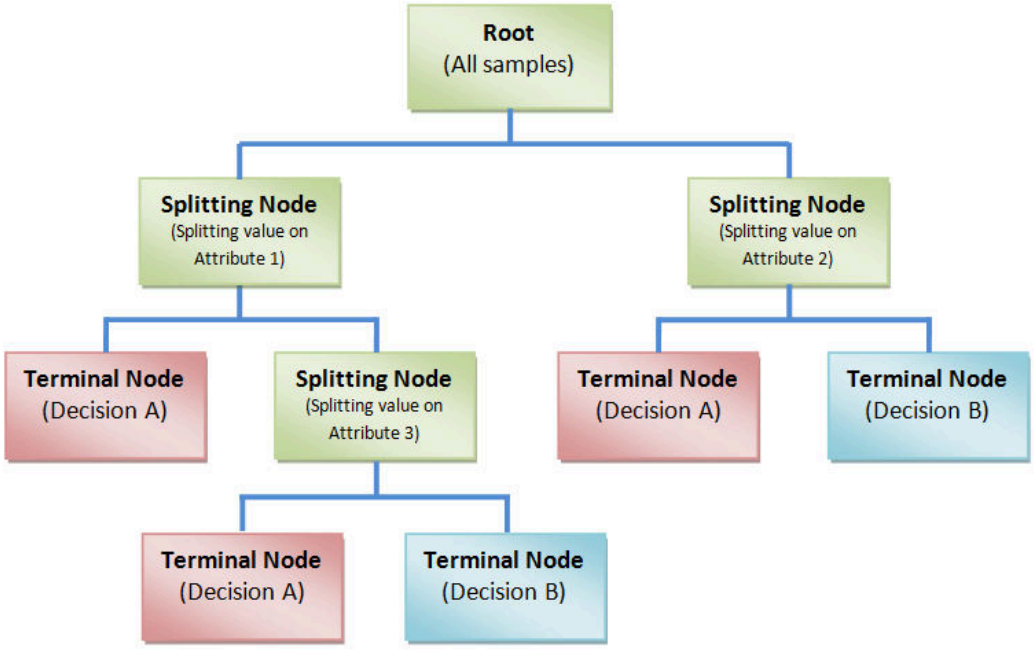

Figure 2.1: Classification Tree Example

After building the tree, when classifying a new case, the new sample is dropped off at the root of the tree. By comparing with the splitting values at each node, the sample will eventually fall into one terminal; one route across the tree is built and the decision is obtained.

According to [37], Decision Trees are grown through a systematic method known as recursive binary partitioning; a "divide-and-conquer" approach where successive questions with yes/no answers are asked in order to partition the sample space [40].

2.1.1.2 Sample Data Format

The sample data are in matrix {X} format and saved in tables. The matrix is composed of a set of **n+1**measurement vectors:

$$X = \{x_1, x_2, ..., x_n, T\} \tag{2.1}$$

Each vector is call an attribute to the DT and peculiarly one of the attributes is the target **T** that the DT makes decision on. The attributes can be either numerical or categorical. Categorical attributes have a finite set of values and the values don't have an intrinsic order; numerical attributes have values in real line and can be sorted in ascending/descending order. In the split process, the node can spilt at any value within the range of the numerical attribute. For example, one numerical attribute $x_1 = \{2, 3.5, 4.5, 7\}$, the splitting value can be 6 or 3 or any value belongs to [2, 7]. On the other hand, the categorical attributes can only split on themselves.

The sample data matrix {X} can also be seen as a composition of **m** measurement vectors:

$$X^T = \{y_1, y_2, ..., y_m\} \tag{2.2}$$

In this composition, each vector is one case from the dataset or called one sample. To conclude, the input data matrix {X} is an **m** by **n+1** matrix: **m** sample cases and **n+1** attributes (including one target vector **T**).

TABLE 2.1: DATA FORMAT FOR A DECISION TREE

	Attribute 1	**Attribute 2**	**…**	**Attribute n**	**Target**
Case 1	A_{11}	A_{12}	…	A_{1n}	T_1
Case 2	A_{21}	A_{22}	…	A_{2n}	T_2
…	…	…	…	…	…
Case m	A_{m1}	A_{m2}	…	A_{mn}	T_m

A_{ij} can be numerical or Categorical

One more point of concern is that as a supervised learning method, the class of each attribute needs to be classified before forming the tree. And due to the nature of the islanding problem, the target is categorical for islanding detection (YES/NO), islanding stability assessment (YES/NO) and islanding location estimate (specified location numbers).

2.1.1.3 Tree Growing Techniques

Before the discussion of the tree growing techniques, several definitions in the DT algorithm are introduced first. These definitions are:

1) Node Impurity

It is defined as the criterion a DT uses to rank candidate splits, or called the heterogeneity of a node. The purity, on the other hand, is a measurement of the class homogeneity. In [41], there is an example for the preparation to compute the node impurity: a classification tree is grown on a categorical target variable **T** taking on values j = 1... J. Every node in the tree is identified by the symbol t, and each node will have an estimated probability distribution for the values of the target variable. There assuming J = 3, at every node we are able to specify the probability of observing **T**= 1, **T**= 2, and **T**= 3 in that node and their probabilities are written p(1 | t), p(2 |t) and p(3 | t), where the probability is conditional on the node under consideration. If the priors are proportional to the data, then these probabilities can be taken to be the observed relative frequencies of each class in the node. [41] The node impurity is computed based on the probability distribution for each node.

2) Cost and Relative Cost

The DT algorithm determines the best tree by testing for error rates or the "misclassification cost". Considering a data sample containing 50 cases, among them the targets have 20 categorical value **A**s and 30 categorical value **B**s. If the tree only contains one node (actually no tree formed), all targets fall into the **B**-category. The misclassification cost or error rate is 0.4 (40%). If the tree has two nodes, the terminal 1 contains 2 **A**s and 22 **B**s and seen as **B**-

category and terminal 2 contains 18 **A**s and 8 **B**s and seen as **A**-category. The new error rate is computed as, noticing the **A**s contains 0.4 of the total sample and **B**s contains 0.6:

For Terminal 1: (2+22)/50*(2/(2+22)) = 0.04

For Terminal 2: (18+8)/50*(8/(18+8)) = 0.16

Total: 0.04+0.16 = 0.2 (20%)

The relative cost shows the improvement for a tree which is further grown from the previous stage, a tree with single node is assigned a relative cost of 1. Using the previous example, the error rate for the two-node tree is 0.2, so the relative cost is computed as:

0.2(new) /0.4(old) = 0.5

The relative cost shows the relationship between the misclassification costs of the mother tree and the child tree. And it is capable in determining the best tree. The relative cost should be smaller than 1 indicating a more efficient tree is grown after new splitting, otherwise the new splitting is judged as inefficient. If we plot the cost and relative costs of a growing tree versus the number of nodes, the optimal tree is the one with the smallest misclassification cost and at the point when the first order differential of the relative cost curve reaches zero.

3) Cost Complexity

This parameter measures the tradeoff between error rates and tree sizes [40], Breiman, Friedman, Olshen and Stone suggest the following cost complexity measure for any tree [41]:

$$\text{Cost Complexity} = \text{Re-}substitution\ Misclassification\ Rate + \alpha(Num.\ of\ Terminal\ Nodes) \quad (2.3)$$

Where: **the re-substitution relative cost** measures the misclassification rate for the data used to grow the tree (the learning pool);

α is the penalty imposed per additional terminal node.

The process of growing the correctly-sized tree consists of three stages, or three major concerns: 1) How to determine the splitting rule basing on accurate and efficient splitting criterion; 2) How to decide a stopping rule for the split process when terminals are reached; and 3) How to assign a class to each terminal node [40].

The first question can be solved by computing the purity /impurity of the nodes. The ultimate goal of a DT is to extract the target vectors into the classification groups which achieve a smallest misclassification error. In other words, achieve a maximum purity of one class of the target vector and the minimum impurity of the equal proportion of all classes in the target vector. When a split achieves the minimum impurity (which is mathematically equal to maximum purity, and is easier for computation) for it descendent nodes, we can say this split is optimal for itself. Many researchers have proposed methods for measuring mode impurity in the last two decades. These methods include: Gini Index, Entropy Impurity, the Twoing criterion, etc. According to [32], the choice of a particular impurity function has very little effect in the forming of the final tree.

The two methods used in the CART® software are introduced below:

1) The Gini Impurity Criterion

The Gini impurity criterion is given by:

$$i(t) = 1 - S \tag{2.4}$$

Where S is the sum of squared probabilities p (j | t) summed over all levels of the dependent variable at the node **t**:

$$S = \sum_{j=1}^{J} p^2(T_j / t) \tag{2.5}$$

If one node consists exclusively of a single class, one of the class probabilities will equal 1, the remaining class probabilities will all equal zero, and the computed diversity index i(t) is zero.

An optimal split **s** at node **t** is should satisfy the option to maximize the decrease in impurity at node **t** achieved by split **s**:

$$\Delta i(s,t) = i(t) - \left[p_L \times i(t_L) + p_R \times i(t_R)\right] \tag{2.6}$$

While the $\mathbf{t_L}$ and $\mathbf{t_R}$ are left and right child node of the existed node **t**; $\mathbf{p_L}$ and $\mathbf{p_R}$ are left and right proportions from the original node **t**.

2) The Twoing Criterion

CART also utilizes another splitting criterion called the Twoing criterion. This is a measure of the difference in probability that a class appears in the left descendant rather than the right descendant node [41]. The method is based on a concept of class separation between the left and right child nodes. One optimal split s at node t should maximize the follow equation:

$$T(s,t) = \frac{p_L \cdot p_R}{4} \sum_{j=1}^{J} \left(\left| p(j|t_L) - p(j|t_R) \right|^2 \right) \tag{2.7}$$

In concept, this method wants to distinguish a class **j** of the target between the two child nodes that it achieves the probability that **j** goes to the left child node differs mostly from the probability that **j** goes to the right. The rule sums the absolute value of the probability differences over all **j** classes.

Once a best split is found, the DT repeats the search process for each child node, continuing recursively until further splitting is impossible or a terminal is reached. A methodology to declare terminal nodes is needed. The method is called the "stopping rule". This is a rule or set of rules that define the termination condition for the splitting. According to [41], every stopping rule examined is shown to produce bad results, "because a node that might not split well at one level might yield very informative splits if the tree-growing process continued just a little further." Nevertheless, two stopping rules are introduced below:

1) There is one effective stopping rule that terminates the splitting when the sample number at one node is below certain threshold. It's simple but sometimes inaccurate because some potential child nodes with high impurity decrease are not considered under such rule.

2) Another heuristic stopping rule is to test the impurity decrease between the mother node and the descendents. If the $\Delta i(s,t) > \varepsilon$, where ε is impurity decrease threshold, the node is identified as a terminal.

The CART program, on the other hand, uses a total different strategy to grow the tree. CART has no stopping rules at all. The tree is grown to its maximum size and to be pruned to optimal size afterwards. The CART features are introduced in the next section.

2.1.1.4 The Classification and Regression Tree (CART) Software

A major innovation of CART is to eliminate stopping rules altogether [41]. Instead of asking when to stop, CART continues to grow the tree till further splitting is impossible, which is called a maximal tree. After obtaining the maximal tree, CART prunes back and removes excessive branches until it reaches the optimal tree, based on the cost complexity characteristic of the tree.

The CART's law to grow the maximal tree is set based on the Gini Impurity Index, as:

1) Define the minimal number of cases that is allowed for an un-terminal node (typically 5 or 10);

2) Considering the sample dataset is an **m** line (m cases) by **n+1** column (n attributes and one target) matrix (see Section 2.1.1.2),setting potential splitting values for certain attribute **l** at node **t,** if the attribute vector is written as $\{\mathbf{x_{l,t}(k)}\}(\mathbf{k = 1, 2,\ldots, m}, 1 \in \{1,2,...,n\})$. When $\mathbf{x_{l,t}(k)}$ is a numerical attribute, all **m** attribute values are sorted in ascend. The potential split values $\mathbf{S_{l,t}} = \{\mathbf{s_{l,t}(k)}\}$ ($\mathbf{k = 1, 2,\ldots, m}$) are:

$$s_{l,t}(k) = \frac{x_{l,t}(k) + x_{l,t}(k+1)}{2} \tag{2.8}$$

When $\mathbf{x_{l,t}(k)}$ is a categorical attribute, the potential split values are the attribute itself: $\mathbf{S_{l,t}} = \{\mathbf{x_{l,t}(k)}\}$ ($\mathbf{k = 1, 2,\ldots, m}$)

3) Compute the decrease in impurity for the split at node t into two child nodes. To achieve this, the subsets of the samples at node t into descendent left (L) and right (R) node are defined as:

$$\begin{aligned} t_L &= \{x_{l,t}(k) \text{if } \le S_{l,k}\} \\ t_R &= \{x_{l,t}(k) \text{if } > S_{l,k}\} \end{aligned} \quad \text{for numerical attribute} \tag{2.9}$$

Or

$$\begin{aligned} t_L &= \{x_{l,t}(k) \text{if } = S_{l,k}\} \\ t_R &= \{x_{l,t}(k) \text{if } \ne S_{l,k}\} \end{aligned} \quad \text{for categorical attribute} \tag{2.10}$$

The decrease in impurity is computed using (2.6):

$$\Delta i(s,t) = i(t) - \left[p_L \times i(t_L) + p_L \times i(t_L)\right]$$

While the $\mathbf{t_L}$ and $\mathbf{t_R}$ are left and right child node of the existed node **t**; $\mathbf{p_L}$ and $\mathbf{p_R}$ are left and right proportions from the original node **t**.$\mathbf{p_L}$ and $\mathbf{p_R}$ are computed as the total case number at the left and right child node over the total case number at node **t**:

$$p_L = \frac{n(t_L)}{n(t)}$$
$$p_R = \frac{n(t_R)}{n(t)} \tag{2.11}$$

At any node **t**, the probability that one of its belonging cases belongs to the target class $\mathbf{T_j}$ is computed by the re-substitution estimator:

$$p(T_j, t) = \pi(t) \cdot \frac{n_t(T_j)}{n(T_j)} \tag{2.12}$$

$\mathbf{n}(\mathbf{T_j})$ is the number of class **j** target, $\mathbf{n}(\mathbf{T_j})$ is the number of class **j** target falls into node **t**, $\boldsymbol{\pi}(\mathbf{t})$ is called the prior probability of node **t**, if not assigned by modeler, $\pi(t) = \frac{n(T_j)}{n}$.

And: $p(T_j|t) = \frac{p(T_j, t)}{p(t)}$ (2.13)

Where $\mathbf{p}(\mathbf{t})$ estimates the probability that a case falls into node **t**.

4) Step 2) and 3) iterates with the consideration of step 1) until no more split can be performed. Then at each terminal, a series of $p(T_j|t)$ (***j = 1, 2… J***) of all J target classes are computed, the terminal will be assigned as class $\mathbf{J_{max}}$ terminal with the highest $p(T_j|t)$ value: $p(T_{J\,max}|t) = \max_j\left(p(T_j|t)\right)$.

The maximal sized DT is likely to be over-fitting for an actual problem. CART always prunes the tree to achieve a best tree. The judgment for pruning process used in CART is the cost

complexity that introduced in Section 2.1.1.3. This parameter measures the tradeoff between error rates and tree sizes and is defined as:

Cost Complexity = Re-substitution Misclassification Rate + α(Num. of Terminal Nodes)

Where: **the re-substitution relative cost** measures the misclassification rate for the data used to grow the tree (the learning pool); and $\boldsymbol{\alpha}$ is the penalty imposed per additional terminal node.

Tracing back from the maximum node number to the single node, the cost complexity at every stage of the tree are computed and the best tree is selected based on the smallest cost complexity.

As a professional data-mining software and the most popular DT algorithm based software, CART exhibits several advantages [41]:

1) CART uses multiple sophisticated methods to assess its accuracy.

The preferred method to assess accuracy is to use a separate test data set (usually 10% the size of the learning sample). However, when data are scarce, CART uses cross validation to accurately assess its goodness of fit. That is, for example, a 10-fold cross validation separates the data into 10 equal subsets. Each time the method uses one subset to test the tree which built from the other nine pieces. This process repeats for ten times. When the 10 replications have been completed, the error counts from each of the 10 test samples are summed to obtain the overall error count for each tree in the full-sample tree sequence. Thus the optimal tree with lowest cost complexity is selected. This method is thought to be very close to the truth [41] and the best value for v-fold is ten or greater. Ten is the default value in CART.

2) Same variable can appear multiple times at the same tree.

This uncovers the context dependency of the effects of certain variables. By contrast, some tree-growing methods use a variable only once in the analysis.

3) CART allows placing non-unitary relative weights on different misclassification errors.

4) Normally, a DT requires the sample dataset to be complete for the training process. However CART can work with variables that have missing values for many cases in the learning sample. By identifying surrogate splitting rules (rules that can substitute for a primary split when data are missing), CART allows cases with incomplete data, increasing the sample size and the reliability of the results.

2.1.2 Decision Tree Algorithm and Non-controlled Islanding

In this section, the proposed method to use decision tree algorithm in islanding contingency detection and identification problem is introduced. A review of several of DT applications in power system islanding assessment has been given in the Section 1.3.3. Although the DT algorithm has been implemented in many power system applications including controlled islanding assessment, its usage in the non-controlled islanding is relatively rare. At the same time, according to the analysis of the historical islanding disturbances that happened in the U.S. power grid in Section 1.2, the conclusion may be drawn that the fast islanding detection helps the operators take correct and fast reaction to maintain the island.

To mimic the situation, we may put ourselves into the position of the system operators. Considering an islanding contingency occurring in a wide area power system, with both the physical and electrical connections broken down the accurate real time information about the island could be very limited to operators outside the isolation. In the past, the island might be known when the frequency jumped back and forth between the high and low limits and caused

the protection scheme to trip loads and units. It might be too late when the operators are alarmed: much load and generation has already tripped. This situation is about to change when the WAMs is put into use. The sharing of information becomes fast and accurate with the respect of the PMU implementation. Now the most feasible and dependable real time measurements tend to be those from the PMUs installed close to the island (or luckily from PMUs installed in the island). The measurements - the voltage phasor, current phasor, load flow and frequency measurements - could be obscure and controversial however they are still the most useful information. The frequency deviation could indicate a potential islanding formation only if any of the PMUs is inside the island. However if we take the worst situation into consideration: all dependable PMU sources are outside the island – no much frequency difference is recorded. In such circumstance, other method in islanding detection is needed. In the analysis, some essential questions are raised and need to be answered:

In a wide area system, how could an operator distinguish and react to an islanding scenario from other system events based only on the information provided by changes in the state variables from outside the island?

With the island state information no longer available or very limited, is it possible to estimate the stability condition of the island and locate the approximate islanded area?

If the essential islanding modes (or most potential islanding regions) are known, does it help in deciding the PMU placements for better islanding detection and identification?

Is it possible to track or monitor an island during its formation with limited information availability?

The DTs used in this study are expected to answer these, especially the first three questions. Though generated offline and from a well studied database, the DT works essentially

online as a special protection scheme for the p.s. dynamic security. DT's fast execution feature makes it very suitable for real-time system security assessment and state prediction. When implemented online with PMU application, for each data refreshing point, the real-time measured system attributes are read by the DT module and processed through the partitioning. The terminal node is picked up almost simultaneously. Time delay in this procedure can be disregarded because most heavy works related to the tree training and testing are performed offline. The DTs are considered adequate for any islanding contingency scenarios that may occur with a high prediction success using simulated and historical islanding database. Besides the database can be updated with refreshed data after the DT module is online when a historian module is installed in the program. The time to re-generate and test the DTs and program new DTs to the system needs to be considered.

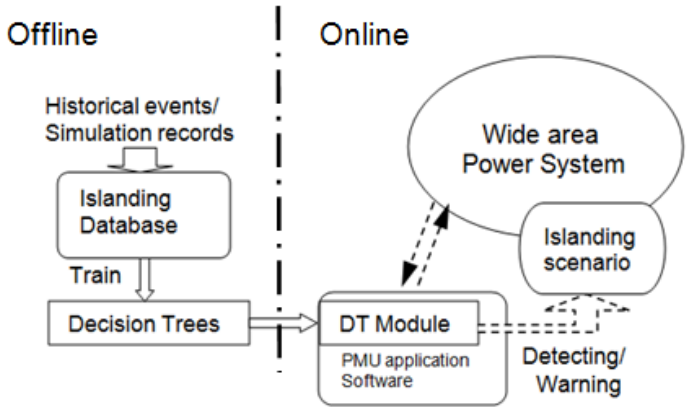

Figure 2.2: DT based Islanding contingency scheme

Fig. 2.2 has demonstrated the process of this DT based method. The offline process includes the islanding database creation and the DT formation for islanding detection using CART; the online process includes the real time system operation monitoring and the online islanding judging module/software.

In this study, the particular system state variables used for wide area system online detection include real-time voltage phasor and current phasor measurements (and/or load flow and frequency variables). Islanding situations happen at low transmission levels involving power plants, there's high probability that the direct access from outside into the isolated area is no longer present after the islanding. Plus the number of PMUs installed in a wide area power system is sometimes limited to the major nodes at its high voltage transmission networks, which is very reasonable due to the cost of PMU implementation. In this study, only the high voltage level buses in the study system are considered as PMU locations and used to form the DTs. Generator variables and lower transmission levels are not concerned in the first place.

2.1.3 Islanding Contingencies Database Creation

The DT based islanding detecting scheme is primarily derived from the islanding database, which is used to generate the DTs offline. To create the database, system operation cases and islanding contingencies are obtained through real event's operating records and through simulations. There are three reasons the dynamic simulations to the study system are needed:

1) The actual islanding cases are limited and unique. It's difficult for the DT to generate correct characteristics or mechanism from limited cases. While it is also unrealistic to perform real world tests, simulations make the thorough investigation on certain system region possible.
2) Applying simulations to system models, some extreme system conditions and scenarios can be tested and analyzed. It helps us to study the system under extreme conditions and boundary situations.

The DT program is updatable and needs to be refreshed in order to make it practical. The historical event records and daily operation records are also major sources of the database. The simulated data is the key to turn this iteration on.

The database creation is principally a reversed process of the DT defining an islanding case. The database includes islanding, other types of faults or contingencies and normal operating cases. One thing is sure that each case's type is known before the simulation is run. In the database, an ISLANDING_DECISION identifier is generated for all inputs: all islanding cases are labeled as "1" while all others are labeled as "0". Besides that, all cases share the same state variable channels.

In the database creation process, two schemes are introduced and used: A System Islanding Detecting Strategy (SIDS) is introduced to distinguish islanding cases from normal system operations and from other contingencies through a system incidence matrix computation. A modified enumeration method is used to select reasonable size of the islanded area based on the system geographical and electrical topologies. In the last procedure, the collected data through simulations and real world records are used to form an intelligent decision tree. The proposed method also includes an Island Severity Index (ISI) which qualifies the long term and transient behavior of the islanded system. The transient index judges the instantaneous impact of the isolation to the main grid. The long term severity index determines how severely the system's operating status will vary from the normal operating criteria with all possible protection schemes carried out after a certain period of time. The ISI serves as an additional option to qualify the stability condition of certain islanding contingency.

2.1.3.1 System Islanding Detecting Strategy

To state this strategy, we first introduce the concept of the incidence matrix and observability matrix [35].

In mathematics, an incidence matrix depicts the relationship between two classes of objects [42]. If the first class is X and the second is Y, the matrix has one row for each element of X and one column for each element of Y. If x and y are related (called incident in this context) then the entry in position (x, y) is 1 otherwise it is 0. A case related to the power system is shown below:

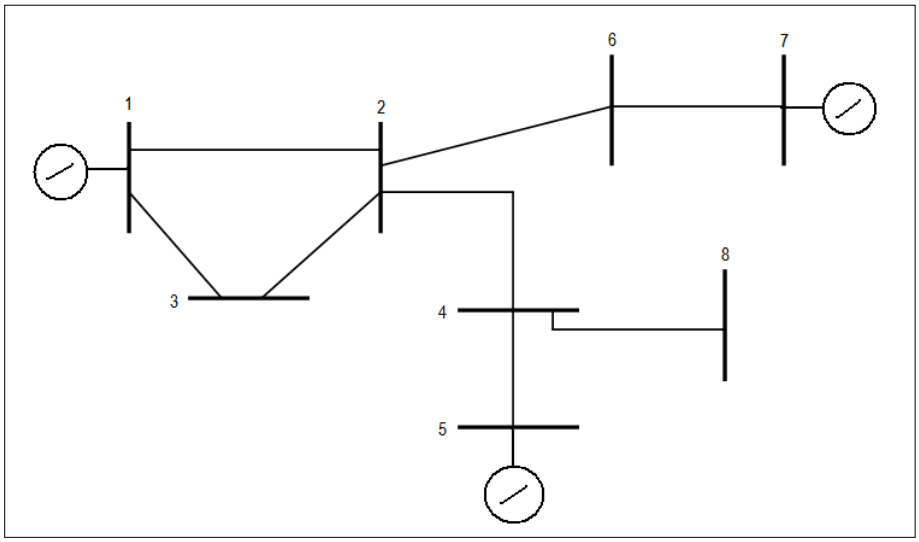

Figure 2.3: 8-bus 3-machine test system

Fig. 2.3 shows the one line diagram of a small scale power system. This system contains eight (8) buses, eight (8) branches, and three (3) generators. We define the X- and Y-class for this system as the bus vector {**b1**, **b2**, **b8**}. In power systems, the incidence matrix is a reversible symmetrical matrix that indicates the connecting condition of a system. Its size is depended on the bus number in the system (for this example, it's 8 by 8). It has all its diagonal elements (bus elements) equaled to 1 which means the bus is connected to the system. For each two buses **i**, **j**

(**i≠ j**) which have transmission line connected, the corresponding elements in the A matrix $\mathbf{A_{i,j}}$, $\mathbf{A_{j,i}}$ (branch elements) are also 1. Zero-valued element $\mathbf{A_{x,y}}$ indicates that the bus **X** doesn't have a connection with bus **Y**. The incidence matrix is symmetrical. Line vector $\mathbf{A_m}$ refers to Bus **m**'s connection status with all system buses. Then for system shown in Fig. 2.3, we can easily obtain the incidence matrix **A**:

$$A=\begin{bmatrix} 1 & 1 & 1 & 0 & 0 & 0 & 0 & 0 \\ 1 & 1 & 1 & 1 & 0 & 1 & 0 & 0 \\ 1 & 1 & 1 & 0 & 0 & 0 & 0 & 0 \\ 0 & 1 & 0 & 1 & 1 & 0 & 0 & 1 \\ 0 & 0 & 0 & 1 & 1 & 0 & 0 & 0 \\ 0 & 1 & 0 & 0 & 0 & 1 & 1 & 0 \\ 0 & 0 & 0 & 0 & 0 & 1 & 1 & 0 \\ 0 & 0 & 0 & 1 & 0 & 0 & 0 & 1 \end{bmatrix};$$

The system observability is referred to the accessibility from one bus to any other. Considering the system in Fig. 2.3, **bus1** is the neighbor bus of **bus2**, in other words, **bus 1** can reach **bus 2** in 1 step. And **bus 1** needs 2 steps to access **bus 6**, or **bus 6** is 2-step observable for **bus 1**. The 1st step depth observability between **bus 1** and **bus 6** is zero and the 2nd step depth observability between **bus 1** and **bus 6** is one [35].

The nth depth system observability matrix is a reversible symmetrical matrix that indicates the system observability from each bus to other buses in a system. It has the same size as the incidence matrix. It has all its diagonal elements equaled to 1 which means the bus is observed by itself. The off-diagonal element in the A matrix $\mathbf{A_{i,j}}$ equals 1 when the row bus **i** is observed by the column bus **j**(**i≠ j**) within certain step **n**. Zero-valued element $\mathbf{A_{x,y}}$ refers to the bus **X** cannot be observed by bus **Y** within step **n**. The incidence matrix is symmetrical. Line vector $\mathbf{A_m}$ refers to Bus **m**'s observability with all system buses. The system observability matrix

changes upon the different setting for the step **n**. There's an easy way to compute the n^{th} depth system observability matrix. That is: compute the n^{th} power of the system incidence matrix and change all non-zero elements to 1.

For the 8-bus 3-machine test system, we have the 2^{nd} and 3^{rd} depth system observability matrices are:

$$2^{nd}:(A)^2=\begin{bmatrix}3&3&3&1&0&1&0&0\\3&5&3&2&1&2&1&1\\3&3&3&1&0&1&0&0\\1&2&1&4&2&1&0&2\\0&1&0&2&2&0&0&1\\1&2&1&1&0&3&2&0\\0&1&0&0&0&2&2&0\\0&1&0&2&1&0&0&2\end{bmatrix}\Rightarrow\underset{none-zero\to 1}{(A)^2}=\begin{bmatrix}1&1&1&1&0&1&0&0\\1&1&1&1&1&1&1&1\\1&1&1&1&0&1&0&0\\1&1&1&1&1&1&0&1\\0&1&0&1&1&0&0&1\\1&1&1&1&0&1&1&0\\1&1&0&0&0&1&1&0\\0&1&0&1&1&0&0&1\end{bmatrix}$$

$$3^{rd}:(A)^3=\begin{bmatrix}9&11&9&4&1&4&1&1\\11&15&11&9&3&8&3&3\\9&11&9&4&1&4&1&1\\4&9&4&10&6&3&1&6\\1&3&1&6&4&1&0&3\\4&8&4&3&1&7&5&1\\1&3&1&1&0&5&4&0\\1&3&1&6&3&1&0&4\end{bmatrix}\Rightarrow\underset{none-zero\to 1}{(A)^3}=\begin{bmatrix}1&1&1&1&1&1&1&1\\1&1&1&1&1&1&1&1\\1&1&1&1&1&1&1&1\\1&1&1&1&1&1&1&1\\1&1&1&1&1&1&0&1\\1&1&1&1&1&1&1&1\\1&1&1&1&0&1&1&0\\1&1&1&1&1&1&0&1\end{bmatrix}$$

In a power system, based on the system topological structure and breaker status, the incidence matrix of the system is obtained. Square the incidence matrix and change all non-zero elements to 1 to obtain the 2^{nd} step depth system observability matrix; cube the incidence matrix and change all non-zero elements to 1 to obtain the 3^{rd} step depth system observability matrix, and so on. The n^{th} step depth system observability matrix has the same rank as the system incidence matrix. The non-zero off-diagonal element in the n^{th} observation depth matrix represents that the line bus can be reached from column bus within n branches.

After multiplying the incidence matrix several times, all elements in the Depth matrix will be 1. In a power system with N buses, the certain iteration number is defined as **Q**. **Q** can be obtained through the system incidence matrix analysis. Taking any two random buses from the system, recording the bus numbers in the shortest path of all existed line paths between the two buses, repeat this to every possible bus-pair combinations in the system and find out the largest bus quantity. This number is the maximum iteration number **Q**. For a system with lines tripped, in incidence matrix view it equals to replacing some 1s in the matrix with 0s. If the tripped line isn't the shortest path between any two buses, the **Q** will not be influenced, otherwise the **Q** need to be recalculated.

And for system containing islands, there's no possibility to make all elements in the depth matrix to be1. The stopping rule is principally generated as:

The **k-1**$^{\mathbf{th}}$ depth matrix is equal to the **k**$^{\mathbf{th}}$ depth matrix, where **k**$\leq$ **Q**.

Proof: in the islanding case, all paths are lost between some bus-pairs. The largest iteration number **k** equals to the longest bus path among those shortest ones of all remained bus-pairs. If we assume all remained paths in the system as a group, it must be a subset of the paths group for the original system. Thus **k** is not larger than **Q**.

The final depth matrix will contain lots of blocks with elements inside each block are either all 0 or 1. From this we can easily find out how many islands are formed and how they forms.

Write the method in mathematical form:

$$A_o^{\,k} = [A^k]\Big|_{A^k_{i,j}>0 \Rightarrow A^k_{i,j}=1} = [A_o^{\,k-1} \cdot A]\Big|_{A^k_{i,j}>0 \Rightarrow A^k_{i,j}=1} \quad \mathbf{k = 1, 2, 3, \ldots, Q} \tag{2.14}$$

$$\text{with the stopping rule, if } \begin{cases} A^{k-1} = A^k \\ k \leq Q \end{cases} \tag{2.15}$$

Then there's isolation occurring in the system structure. The principle of this method is illustrated using the same test system shown in Fig. 2.4.

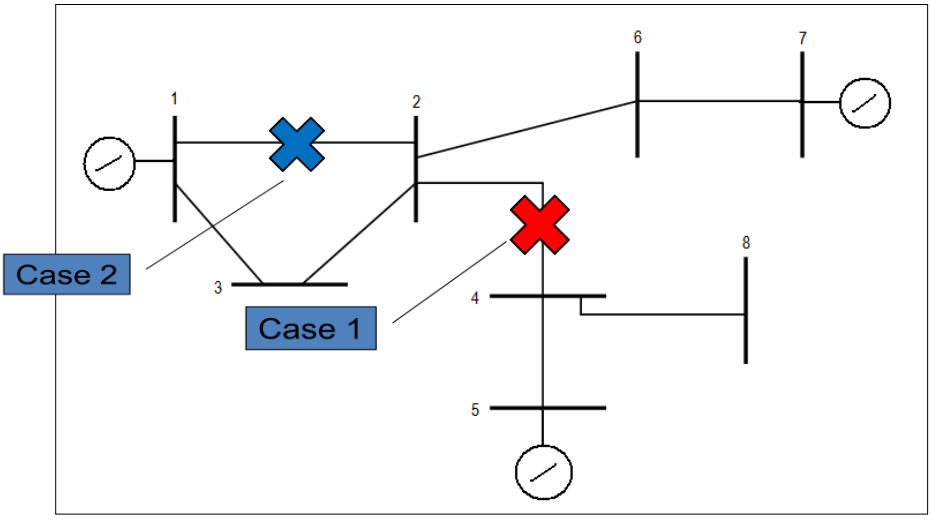

Figure 2.4: 8-bus 3-machine test system with branch disconnections

The system structure data can be expressed in two matrices:

Generator matrix: $G = [1 \quad 5 \quad 7]$;

Incidence matrix:

$$A = \begin{bmatrix} 1 & 1 & 1 & 0 & 0 & 0 & 0 & 0 \\ 1 & 1 & 1 & 1 & 0 & 1 & 0 & 0 \\ 1 & 1 & 1 & 0 & 0 & 0 & 0 & 0 \\ 0 & 1 & 0 & 1 & 1 & 0 & 0 & 1 \\ 0 & 0 & 0 & 1 & 1 & 0 & 0 & 0 \\ 0 & 1 & 0 & 0 & 0 & 1 & 1 & 0 \\ 0 & 0 & 0 & 0 & 0 & 1 & 1 & 0 \\ 0 & 0 & 0 & 1 & 0 & 0 & 0 & 1 \end{bmatrix};$$

The longest path: 5-4-2-6-7 or 8-4-2-6-7, so the **Q** = 4. The incidence matrix **A** needs four iterations (**Q** = 4) to reach full 1 matrix by multiplying itself.

The upper diagonal shows the connection conditions, there are 8 lines in the system and the total tripping combination is 255, if we only concern tripping 4 or fewer lines, the total combination number is 162.

When applying islanding analysis, we randomly trip 1 and 2 line(s) in the system:

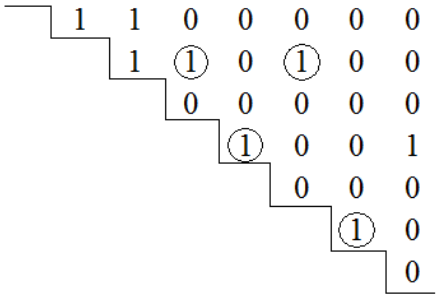

Tripping the line circled in the upper diagonal part of the incidence matrix will create an island while tripping others will not. Three cases are discussed below:

Case 1: Tripping line 2-4 in the system, this will cause 2 islands. When multiplying the incidence matrix, the 3rd depth matrix is equal to the 4th, which means the final depth matrix is reached. The 3rd depth matrix shows 4 blocks in the diagonal: Bus 1-3, 4-5, 6-7 and 8. The off-diagonal blocks show the relationships between each diagonal bus group. When elements are 1, this means the two blocks are in the same island, otherwise are not. This offers a way to distinguish islands. It's easy to find the system split into two islands: 1-3, 6, 7 and 4, 5, 8.

$$\underset{\text{none-zero}\to 1}{(C_1)^3} = \begin{bmatrix} 1 & 1 & 1 & 0 & 0 & 1 & 1 & 0 \\ 1 & 1 & 1 & 0 & 0 & 1 & 1 & 0 \\ 1 & 1 & 1 & 0 & 0 & 1 & 1 & 0 \\ 0 & 0 & 0 & 1 & 1 & 0 & 0 & 1 \\ 0 & 0 & 0 & 1 & 1 & 0 & 0 & 1 \\ 1 & 1 & 1 & 0 & 0 & 1 & 1 & 0 \\ 1 & 1 & 1 & 0 & 0 & 1 & 1 & 0 \\ 0 & 0 & 0 & 1 & 1 & 0 & 0 & 1 \end{bmatrix}$$

Case 2: Tripping line 1-2 in the system, this won't cause an island. The matrix ends up in full 1.

$$\underset{\text{none-zero}\to 1}{(C_2)^4} = \begin{bmatrix} 1 & 1 & 1 & 1 & 1 & 1 & 1 & 1 \\ 1 & 1 & 1 & 1 & 1 & 1 & 1 & 1 \\ 1 & 1 & 1 & 1 & 1 & 1 & 1 & 1 \\ 1 & 1 & 1 & 1 & 1 & 1 & 1 & 1 \\ 1 & 1 & 1 & 1 & 1 & 1 & 1 & 1 \\ 1 & 1 & 1 & 1 & 1 & 1 & 1 & 1 \\ 1 & 1 & 1 & 1 & 1 & 1 & 1 & 1 \\ 1 & 1 & 1 & 1 & 1 & 1 & 1 & 1 \end{bmatrix}$$

Case 3: Tripping line 1-2, 4-8 in the system. The generator matrix is used to ensure every island contains at least one generator thus make it an island. The computation stops at the 5th multiplying. It's easy to see the system is split into 2 parts: Bus 1-7 and 8. However checked with the generator matrix, Bus 8 is not a generator bus so no island is created.

Using this method, we can easily generate and identify any islanding cases by manually creating contingencies in a study system, regardless of the system size.

The islanding detecting strategy works with the system structure information. Failure to achieve a full-1 matrix demonstrates a physical structure separation in the system. If the exact structure of the power system is known and can be updated within micro-seconds (i.e. all breakers and branches status in the system are monitored by PMUs), this method itself could be an efficient tool in system islanding determination. However, in most power systems such information could not be obtained thoroughly or simultaneously, which means at the present time, we need to judge an islanding contingency with limited synchronized system measurements that could be monitored through the PMUs, such as voltage, current and real/reactive power variables.

2.1.3.2 The modified enumeration method in islanding contingencies formation

When starting the islanding simulation in a wide-area system, a variety of islanding locations are selected. The determination of the centers of the islanding in this study is considered with such options: 1) The electrical central points or major joints of the power system; 2) Areas with large load consumers and relatively vulnerable transmissions; 3) A subsystem where the major tie-lines to each other region radial in topology and geographically long; 4) Areas which have historical islanding contingencies /cascading hidden failures.

The involved islanding region size is another concern. In practice, the islanding contingencies are formed within certain range. Historically the islanding disturbance are majorly caused by bad weather or nature conditions like Lightning storms, hurricanes or extreme cool/hot weather; or cascading breaking down due to hidden failures or equipment failures. No matter which reason causes the disturbance, the isolated regions had their boundaries. For the environmental disaster cases, the region is generally quantified by the geographical distances of the buses in the wide area system; for the cascading failure caused cases, the region can be quantified by the electrical distances.

However both islanding factors can be alternatively described by converting them to the bus observation depth matrix. For a power system, based on the system structure and breaker status, the incidence matrix of the system is obtained. As mentioned in Section 2.1.3.1, the system observability matrix could be easily obtained by incidence matrix multiplication. The certain geographical and electrical distance could be equivalently converted by certain observation depth **n**. Changing the value of **n** indicates involving larger/smaller area geographically and/or implementing a longer/shorter hidden failure chain. More introduction of this method can be found in [29].

To simulate a potential islanding case in the study system, once locating the islanding center, the program trips one line at the boundary to test the system isolating condition at every single branch around the boundary, and then move to trip multiple lines. Multiple lines are randomly selected from the system which will create a huge number of combinations. The complete testing combinations for tripping up to 3 lines in a 1000 bus, 1500 branch system could be more than 500 million; which is not desirable for simulation. There are too many unreasonable combinations counted including some unreasonable combinations that may introduce an islanding condition. By applying the observation depth selection, the enumeration random branches tripping is limited only within certain observation depth, in other words, inside certain geographical and electrical distances. Those useless combinations are eliminated, tremendous time is saved. By setting observation depth **n** = 5, the combinations number decreases to around 50 thousand for the same system mentioned above.

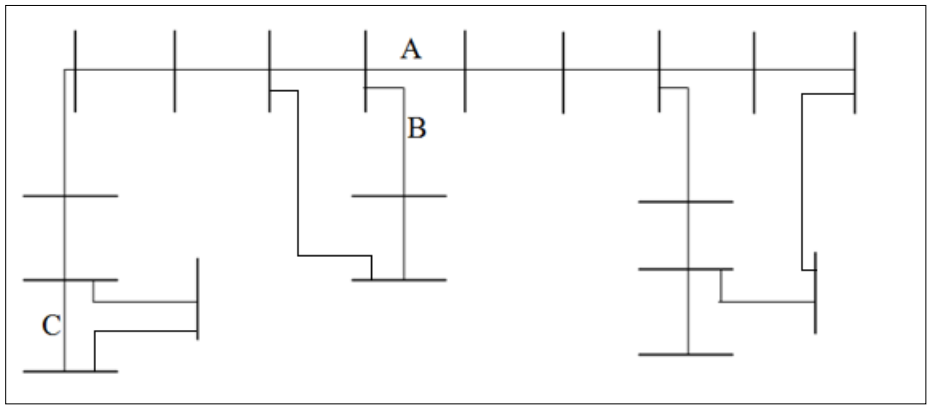

Figure 2.5: Various branch tripping locations

As shown in Fig. 2.5, for example, tripping line A will create an island in the system, tripping lines A and B will cause the same islanding case and this combination is reasonable because the geographic and electrical distances between the two lines are close; however tripping line A and C is a less-likely combination which leads to the same result but not realistic. By the

increase of the system scale, the unreasonable islanding combinations will increase significantly; the modified depth first method largely eliminates those cases by setting up a proper threshold for the line tripping range.

2.2 The Islanding Severity Index (ISI)

In this section, the concept and operation of the islanding severity index (ISI) is introduced. The ISI is a proposed method for ranking the system transient behavior and severity level of islanding contingencies. The ISI works as an additional tool to assist the DTs in islanding severity determination. The major computation and programming works of the index are done offline with the islanding database while the ISI works online to execute the severity computation and judgment at the same rate as the updating of measurements.

2.2.1 The Concept

In power system voltage and angle stability studies, an index method called Voltage Stability Index (VSI) is widely used. The VSI is generated from the basic power flow equation and/or energy functions. This method uses an Index that shows the system's stability condition and can be used to estimate the systems operating states. The mathematical expression of a VSI is often written as a polynomial containing the systems real-time measurements such as voltage magnitudes, phase angles, bus injected power and branch power flow values, etc. [30].

The index can be different by using different power system models and target parameters. The values of VSI are distinctly different in normal condition and contingencies for a power system. The changing process of the VSI values in the region from no loading condition to maximum permissible loading condition will also reflect the system's stability trend from stable to unstable. The point when system lose stability is called the optimal point (or diverge point) in VSI. Some of the indices apply normalizations using this optimal value of the index to maintain the index values between settled thresholds [30, 31].

Voltage magnitude is the most often used parameter in voltage stability index studies. A typical Voltage Stability Analysis considering voltage magnitude [31] is based on a simplified 2-bus Thevenin Equivalent power system with line resistance neglected. The approximate power flow equations through sending and receiving ends are obtained. So the P-V characteristic and voltage stability limit for power transfer at specific load bus are obtained from the transformation of the power flow equations.

A modified VSI method, Fast Voltage Stability Index (FVSI) [44] is based on the previous discussion about basic voltage stability index mentioned above. According to this method, some more approximations were made to simplify the system characteristics. The author only considered the relationship between the voltage magnitude and the reactive power at load receiving end.

Apart from voltage magnitude, other parameters can also be used for the investigation of power system stability. M. Nizam, A. Mohamed and A. Hussain developed a static method called power transfer stability index (PTSI) [45]. PTSI is based on the ratio of the apparent power transferred and the maximum power that can be transferred. To obtain the expression of the maximum apparent power, the authors use the load impedance derivative of the apparent power. The VSIs have been proved to be accurate and efficient in voltage stability application in many circumstances.

Some other VSI methods consider using the system admittance or impedance matrix rather than making equivalent transformation of the system. One method is Voltage Collapse Prediction Index (VCPI) [46]. This method requests the system network admittance matrix to be formed as an equation describing the voltage phasor at specific bus. The value of VCPI varies between 0 and 1. The closer the index is to 1 means the system is closer to lose its stability.

For the power system islanding stability concern, researchers face a similar problem which can be solved by analyzing system state variables and thresholds. However, there is no specific severity index for judging islanding cases yet. The islanding cases, which differ from the normal contingencies, show a large degree of diversity due to different system's structure and geographic characteristics. In some cases, the islanded region may contain balanced power generation and loads after the transients. This does not mean the region is stable, on the contrary, losing its interchange ability with the main grid; the system may become extremely vulnerable for further power oscillation. This has been proven by many cases listed in Section 1.1 and Appendix A. In such cases, while the system frequency was stable with or without applying under-/over-frequency protection scheme, the balance could only had been maintained for a few minutes before the new oscillation formed.

Such behavior may not be reflected from common system state variables for normal VSIs. While deciding the islanding severity, the transient power mismatches, the machines' power generation and the machines' inertia are selected as the state variables in the proposed method. The power mismatch is considered to be the essential state variable that hazards the islanding situation. An overwhelming power mismatch in the island transient will inevitably introduce oscillation and lead to an unstable island. The machines' power generation shows a margin of the island generation capacity in order to keep the stability. The machines' inertia time constant, as the neutral machine characteristics, could determine the final power re-dispatch in a longer time period.

The Islanding Severity Index is defined as two components:

1) The long term index: the summation of the power mismatch over the machines total inertia time constant in each isolated area.

$$m_{islanding}(ISI) = \sum_{i=1}^{N} \frac{M_i}{H_i} \text{ while } \quad H_i = \sum_{j=1}^{N_i} H_{ij} \tag{2.16}$$

$\mathbf{H_i}$ is the total inertia time constant of the isolated area **i**; $\mathbf{M_i}$ is the total power mismatch of the isolated area **i**; **N** is the number of isolated areas in the islanding contingency.

The machines' inertia time constant is used to compute the island's long-term stability because this machine characteristic determines the final power dispatch within the island after it survives the transient power and frequency oscillation. It may also reflect the system's reaction time to damp the power oscillation.

2) The instant index: the summation of the power mismatch over the machines total real power generation in each isolated area.

$$m_{islanding}(ISI) = \sum_{i=1}^{N} \frac{M_i}{P_i} \text{ while } P_i = \sum_{j=1}^{N_i} P_{ij} \tag{2.17}$$

$\mathbf{P_i}$ is the real power generation in the isolated area **i**. The overall power generation of the island shows its capacity from the system margin to overcome the power oscillation in real time. If the transient power mismatch is too large for the machines to handle, the island voltage stability may collapse.

The state variables used in the index computation are partly from the real time measurements, partly from pre-saved system data. When the system is under normal operation, the generator power outputs are stable and constant. When the islanding contingency occurs, the power output measurements from wide area measuring units are collected and sent to the online module and the index is computed simultaneously. The maximum index values are reached at the contingency occurring point and selected. As its name indicates, the instant index shows the instantaneous impact of the isolation to the main grid and how severe it could be during the

transients. For a very short time, while the protection scheme has not reacted to the contingency, this index is capable to determine the maximum hazard the contingency could cause. The long term severity index helps determine how severely the system's operating status will vary from the normal operating criteria with all possible protection schemes carried out after certain period of time. Excessive generations and/or less-important loads are tripped, branches are tempted to reclose and switching shunts are put into use to balance the voltage magnitudes and angles.

This index is very useful as it allows researchers to study the islanding response of certain system quickly. For any study system, after analyzing potential islanding cases the island severity could be computed for all conditions. The stability of the islands in long term with certain protection scheme applied could also be estimated. The ISI could update itself with changing measurements and status. In the real world, the continuous updating of the long term and instant ISI will benefit from the installation of phasor measurement units and advanced communication system.

2.2.2 Adapted Real Time ISI Computation

In principle, the ISI could be computed in real time if important measurements such as generator outputs and load conditions are obtained simultaneously. In some situations, the only data source is local real time measurements as voltage, current phasor, load flows and frequencies. For the dynamic characteristics of the units, we have following formulas describing the transient behaviors of the units at the generator bus:

$$\omega = \frac{\mathrm{d}\theta}{\mathrm{dt}},\ \mathrm{f} = \frac{\omega}{2\pi} \qquad (2.18)$$

$$\frac{\mathrm{d}\omega}{\mathrm{dt}} = \frac{1}{2\mathrm{H}}(\mathrm{T_m} - \mathrm{T_e}) = \frac{1}{2\mathrm{H}}(\mathrm{T_m} - \mathrm{P_e})$$

While θ is the machine angle; ω is the machine rotor angle velocity; **H** is the machine's inertia time constant; $\mathbf{T_m}$, $\mathbf{T_e}$ are the machine's mechanic and electrical torque; $\mathbf{P_e}$ is the machine's electrical load.

When a contingency occurs and the island forms, the transient power flow oscillates and re-dispatches within the isolated area. The sudden unmatched power between generation and loads leads to an unbalance between the mechanical power and electrical power, which is finally reflected as an instantaneously unmatched torque.

Assuming the relationship between the two unbalances is:

$$P_{GEN}(t) - P_{loads}(t) = K \cdot (T_m(t) - P_e(t)) = K \cdot (T_m(t) - T_e(t)) \tag{2.19}$$

K is the power unbalance coefficient, which remains constant in the computation and has no unit, so

$$ISI\_longterm(t) = \sum_{i=1}^{N} \frac{M_i(t)}{H_i} = \sum_{i=1}^{N} \left| \frac{P_{GEN\_i}(t) - P_{load\_i}(t)}{H_i} \right|$$

$$= \sum_{i=1}^{N} \left| \frac{K_i}{H_i} \left| T_m(t) - T_e(t) \right|_i \right| = \sum_{i=1}^{N} \frac{K_i}{H_i} \cdot 2H_i \frac{d\omega_i}{dt} = \sum_{i=1}^{N} 2K_i \frac{d\omega_i}{dt} = \sum_{i=1}^{N} 2K_i \frac{d^2\theta_i}{dt^2} \tag{2.20}$$

The long-term ISI is transformed into a summation of the **2K** times the time derivative of the generator angle velocity, or the frequency change in respect of the time at isolated area **i**. At the same time, we have:

$$ISI\_instant = \sum_{i=1}^{N} \frac{M_i}{P_i} = \sum_{i=1}^{N} \left| \frac{P_{GEN\_i} - P_{load\_i}}{P_{GEN\_i}} \right| = \sum_{i=1}^{N} \left| \frac{K_i}{P_{GEN\_i}} \left| T_m - T_e \right|_i \right|$$

$$= \sum_{i=1}^{N} \frac{H_i}{P_{GEN\_i}} \cdot ISI\_longterm_i \tag{2.21}$$

The modified index can be updated with system parameters like generator outputs recorded by CT/PTs or PMUs at stations and time derivatives of generator angles recorded by phasor measurement units.

It can be seen that when apply the adapted ISI method, the long term ISI becomes the summation of the weighted (**2K**) frequency changes of all islands in the disturbance. In other words, the severity of the islanding disturbance is in direct ratio to the frequency change over time. If the system has PMUs installed in the island, they will be the best devices to monitor the frequency and to estimate the islanding severity. Or if the direct frequency measurements are not reached, the frequency changes could be computed using units angle variables inside the islands.

The proposed decision tree algorithm has a function to estimate island's severity level using the database records. This ISI works as an additional strategy. The joint of the two methods will be introduced in Chapter Four.

2.3 The Optimal PMU Placements using BIPA

In this section, another issue related to the islanding disturbance monitoring and detection is introduced. That is, an optimal PMU placement strategy using binary integer programming algorithm with the consideration of system generator bus coverage and redundancy problems.

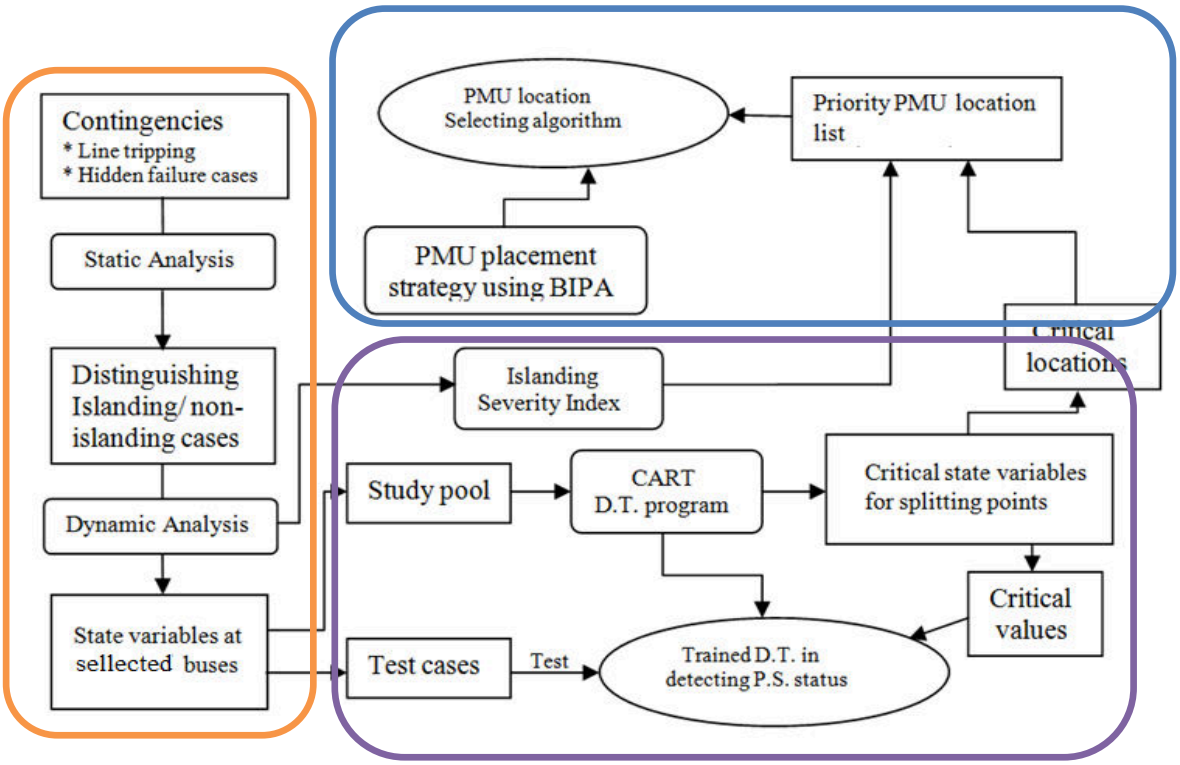

Figure 2.6: The Islanding Analysis Method

Fig. 2.6 has shown the whole picture of the islanding analysis method. The brown circled process is the offline islanding database creation stage, which has been demonstrated in Section 2.1.3; the purple circled process is the main body of the DT algorithm for online islanding detecting and severity assessment. While in the tree forming process, the major splitting points can be used to judge the corresponding critical monitoring locations in the study system. This could be used for PMU placement locations with islanding consideration.

If we want to design the optimal PMU placement strategy, there are many other aspects need to take consideration and many rules to be followed. Some major optimal PMU placement methods are introduced in the following section.

2.3.1 The Introduction of PMU Placement Methods

The invention and implementation of time synchronized PMUs in power systems have brought a revolutionary improvement in power system monitoring, state estimation, fault detecting, and protection, etc. The PMU monitors the behaviors of the buses and branches by recording time-stamped measurements with very accurate techniques where the PMU is located and within the one-step-away region from the PMU.

To achieve a full observability of the system, a set of PMUs need to be installed to form coverage of all system buses. The locations and number of PMUs are not identical. One PMU set with full coverage and least PMU number is called an optimal set for the power system. Optimal sets may not be identical either. Many methods were raised to deciding the optimal PMU set for power systems, including genetic algorithm, Tabu search and matrix reduction algorithm[22, 34].

In 1993, Baldwin & Mili introduced a dual search algorithm consisting of the Simulated Annealing based method and a modified bisecting search [35] to find the optimal placement of PMUs sets. They concluded that PMUs are required only in 1/4 to 1/3 of the network buses to ensure a full observability.

The genetic algorithm (GA) is a search heuristic that mimics the process of natural evolution. It is widely used to generate useful solutions to optimization and search problems [49]. The genetic algorithm works out the best solutions to optimization problems by applying evolution through generations of strings which encode candidate solutions. The algorithm usually starts the evolution from a population of randomly generated individuals. It evaluates the

fitness of all individuals at present generation and selects the ones with best fitness to grow the new generation. This iteration will continue until either a maximum number of generations have been produced, or a satisfactory fitness has been reached for the solution.

Tabu search is a local search method created by Fred W. Glover and in 1986 and formalized in 1989 [47, 48], local searches take a potential solution to a problem and compare its immediate neighbors to determine an improved solution. This method could face the problem that many solutions are equal in fit so it may stop in the middle of optimization. Tabu search uses memory structures in order to avoid repeatedly generating routes. This method can response to certain stopping criterion or rules and is good for combinatorial optimization problems like PMU optimal placements.

In another research, Nuqui used spanning trees of the power system graph to find the optimal location of PMUs and extended the application of simulated annealing for the communication facility restrictions[36].

Those methods have their advantages: they are fast and computable, for a wide-area system with thousands of buses, which the enumeration method can't be applied; those methods can still work because of their recursive characteristics; the results of these methods are fairly accurate too. Their shortages are also distinct: the PMU set decided by these methods may not actually be the true optimal PMU set but surrogates very close to the optimal. However with the increase of the system scale, the accuracy of the results will decrease. Secondly the starting point for those methods is essential according to their characteristics; a change of starting point will lead to completely different results for PMU locations. So the placement is not repeatable when the analytics is repeated. The last thing is those methods are difficult to understand and program.

They contain many steps and selections in each step so that it's hard for people to implement them into practical usages.

The proposed method is using the binary integer programming method, which is a kind of binary enumeration method that covers every possible PMU placement combination, to effectively derive the optimal placement.

2.3.2 Some Definition and Backgrounds in PMU Observability

1) Power System Incidence Matrix [**A**]

In power systems, the incidence matrix is a reversible symmetrical matrix that indicates the connecting condition of a system. Its scale is depended on the bus number in the system. It has all its diagonal elements (bus elements) equaled to 1 which means the bus is connected to the system. For each two buses **i**, **j** (**i≠ j**) which have transmission line connected, the corresponding elements in the A matrix $\mathbf{A_{i,j}}$ **,** $\mathbf{A_{j,i}}$ (branch elements) are also 1. Zero-valued element $\mathbf{A_{x,y}}$ refers to the bus **X** doesn't have a connection with bus **Y**. The incidence matrix is symmetrical. Line vector $\mathbf{A_m}$ refers to Bus **m**'s connection status with all system buses.

2) PMU Observability Matrix **O** (N by 1 vector)

PMU observability for certain bus **K** implementing **m** PMUs is an N by 1 column vector which is m times the $\mathbf{K^{th}}$ column in the incidence matrix. And the PMU observability matrix is the sum of each bus observability vector with PMUs installed:

$$O = \sum_i m_i \cdot A_i \tag{2.22}$$

while: **i** -**ith** bus that with one or more PMUs installed;

$\mathbf{m_i}$- number of PMUs installed at **ith** bus;

$\mathbf{A_i}$ -**ith** column of the power system incidence matrix.

3) Observability Redundancy and Observability Region

Observability redundancy is the extent how the buses in the systems are monitored by PMUs. Each bus has its own observability depth which is the corresponding element in the observability matrix, when the observability redundancy is:

a) = 0: the bus is not monitored by any PMU;

b) = 1: the bus is monitored by one PMU;

c) >1: the bus is monitored by multiple PMUs.

Observability region is the area monitored by PMUs. It can be increased by adding new PMUs at un-monitored area.

2.3.3 Theorems and Assumptions in PMU Placement

In PMU placement scheme, one bus in the power system is defined as observed when a PMU is directly located at that bus or at its neighbor bus which has at least one branch connected to that bus. Otherwise, that bus is defined as unobserved. There's one exception when there are only zero-injection buses between the PMU located bus and the destination bus, that bus might be observed. One bus can be observed by multiple PMUs and the number of reached PMUs is defined as the PMU observability at certain bus.

When every bus in a power system is at least observed by one PMU, we may say a complete observability is achieved. The PMU set to achieve a complete observability with least PMU quantity is called an optimal PMU set. The optimal PMU set for a power system may not be unique.

According to the principle of PMU placement and the power system topology, we can introduce the following theorems and assumptions:

1) The PMU observability at certain bus can be increased either by placing PMUs at that bus or its neighbor buses which have no PMUs installed yet or placing additional PMUs at that bus or its neighbor buses that already have a PMU installed. The difference for the two conditions is that for the former case, the implementation of the PMU may increase the power system's observability region (more buses are observed by placing the PMU) and the latter one is not. And we can easily obtain the maximum bus observability with none of the PMUs placed at the same bus equals to one plus the number of branches connected to that bus.

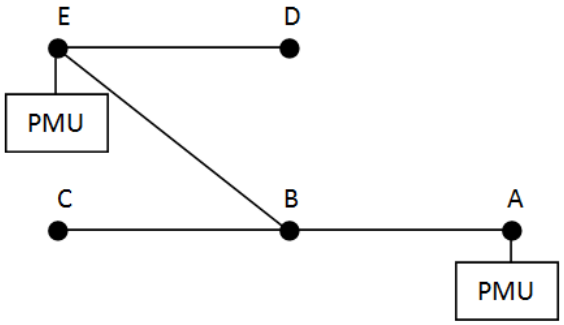

Figure 2.7: The PMU Observability Increase

Consider a system network shown in Fig. 2.7, Bus-B is monitored by PMUs at Bus-A and E, the observability is 2. Now we want to increase the observability to 3. We either can put a PMU at Bus-B or C or add one at Bus-A and E. The differences between two methods listed in the table.

TABLE 2.2: PMU OBSERVABILITY INCREASE METHODS

Differences	Place a PMU at PMU-existed Bus	Place a PMU at non-PMU-existed Bus
System observability region	Doesn't increase when new PMU added	May increase when new PMU added
certain bus is removed from the system	Loss all observability from that bus	Keep observability from other buses

The maximum bus observability with none of the PMUs placed at the same bus equals to one plus the number of branches connected to that bus.

2)The solution to an optimal PMU placement problem must be a PMU set with all PMUs placed at different buses.

Proof: when a PMU is placed at PMU-existing Bus, the system observability region doesn't increase. If a PMU set contains overlapped PMUs, it can be removed from the set without losing any observability region.

3) If a PMU placement set $X_1 = \{a_{11} \quad a_{12} \quad \dots \quad a_{1m}\}$, is a solution to the optimal PMU placement problem of the system, any subset $X_{1K} \subseteq X_1$ is an optimal PMU placement of the region which is observed by the PMUs in the subset $\mathbf{X_{1K}}$.

Proof: if there exists one subset $\mathbf{X_{1K}}$ is not the optimal placement of the region that is observed by the PMUs in $\mathbf{X_{1K}}$, the optimal PMU set in that area, say $\boldsymbol{X'_{1K}}$ can replace the part of $\mathbf{X_{1K}}$ in set $\mathbf{X_1}$ and a new optimal set with fewer PMUs is obtained, which is impossible.

4) If a system has its optimal PMU placement set containing m PMUs. To achieve an observability redundancy **B**, the minimal number of PMUs needed is a summation of a group of subsets of the optimal set. The minimal PMUs needed for $\mathbf{B^{th}}$ observability redundancy will be no larger than $B \cdot m$.

Assume existing a PMU placement set

$X_1 = \{a_{11} \quad a_{12} \quad ... \quad a_{1m}\}$ **m** is the number of PMUs

is a solution to the optimal PMU placement problem of the N-bus system. We can solve the redundancy problem following the sequence below:

a) Solve the 1st dimension of redundancy **B**. The result will be the same as the optimal PMU set of the system. Then we calculate the observability redundancy based on the optimal set, subtracting it from the redundancy requirement, obtaining the new redundancy requirement for each bus. (Some bus's redundancy requirement may be satisfied in this step then the undated requirement will become zero.)

b) Solve the 2nd dimension of the redundancy. This is equal to solve the optimal PMU set of the undated redundancy problem. According to Theorem 3, the solution will be a subset of the optimal PMU set of the system. Calculate the observability redundancy based on the optimal subset, subtracting it from the redundancy requirement obtained from last step, obtaining the new redundancy requirement.

c) Repeat step b) until the redundancy requirement for each bus becomes zero.

The minimal PMUs needed for **B**th observability redundancy will be no larger than $B \cdot m$. One extreme condition is that under the optimal PMU set each bus is monitored with only one PMU. Then the minimal PMU number will definitely be $B \cdot m$. If the system only has one optimal solution, the $B \cdot m$ PMUs will be at the m buses and each bus will place B PMUs; on the other hand, if the system has more than **B** optimal solutions, the $B \cdot m$ PMUs can be at $B \cdot m$ different buses, no overlapping occurs.

If we consider all PMUs are placed at different buses and the solution is **P**. $P \geq B \cdot m$.

5) The converse proposition of 3) is not always correct. If we split the system into small islands, the combination of the optimal PMU sets in each island may not be the optimal solution to the whole system. The two sets are equal only when all the boundaries between each island are coverage boundaries of the PMUs in the optimal PMU set of the whole system. Otherwise a solution close to the optimal one will be obtained.

2.3.4 The Modified Bus Reduction and PMU Placement Scheme

In power system PMU placement study, bus reduction is a very useful tool in computation simplification especially when dealing with large scale system. The power system models in present study contain virtual buses and zero-injection buses. Virtual buses refer to the buses added into the power system model for modeling use but do not exist in the real world. Fig. 2.8 shows the reduction of virtual buses (the shorter buses are virtual buses and they are removed from the system after reduction).

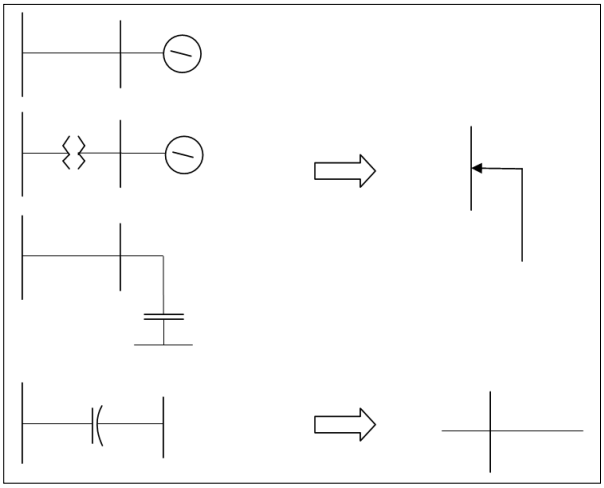

Figure 2.8: Virtual bus reduction

In PMU placement computation, a path with pure zero-injection buses doesn't influence the observability of PMUs at one end. And all zero-injection buses with only two branches connected can be removed from the system.

The reduction methods above could be applied to all power system models and all nodes are treated equally independent of their connection to generators. Similarly, the previous methods mentioned in Section 1.3.2 treats all nodes in the power system indifferently. For a simplified computation, they require a bus reduction before starting the computation. The ultimate goal for them is to generate the optimal PMU sets. So the PMU implementation spots may locate at any place that satisfies the optimal computation. Sometimes, these spots are accurate but vulnerable under islanding disturbances. Fig. 2.9 shows a dangerous example. The PMU located bus is capable to monitor the right generator bus when the system is united; all zero-injection buses are removed during bus reduction process. However in the real world when the right part is isolated, its connection breaks down and the observability to generation is lost.

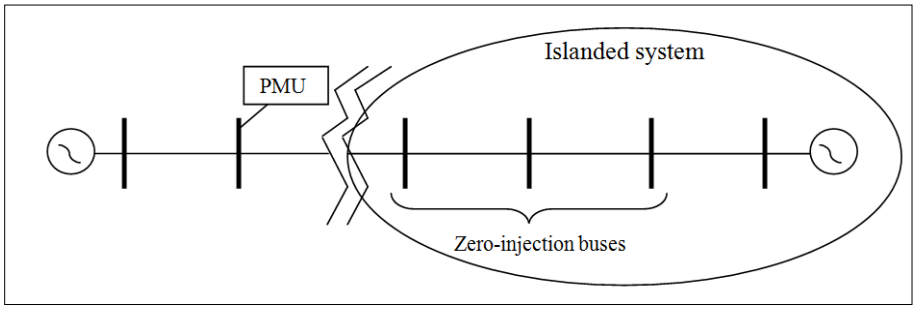

Figure 2.9: Traditional PMU placement loses observability in islanding case

Some specific restrictive options need to be added to the existing reduction scheme to meet this problem. In practical, the islanding contingencies are formed within certain range. It's analyzed with the formation of the islanding contingency. Historically the islanding disturbance are primarily caused by bad weather or nature phenomena like Lightning storms, hurricanes or

extreme cool/hot weather; or cascading breaking down due to hidden failures or equipment failures. No matter which reason causes the disturbance, the most directly involved buses and branches sit within a certain region. For the environmental disaster caused cases, the region is mostly determined by the geographical distances of the buses in the wide area system; for the cascading failure caused cases, the region is generally decided by the electrical distances. Finding the optimal PMU set under those restrictions is still our goal. These restrictive options may include:

1) Certain zero-injection buses are preserved in the system model reduction procedure because their geographical information in the real world might be essential in the islanding analysis criteria;

2) To monitor a generator bus, a PMU need to be placed at the near end at the generator bus rather than a far distance bus. This prevents the cases described in Fig. 2.8.

2.3.5 Binary Integer Programming Algorithm (BIPA)

Traditional PMU placement methods can be divided into two groups: enumeration method and zero-regressive methods as simulated annealing strategy, genetic algorithm and Tabu search. Binary integer programming method belongs to the former however, it converts the placement selection from graphical search to binary and linearized problem, saving enormous computation time.

To find the minimal PMUs needed, for the system observability problem, the expression of the method can be written as:

$$\begin{aligned} &\min\ f' \cdot X \\ &\text{while } A \cdot X \geq b \end{aligned} \tag{2.23}$$

In the equation:

A- the system incidence matrix, N by N; it has all its diagonal elements (bus elements) equaled to 1 which means the bus is connected to the system. For each two buses **i**, **j** ($i \neq j$) which have transmission line connected, the corresponding elements in the **A** matrix $\mathbf{A_{i,j}}$, $\mathbf{A_{j,i}}$ (branch elements) are also 1. Zero-valued element $\mathbf{A_{x,y}}$ refers to the bus **X** doesn't have a connection with bus **Y**;

X - the PMU placement vector, N by 1; each element representing the number of PMUs need to be installed in the corresponding bus;

b – the objective vector; N by 1, with each element representing the number of PMUs the corresponding bus is observed by;

f - the linear inequality constraints vector; it's an N by 1 vector with each element is equal to 1.

For optimal PMU placement, the problem turns to:

$$\begin{aligned} &\min\ f'\cdot X \\ &\text{While}\ \ A\cdot X \geq b\ \ b = \begin{bmatrix}1 & 1 & \dots & 1\end{bmatrix}^T \end{aligned} \tag{2.24}$$

According to the Theorem 2, in an optimal PMU placement problem, **X** will only contain 0 or 1. The Problem is purely binary.

Restrictive conditions can be added into the binary problem, and then the problem turns to:

$$\begin{aligned} &\min\ f'\cdot X \\ &\text{while}\quad A\cdot X \geq b \\ &\qquad A_{EQ}\cdot X = b_{EQ}\ \ A_{EQ}, b_{EQ}\ \text{are restrictive matrices} \end{aligned} \tag{2.25}$$

When the redundancy is considered, **X** and **b** may contain values larger than 1. When this happens, according to the Theorem 4, **b** can be separated into several binary vectors which are

used to calculate optimal PMU sets after each update of the redundancy requirements. And for **b**, there will be a solution ***X'*** as the optimal PMU set. The summation of all ***X'*** vectors will be the system's optimal solution to the redundancy problem.

The binary integer programming method separates the redundancy problem into iterations of optimal problems. For a system redundancy of **K**:

$$\text{Stage 1: } \min f' \cdot X_1 \qquad b = K \cdot [1 \quad 1 \quad ... \quad 1]^T \tag{2.26}$$

$$\text{while } A \cdot X_1 \geq b_1 \qquad b_1 = [1 \quad 1 \quad ... \quad 1]^T$$

$$O_1 = \sum_i m_i \cdot A_i, i \in \{X_1\} \; b_2 = b - O_1$$

Stage 2: $\min f' \cdot X_2$

while $A \cdot X_2 \geq b_2'$ b_2' is the optimal requirement for the same system area of $\mathbf{b_2}$

$$O_2 = \sum_i m_i \cdot A_i, i \in \{X_2\} \; b_3 = b_2 - O_2$$

Repeat stage 1 and 2 until all elements in $\mathbf{b_j} = 0$

$$\text{Then} \quad X = \sum_j X_j \tag{2.27}$$

The binary programming method in solving PMU placement problem has apparent advantages:

1) Fastness; the time for PMU placement calculation using enumeration method is extremely large. It is even impossible using enumeration method in large scale system (1000 bus and more) due to the extreme large number of combinations.

2) Accuracy; the enumeration method is the most accurate method. It can find out all optimal combinations for any settled requirement. Any other methods, like simulated annealing strategy, genetic algorithm or Tabu search may not return the optimal solution in one run because the optimal solution is strongly related with the starting point. However, the binary programming

method, due to its simplicity, could solve the large scale system problem and return the optimal solution obtained from binary level.

3) Simpler to program; all data are converted into binary matrices that any mathematical software like MATLAB can easily process and use to solve the problem.

CHAPTER 3: SIMULATIONS AND RESULTS

3.1 Testing Results on Simulated Islanding Database

The strategies related to the islanding contingency database formation have been tested on several study systems, including IEEE-14, 30, 57, 118, 300, WECC-128, East coast full-loop system, etc. The details of the study system models can be found in Appendix B.

3.1.1 Test on System Islanding Detecting Strategy

The system islanding detecting strategy has been tested using multiple systems and proven to be correct and accurate. Its concept and operating procedures on one specific 8-bus system example are demonstrated in Section 2.1.3.1. The logic of building up the islanding detecting strategy is Fig. 3.1:

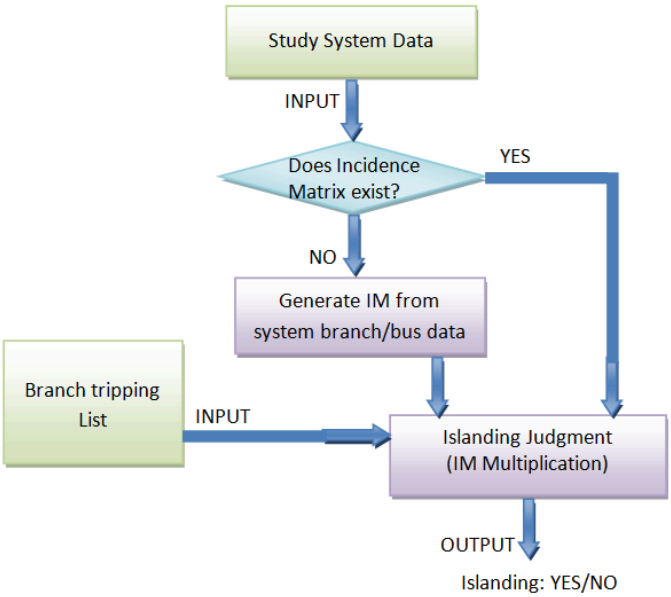

Figure 3.1: Islanding detecting Strategy Logics

The Input for the detecting module contains two parts: one is the study system static data that describes the system in stationary situation (no dynamic data needed); the other one is the branch tripping list which includes all tripping conditions need to be tested in the study system. The program reads in the system data and save it into its working space. Then it searches for the system incidence matrix (IM). If the IM does not exist, the program will generate the IM from system branch and bus data. In the next stage, the IM and the branch tripping list are delivered to the Islanding Judgment module and the IM computation is applied. The outputs generated from this module include the islanding condition and a brief summary about the size of the generation and loads inside the island.

3.1.2 Test on the modified enumeration method

The coverage of the modified depth first method has been tested and compared to the enumeration method. The test results are listed in TABLE 3.1 [29].

TABLE 3.1: COVERAGE TEST FOR DEPTH FIRST METHOD [29]

Test Model (Max. tripping = 3)	**Enumeration Method**		**Modified Depth First Method**		
			Depth = 2		
	Combos tested	Islanding case formed	Combos tested	Islands formed	Coverage%
IEEE-14	1350	253	999	143	56.52
IEEE-30	11521	1024	3246	245	23.93
IEEE-57	79157	80	6434	20	25
IEEE-118 (up 2 lines)	16110	890	2185	49	5.51
IEEE-300 (up 2 lines)	83845	13786	4073	513	3.72

TABLE 3.1, CONTINUED [29]

Modified Depth First Method								
Depth = 3			Depth = 4			Depth = 5		
Combos tested	Islands formed	Coverage %	Combos tested	Islands formed	Coverage %	Combos tested	Islands formed	Coverage %
1343	246	97.2	1350	253	100	-	-	-

8414	701	68.5	11136	963	94.0	11521	1024	100
19246	34	42.5	37219	49	61.3	54882	64	80
3976	97	10.9	5964	182	20.5	8092	286	32.1
7450	1039	7.5	11865	1660	14.0	17048	2760	20.0

The test results illustrate that, while applied in small scale system, the modified enumeration method (the depth first method) is a good substitute for the enumeration method. When the system complexity increases, more unreasonable combinations are created through computation and needed to be disregarded. While taking more time in computation, the enumeration method could not distinguish them efficiently. On the other hand, the modified depth first method could concentrate its work on forming islands in the given region, which prevents recording the unreasonable combinations and saves enormous time. Taking the IEEE-118 system as an example, when applying the enumeration method, it will take more than 1 day for computing the islanding combos caused by triple-line tripping. While setting the observability depth to 4 in modified depth first method, 182 cases are recorded for tripping up to 2 lines and 7,412 cases for tripping up to 3 lines. And the total computation time is 15 minutes.

3.1.3 Tests on DT based Islanding Detection

3.1.3.1 Study System Description

The decision tree algorithm has been carried out on several system models for testing. The results showed that this method works very well with large scale full loop systems. One of the major study systems used is a modified MMWG 57,000 Bus Eastern Coast Power Grids model. The selection of islanding locations is made on the system model within Dominion Virginia Power (DVP) territory. The Virginia power system territory characteristics have been introduced in Chapter 1. In this stage, a total number of 190 islanding contingency cases inside the DVP are selected, generated and recorded, with 300 non-islanding contingency and normal

operating cases to form the database (100 normal operation cases; 100 short circuit, 100 rapid load changing and line tripping cases). The dynamic simulations are done using Python compiled PSS\E (32.03 version).

As discussed in previous sections, to simulate the practical situations in a wide area system, only measurements from the highest voltage transmission networks are considered. The channels of the simulation outputs are the voltage and current phasor (real time load flow) measurements at the 500kV level buses inside the DVP system.

A) The DVP Area Model Revision of the MMWG 57,000 Bus System

When the MMWG model is modified for simulations, some revisions of the DVP system are adopted for a better precision. Presently, the most accurate PSS\e models of the DVP area are six static load flow cases with annual differences of loads, generations and topologies. On the other hand, the MMWG file, which is a 2008 load version, contains a Dominion transmission network with simplified topology and dynamic data. Some modifications are adopted between the MMWG 2008 model and the 2011/ 2012 summer load models.

Revisions include:

1) Using the 2011/2012 DVP system topology to replace the 2008 simplified DVP subsystem in the MMWG model;
2) Revising the boundary conditions and tie-lines, adding existing tie-lines which were neglected in the MMWG model;
3) Modifying some system parameters and state variables in the MMWG model;
4) Building up the new dynamic file and conversion options for dynamic simulations.

Tables 3.2 and 3.3 list the differences of the two models at the DVP boundary and bus numbers:

TABLE 3.2: STUDY SYSTEM TIELINE COMPARISON

Tie-line Comparison	2008 MMWG	2011/2012 Summer load
DVP – PJ&M	1 branch	1 branch
DVP – PEPCO	1 branch, simplified	1 branch
DVP – AP	7 branches	10 branches
DVP – AEP	10 branches	10 branches
DVP – CPLE	7 branches, simplified	7 branches

TABLE 3.3: STUDY SYSTEM BUS COMPARISON

		2009_Nofull	2011_Summer	2012_Summer
DVP Total		886 Buses 23 To Buses	1022 Buses 24 To Buses	1032 Buses 24 To Buses
DVP Region	500KV	26	31	31
	230KV	284	333	341
	138KV	12	14	14
	115KV	383	448	449
	69KV	35	36	36
	34.5KV	2	3	3
	13.2-26KV	124	157	157
Generator bus Comparison	Total	156	163	163
	230KV	5	6	6
	138KV	1	1	1
	115KV	11	9	9
	26KV	0	1	1
	25KV	2	2	2
	24KV	4	4	4
	22KV	11	12	12
	20.5KV	6	6	6
	20KV	1	1	1
	18KV	23	26	26
	14.4KV	8	8	8
	13.8KV	77	77	77
	13.2KV	7	7	7

The islanding contingency database is created mainly to testify the decision tree algorithm in islanding assessment. We use the modified 2011 summer case model. The 2012

summer case model is used for further research that will be introduced in later sections and next chapter.

B) The Islanding Database Case Selection

B.1 Islanding Contingency Cases Selection

While selecting the islanded area, we started a thorough search in the DVP territory. The major concerned possible islanding centers are:

1) The electrical central points in the Dominion system;

2) Areas with large load consumers and relatively vulnerable transmissions;

3) Some regions in the DVP that the connection is radial in topology or geographically long;

4) Some areas close to the Atlantic coast.

Once the islanding center is located, the program trips one line at the boundary to test the system isolating condition at every single branch around the boundary, and then move to trip multiple lines. As we discussed in Chapter 1, the Virginia Power System is analyzed as "some portions of the transmission system are more heavily loaded than others. This may become the major weak point to the system in case it splits into parts because the islanded area may face unbalance generation-load situations. At the same time, The Virginia Power system is along the east coast of the United States, and is affected by windstorm and thunder storms." The test results show one obvious pattern that in many islanding cases, tripping 2 or 3 branches within a small distance will make certain region in the DVP isolated. This in some extent demonstrates the radial topology structure in certain part of the DVP system is vulnerable to islanding situations.

Some islanding cases obtained through the islanding detection strategy and the modified depth method is listed in TABLE 3.4.

TABLE 3.4: SELECTED SIMULATED ISLANDING CASES

Case number	Lines Tripping Combo	Islanded Buses	Island Generation	Island Loads	Island Gen ID
1	314579-314583	314579, 314591, 314605, 314627, 315136, 315137, 315138	165+j18.3	69.718 +j29.931	315136, 315137, 315138
2	314150-314212 314218-314222	314212, 314215, 314222, 315043, 315044, 315045, 315046, 315047, 315048	606+j74.4	49.771 +j21.913	315043, 315044, 315045, 315046, 315047, 315048
3	314232-314766 314745-314777	314766, 314777, 315177, 315178, 315179, 315180	218-j11.2	19.085 +j3.254	315177, 315178, 315179, 315180
4	314236-314289 314253-314257	314253, 314289, 315067, 315068, 315069, 315070	348+j84.8	31.979 +j11.118	315067, 315068, 315069, 315070
5	314276-314339 314307-314311	314311, 314339, 315083, 315084, 315085, 315086	210+j14.8	40.016 +j8.604	315083, 315084, 315085, 315086
6	314579-314583 314579-314591	314579, 314605, 314627, 315136, 315137, 315138	165+j18.3	41.331 +j20.864	315136, 315137, 315138
7	314579-314583 314611-315139	314579, 314591, 314605, 314627, 315136, 315137, 315138; 315139	275+j9.9	69.718 +j29.931	315136, 315137, 315138, 315139
8	314579-314583 314611-315141	314579, 314591, 314605, 314627, 315136, 315137, 315138; 315141	275+j9.9	69.718 +j29.931	315136, 315137, 315138, 315141
9	314747-314744 314763-314774	314746, 314744, 314748, 314754, 314762, 314763, 314868, 315171, 315170	227-j12.6	71.44 +j24.262	315171, 315170
10	314524-314541 314526-314534	314534, 314541, 314826, 314827, 315115	67.2+j1	11.898 -j1.886	314541, 315115
11	314067-314068 314074-314094	314067, 314070, 314094, 315001, 315002	98-j12.4	151.496 +j44.532	315001, 315002
12	314666-314689 314694-314712	314667, 314671, 314515, 314666, 314700, 314705, 314712, 314348, 314354, 314670, 314680, 314685, 314727, 314728, 314729, 314730, 314731, 314732, 314733, 314734, 314735, 314736, 314737, 314738, 314739, 314740, 314789, 315156, 315165, 315166	147.5-j11.9	78.362 +j21.696	315156, 315165, 315166

The major transmission voltages in the DVP are 500kV, 230kV and 115kV. The DVP system contains (31) 500kV buses, (349) 230kV buses and (449) 115kV buses. Each voltage level composes its own transmission network and exchanges power at major substations. The 500kV network is interconnected and considered robust. There are certain parts at 230/115kV that are radial and easy to be separated. One big composition of the islanding cases occurs at the low voltage transmission (230/115kV) / distribution (69/35kV) and transformation (13.2 - 22.5kV) networks surrounding certain power plants.

Another point needs to be noticed in the islanding case generation process, is that there are some cases that lead to islanding contingencies in the simulation however in the real system

that they may be prevented by the Dominion's protection schemes for plants. In the first stage, we selected 190 cases by tripping up to 3 branches in the study system.

B.2 Non-Islanding Simulation Cases Selection

The non-islanding database is composed of such types of system simulations: normal operation cases with varying load conditions; short circuit fault cases; rapid load changing cases and line tripping cases.

The normal operation cases reflect the daily operation conditions of the study system. We start from the summer peak load model and randomly apply load change at 10% of the load buses in the DVP. The load change range is within [90%, 110%];

Rapid load change cases occur at the major load buses in the system, a rapid load increase indicates a jump of the load consumption at the local bus. This is simulated as linear load increase of an amount of the 100% of the original load within 5 seconds in the PSS\e.

Bus fault cases are carried out at the 230kV and 115kV buses at the DVP. The locations of the tripping are randomly selected. The fault type selected is the three-phase short circuit. The faults are considered as permanent faults that last for the rest of the simulation.

Line tripping cases are carried out from 35kV to 500kV at the DVP. We are interested in 500kV line tripping cases in the DVP thus we put several such cases into the database. We also check the islanding condition to make sure none of the line tripping cases overlaps with the islanding cases. These trips are considered as permanent faults that last for the whole simulation.

3.1.3.2 Decision Tree Prediction Assessment

The channels of the simulation outputs are the voltage and current phasor (converted from real time load flow) measurements at the 500kV level buses inside the DVP system. The

time stamped simulation results are converted into EXCEL file and used to generate the DTs for islanding prediction and estimation purpose. In this section, the prediction assessment of each specific tree is analyzed.

A) The DT for Islanding Detection

The whole islanding database is used to generate this tree. Two methods are used in tree formation: the 10% test sample method and 10-fold cross validation method [42]. Table 3.2 shows the decision tree prediction success at different tree sizes.

From the fourth column it can be seen that a full-size tree using 10-fold cross validation method can achieve 98% accuracy for islanding detection basing on the database. In other words, any islanding case that randomly picked up from the database will have a 98% chance to be identified correctly using the presented DT. Of course the prediction success rate is largely relevant to the database size and case selection. The test results have proven that based on a well-established and updatable database, that the DTs reaching high prediction success indicate the DT method is capable for online islanding detection and identification. The table also shows the prediction success for a smaller sized tree with smaller variable importance. For the 10-fold cross validation DT, if we choose to prune the tree to three or two nodes, the prediction success will drop to 96.73 and 93.06 percent, which is still fairly high. However, for tree with fewer than 20 nodes, the tree is considered to be simple and having less chance to over-fitting. The prune process is not recommended at that level.

TABLE 3.5: DECISION TREE PREDICTION SUCCESS

Tree size (Nodes number)		Variable importance	Prediction success		Relative cost
			Learn	Test	
10% test sample	4	16	99.78%	97.73%	0.067
	3	10	98.65%	95.45%	0.133
	2	6	94.62%	90.91%	0.267
10-fold cross validation	4	18	99.59%	98.16%	0.038
	3	12	98.57%	96.73%	0.078
	2	6	94.29%	93.06%	0.179

The decision tree generated by CART is shown in the Fig. 3.2. This tree is generated using 10-fold cross validation. Major structures and splitting options are noted in the tree block diagram. In this particular tree, the major splitting points are voltage angles, real power and reactive power measurements. The tree is very simple yet achieves a high accuracy.

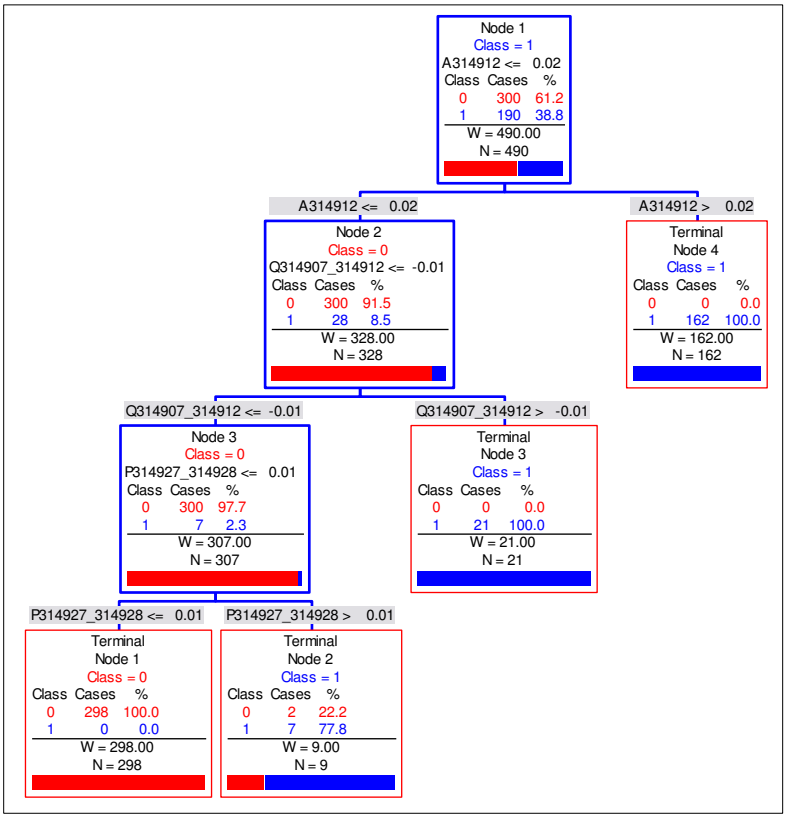

Figure 3.2: Decision tree splitting diagram using 10-fold cross validation

The DTs are also useful for the PMU placement assessment. When forming the trees, the primary split variables are referred to as having the most effluence to the prediction accuracy. The places where these variables are measured are also the critical PMU locations for implementation of islanding detection application. In this test, all state variables are from 30 locations at the 500kV network; among them are the major substations with PMUs installed. The measurements at those locations show exactly what the PMUs may see when an island form in a lower voltage area and how this island would influence the major 500kV transmission network. For a tree using 18 system variables in determination, the variables may just come from 4 different locations.

B) Islanding Behavior Groups

A successive study of the islanding characteristics of the 190 islanding cases was carried out. Major islanding cases were run for 20 seconds and the angle variables of the involved generators were tracked. Three types of islanding categories were obtained

B.1 Category 1:

- Machines in the islands are angle coherent;

- The islanded area remains stable;

- The islanded machine angles have a relatively larger oscillation in a different direction compared with the main grids;

- In some cases, the islanded area is connected with tie-lines outside the Virginia area. Although a Virginia region is physically islanded it still receives power delivered from outside the area. (This is due to: the islanding detecting strategy is applied within the partial incidence matrix of the DVP, thus some of the boundary tie-lines are kept in some cases. However, these

cases are still thought islands – not a physical but an electrical island for which the utility losses the control of the island.)

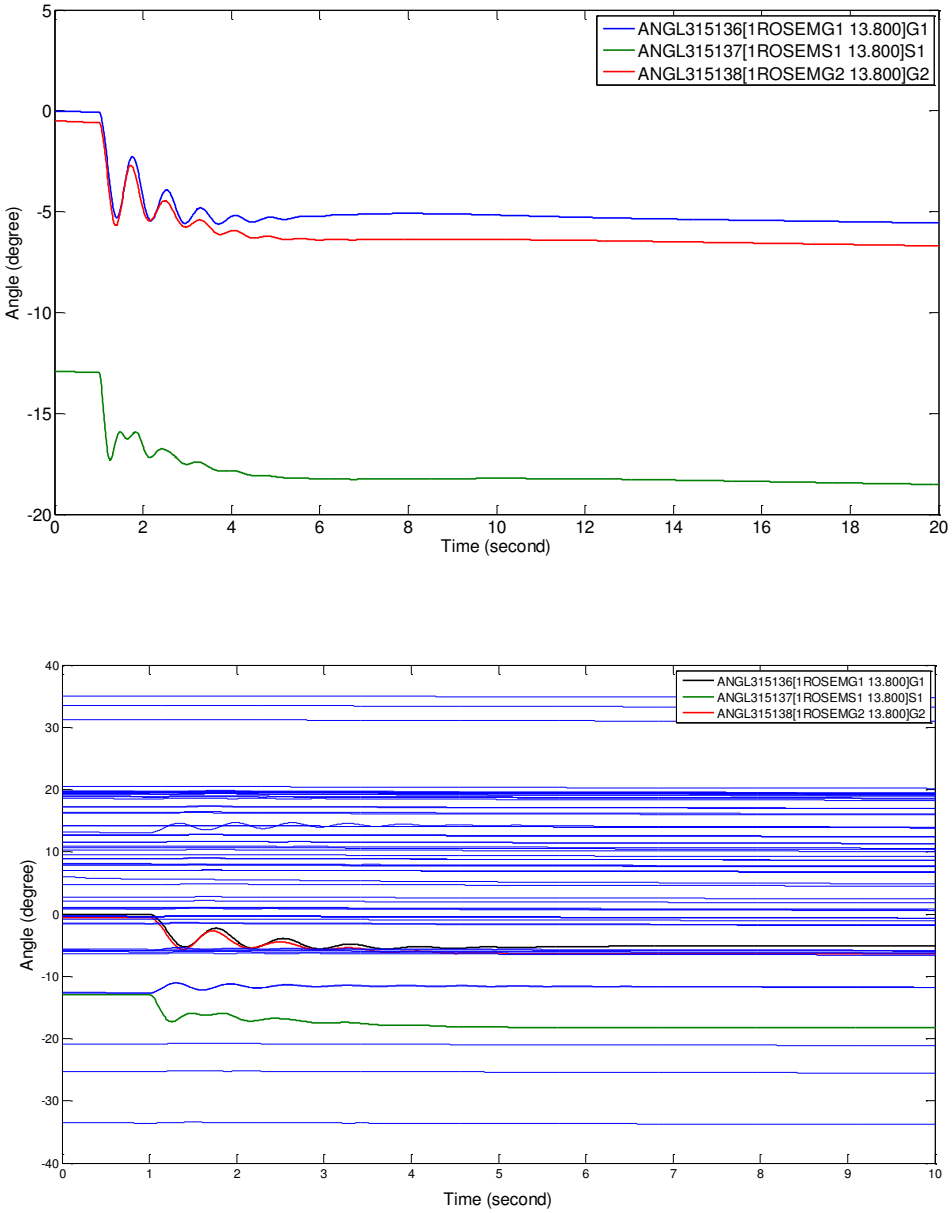

Figure 3.3: Machine angles oscillation of category 1 cases

B.2 Category 2:

- Machines in the islands are angle coherent;

- The islanded area lost stability after the contingency;

- The islanded machine angles go up because of a mismatch between loads and generation; the angles in the main grid go to the opposite direction. Protection actions are needed.

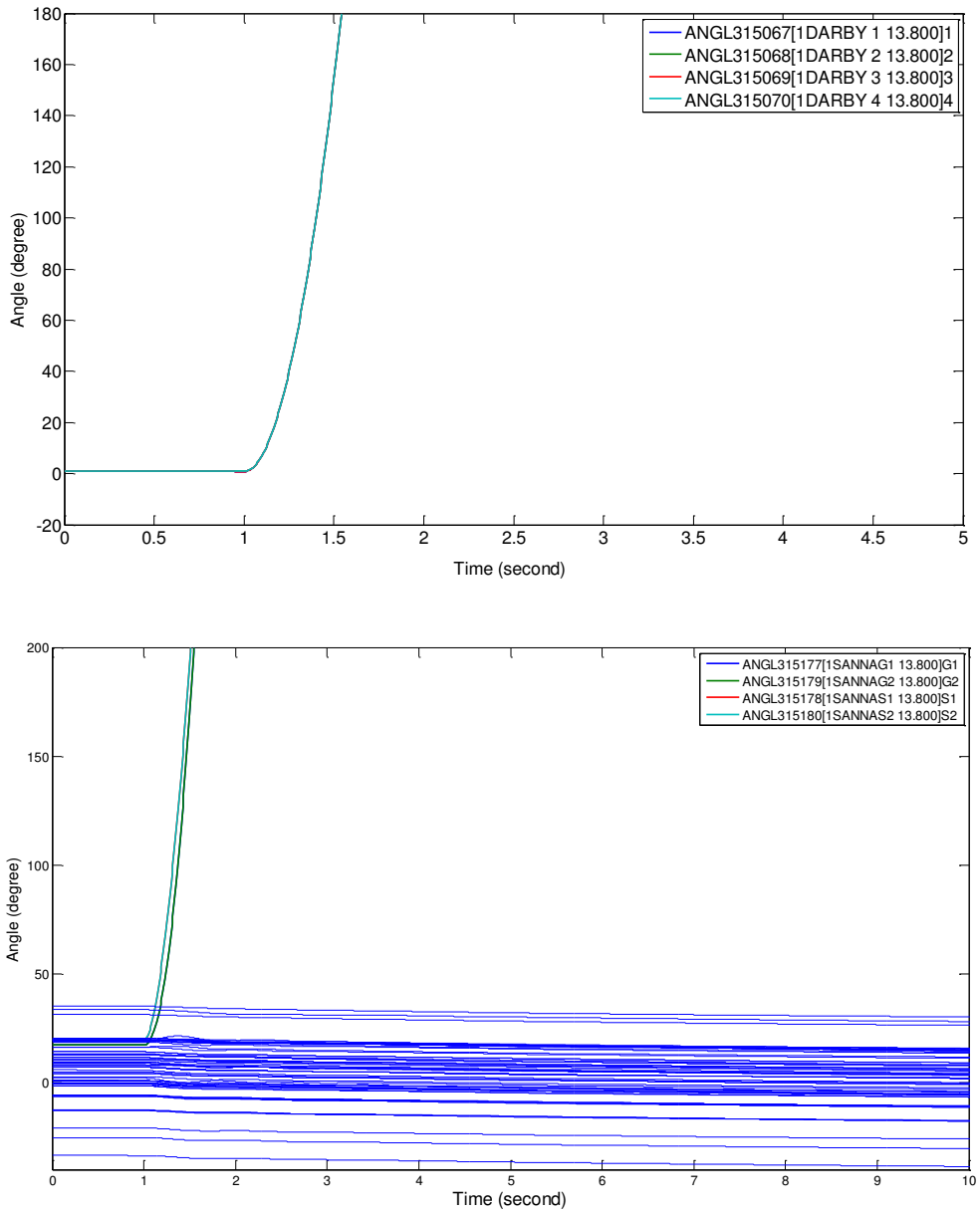

Figure 3.4: Machine angles oscillation of category 2 cases

B.3 Category 3:

- Machines in the islands are angle coherent;

- The islanded area remains stable after the contingency and the islanded machine angles go along with the main grid.

- Some machines not included in the island but near the boundary are influenced more by the contingency. Sometimes the generators related to the islanded area lost stability.

- In some cases, the islanded area is connected with tie lines outside the Virginia area.

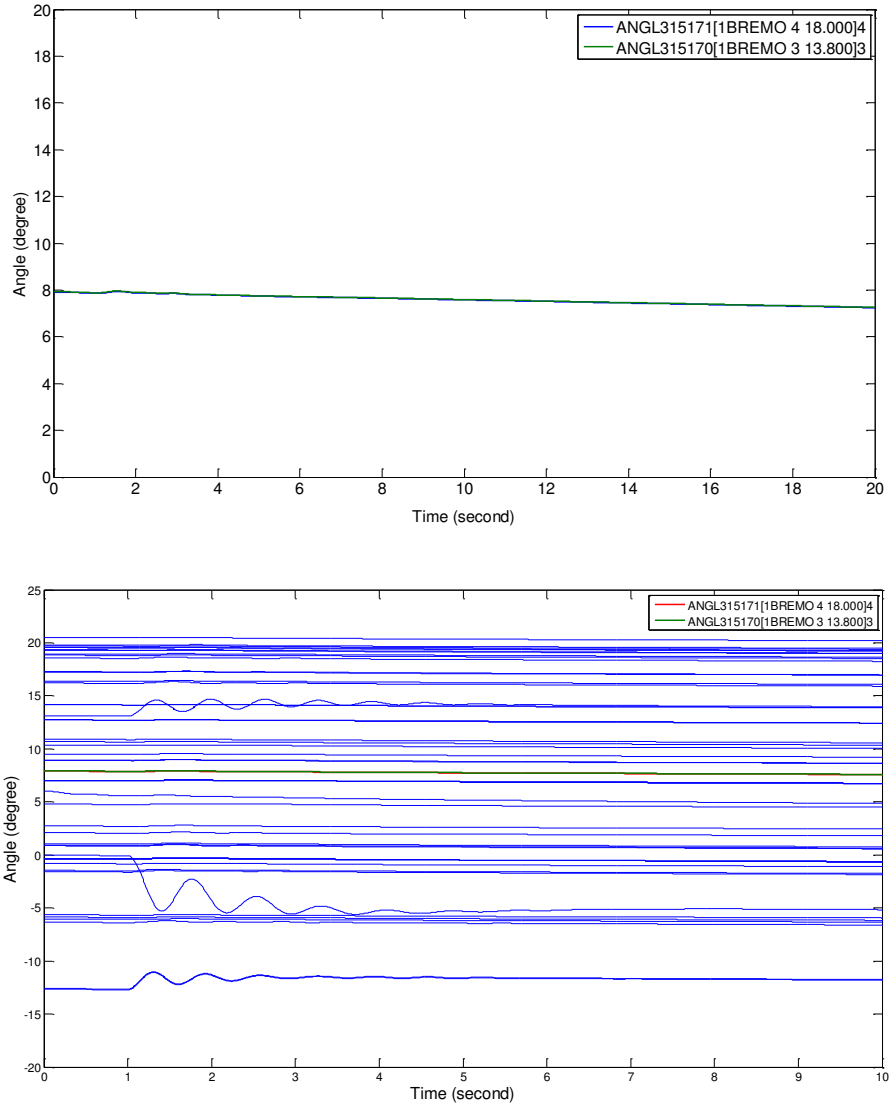

Figure 3.5: Machine angles oscillation of category 3 cases

C) The DT for Other Islanding Issues

As it was stated previously, the islanding contingency database is created mainly to test the decision tree algorithm in islanding detection. While the DT algorithm can achieve more functions including islanding location estimation, islanding stability assessment or islanding area estimation. Tests on these functions are made using different islanding databases, corresponding decision trees are obtained and analyzed. A brief introduction of the specialized islanding database used for such purposes as well as for the islanding severity index usage is given in Section 3.2. The detailed database introduction and DT analysis are given in Chapter Four.

3.2 Testing Results on Islanding Severity Index

The ISI is a proposed method for ranking the system transient behavior and severity level of islanding contingencies. The ISI works as an additional tool to assist the DTs in islanding severity determination. The method itself is a very useful tool in power system islanding analysis. It offers a way to qualify and quantify the islanding severity for any islanding scenarios proposed in a study system both offline and online. In the offline analysis, it can help judging the underlying weakness points of a study system under unbalanced power condition.

A successive islanding severity test of the (190+300) islanding database was carried out on selected islanding cases based on the islanding groups analysis. The long-term and instant ISI values were calculated via equation (2.20) and (2.21). Table 3.5 shows 10 typical islanding contingency cases taken from the database. According to the computation, category 2 islanding cases have relatively larger ISI instant and long-term values than the category 1 and 3 cases. Islanding case with a higher instant ISI value show larger angle oscillations; while it doesn't necessarily mean it has a higher long-term ISI value which is related to the generators' inertia and have effect to their power re-dispatch characteristic. Those Island cases with huge generation have correspondingly much larger long-term ISI values however a large ISI value does not indicate the machines in the island will lose stability. There are also some meter islanding cases in the system; case 7-10 all have inter-area tie-lines connected with the islanded area. Although in these cases they have relatively high instant and long-term ISI values, the islanded areas are still stable, however the influences to the system is more severe than category 1 cases, which are also shown as the more severe angle oscillations at boundary generators.

TABLE 3.6: ISLANDING SEVERITY INDEX ANALYSIS

Case #	Island Generation	Mismatches		Inertia Combo	Category	ISI_ Instant	ISI_ long-term
		P	Q				
1	165+j18.3	-63.42	8.469	15.3	1	0.384	4.145
2	3030+j397.2	3030	397.2	52.92	2	1	57.256
3	1744-j254.2	-429.2	-385.8	20.22	1	0.246	21.226
4	606+j74.4	556.23	52.487	27.54	2	0.918	20.197
5	348+j84.8	316.02	73.682	26	2	0.908	12.155
6	275+j9.9	46.582	0.069	15.3	1	0.169	3.0446
7	227-j12.6	92.111	-32.85	6.82	3	0.406	13.506
8	227-j12.6	84.76	-36.06	6.82	3	0.373	12.428
9	147.5-j11.9	95.738	-53.60	6.232	3	0.649	15.362
10	147.5-j11.9	118.67	-47.22	6.232	3	0.805	19.042

For the major ISI analysis, a different set of data is used to compose the database. We narrowed our simulations into one smaller region which is considered to be the most potential islanding location in the DVP. A series of islanding cases are formed on the selected locations, and the islanding severity index is computed. A curve-fitting approach is used to simulate the frequency oscillations of the isolated area to help demonstrate how the index ranks the severity of the event. All contingency dynamic simulations are done using Python compiled PSS\E (32.03 version).

3.2.1 The Creation of the Islanding Database for ISI

The creation process includes four stages:

1) Based on the geographical distribution of the transmission network around selected islanding location, the system one-line diagram is made;

2) The one line diagram of the selected area is separated into four partitions (0-3) for a convenient load calculation. The partition determination is based on the system topology characteristics and load condition;

3) The determination of the isolated area is first performed based on the geographic map in Fig. 3.6 and 3.7. The isolated area analysis starts from the selected sub-station and radiates outwards. For each of the two directions, the transmission lines come out of the station circles with increasing radius which indicates a growth of the possible islanding areas along the transmission paths. The potential islanding regions are labeled by the cut-off locations using red and purple dotted lines.

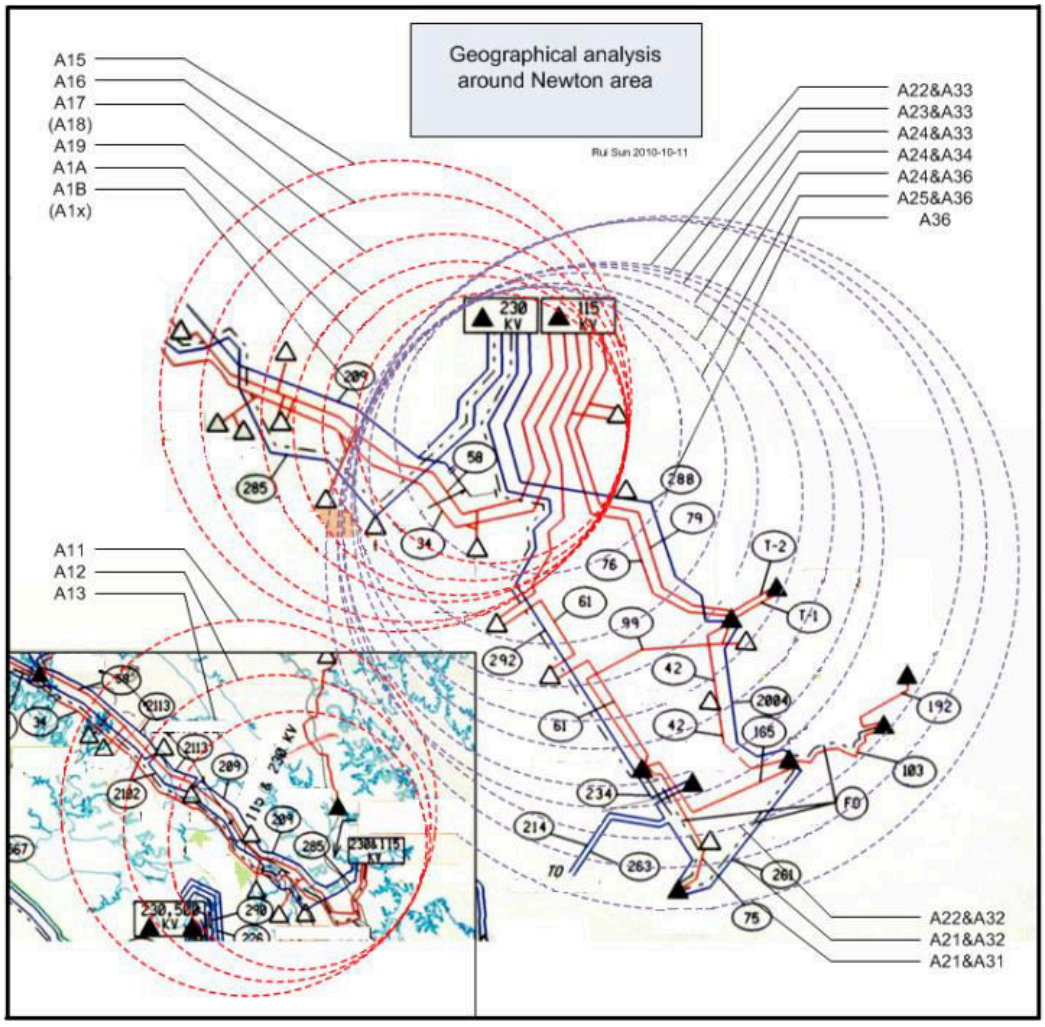

Figure 3.6: Geographic diagram around the selected area

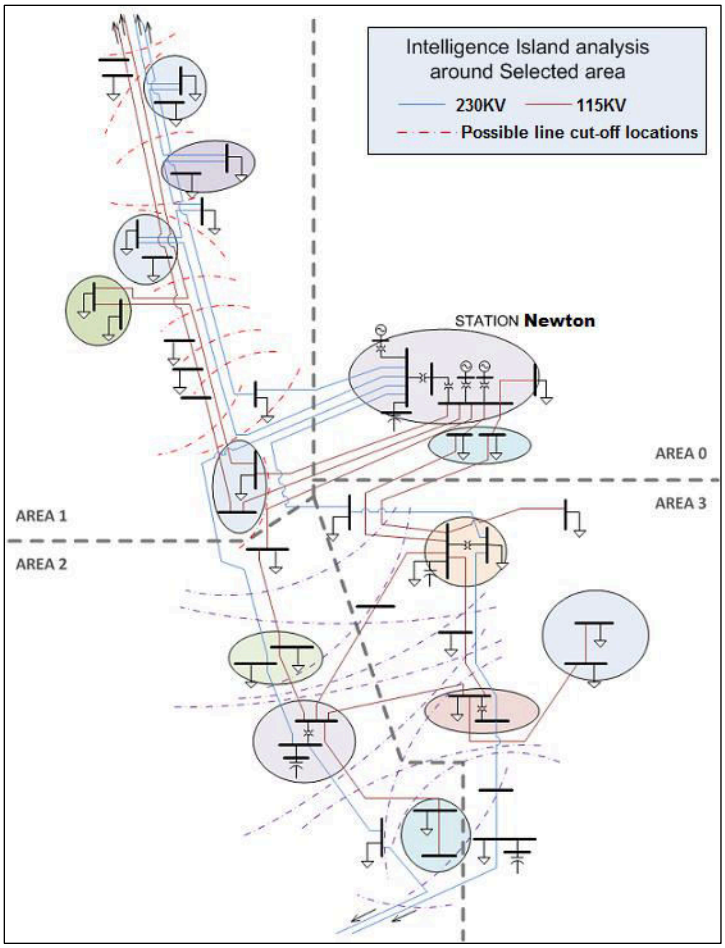

Figure 3.7: Islanding cut-offs around the selected area

4) A total number of 130 islanding cases within the selected area are simulated in PSS\e 32.03, with the network frequency dependence function turned on. The largest load condition simulated for an island is 1130.8MW and -54MVar.

An under-frequency load shedding scheme for the DVP is simulated, which is shown in Table 3.7:

TABLE 3.7: UNDERFREQUENCY SHEDDING SCHEME

Underfrequency Shedding	
f < 59.3 Hz	Shed 10% load
f < 59.0 Hz	Shed 20% load
f < 58.5 Hz	Shed 30% load

A maximum of 30% load will be shed during the protection operation. The time for communication delay and relay/breaker operation for each shedding is 0.2833 second. If after the three stages the frequency of the island is still below 58.5Hz the whole isolated area will be tripped, in other words, the island is considered unstable.

In 130 cases, without load shedding, there are 68 cases with steady frequency over 59.3 Hz and 23 cases below 58.5 Hz. For any case when the frequency drops below 58.5 Hz, a load shedding protection will be applied. For 75 cases, 17 cases apply 10% load shedding only, 30 cases apply 20% load shedding and 28 cases apply 30% load shedding. After applying the load shedding scheme, there are 4 cases with frequency still below 58.5 Hz.

3.2.2 ISI Computation and Analysis

Using the equations derived from (2.20) and (2.21), the index values before load shedding and right after the shedding are computed differently as:

$$ISI\_longterm(ini) = \left| \frac{P_{GEN\_ini} - P_{loads\_ini}}{H_{GEN}} \right|$$

$$ISI\_instent(ini) = \left| \frac{P_{GEN\_ini} - P_{loads\_ini}}{P_{GEN\_ini}} \right| \quad (3.1)$$

And:

$$ISI\_longterm(post) = \left| \frac{P_{GEN@shedding} - P_{loads\_p}}{H_{GEN}} \right|$$

$$ISI\_instent(post) = \left| \frac{P_{GEN@shedding} - P_{loads\_p}}{P_{GEN@shedding}} \right| \quad (3.2)$$

TABLE 3.8: ISI FOR THE STUDY SYSTEM

Case #	P_ld (ini)	P_ld (post)	Freq. w/o shed	Final Freq.	ISI_Long(ini)	ISI_Long(post)	ISI_Instant(ini)	ISI_Instant(post)
1	1139.7	797.79	51.041	58.577	**60.96**	19.60	**1.175**	0.199
2	1039.4	727.58	58.256	58.860	**51.03**	19.22	**0.984**	0.211
3	1039.4	727.58	58.289	58.805	**51.03**	19.57	**0.984**	0.214
4	995.4	696.78	58.419	58.930	**46.67**	18.02	**0.900**	0.207
5	916.6	733.28	58.658	59.109	38.87	8.42	0.749	0.104
6	877.8	702.24	58.769	59.220	35.03	8.66	0.675	0.111
7	799	639.2	59.008	59.430	27.23	15.83	0.525	0.200
8	715.4	643.86	59.259	59.424	18.95	7.87	0.365	0.110
9	665.4	598.86	59.418	59.573	14.00	12.46	0.270	0.174
10	1112.3	778.61	27.811	31.571	**58.25**	**51.60**	**1.123**	**0.401**
11	1012	708.4	31.221	43.118	**48.32**	**48.59**	**0.931**	**0.409**
12	1012	708.4	58.368	58.886	**48.32**	18.11	**0.931**	0.205
13	968	677.6	58.498	59.007	**43.96**	18.59	**0.847**	0.217
14	889.2	711.36	58.738	59.187	36.16	8.29	0.697	0.105
15	850.4	680.32	58.849	59.295	32.32	16.41	0.623	0.196
16	771.6	617.28	59.089	59.505	24.51	15.51	0.473	0.202
17	688	619.2	59.340	59.506	16.24	12.90	0.313	0.174
18	638	638	59.500	59.500	11.29	11.29	0.218	0.218
19	1071.2	749.84	30.283	45.788	**54.18**	**47.02**	**1.044**	**0.388**
20	986.9	690.83	43.980	58.226	**45.83**	**38.06**	**0.883**	**0.358**
21	886.6	709.28	58.709	59.249	35.90	8.72	0.692	0.110
22	886.6	709.28	58.739	59.202	35.90	16.77	0.692	0.193
23	842.6	674.08	58.869	59.318	31.54	16.32	0.608	0.196
24	763.8	611.04	59.109	59.528	23.74	15.40	0.458	0.203
25	725	652.5	59.222	59.405	19.90	13.58	0.384	0.174
26	646.2	581.58	59.462	59.631	12.10	7.67	0.233	0.118
27	562.6	562.6	59.714	59.714	3.82	3.82	0.074	0.074
28	512.6	512.6	59.870	59.870	1.13	1.13	0.022	0.022
29	1158.4	810.88	46.612	58.565	**62.81**	21.51	**1.211**	0.211
30	1019.5	713.65	58.221	58.895	**49.06**	18.38	**0.946**	0.206
…								
93	220.8	220.8	61.799	61.799	30.02	**30.02**	**0.579**	**0.579**
94	1006.8	704.76	58.237	58.978	**47.80**	18.24	**0.921**	0.207
95	867.9	694.32	58.672	59.277	34.05	8.61	0.656	0.111
96	851.4	681.12	58.762	59.322	32.42	8.53	0.625	0.112
97	751.1	600.88	59.117	59.596	22.49	15.56	0.433	0.207
98	666.8	600.12	59.313	59.615	14.14	8.17	0.273	0.121
99	566.5	566.5	59.675	59.675	4.21	4.21	0.081	0.081
100	566.5	566.5	59.698	59.698	4.21	4.21	0.081	0.081
101	522.5	522.5	59.831	59.831	0.15	0.15	0.003	0.003
102	443.7	443.7	60.015	60.015	7.95	7.95	0.153	0.153
103	404.9	404.9	60.122	60.122	11.79	11.79	0.227	0.227
104	326.1	326.1	60.708	60.708	19.59	19.59	0.378	0.378
105	242.5	242.5	61.100	61.100	27.87	27.87	0.537	**0.537**
106	192.5	192.5	64.779	64.779	32.82	**32.82**	0.633	**0.633**
107	1006.8	704.76	58.237	58.978	**47.80**	18.23	**0.921**	0.207
108	867.9	694.32	58.672	59.277	34.05	8.60	0.656	0.111
109	851.4	681.12	58.762	59.322	32.42	8.53	0.625	0.112
110	751.1	600.88	59.117	59.596	22.49	15.56	0.433	0.207
111	666.8	600.12	59.313	59.615	14.14	8.16	0.273	0.121
112	566.5	566.5	59.675	59.675	4.21	4.21	0.081	0.081
113	566.5	566.5	59.698	59.698	4.21	4.21	0.081	0.081
114	522.5	522.5	59.831	59.831	0.15	0.15	0.003	0.003
115	443.7	443.7	60.015	60.015	7.95	7.95	0.153	0.153
116	404.9	404.9	60.122	60.122	11.79	11.79	0.227	0.227
117	326.1	326.1	60.708	60.708	19.59	19.59	0.378	0.378
118	242.5	242.5	61.100	61.100	27.87	27.87	0.537	**0.537**
119	192.5	192.5	64.781	64.781	32.82	**32.82**	**0.633**	**0.633**
120	926.1	648.27	58.482	59.183	**39.81**	18.28	0.767	0.222
…								

The analysis starts from the comparison between the scenarios with and without a load shedding scheme. The 4th and 5th column in Table 3.7 are the frequencies of the island with and without load shedding after 20 seconds. Under-frequency and over-frequency cases are shown in bold in first column. The load shedding action effectively improves the stability of the islands. By applying the load shedding scheme, the number of unstable islanding cases decreases from 23 to 4, considering the system has come back to steady state for most stable cases at 20 seconds after the contingency. This change is precisely demonstrated by the values of the long-term index. For the selected area, a severe threshold at 38 can be set for long term ISI, all cases with higher long-term values are proved to be unstable. With load shedding, most large long-term values have turned small, while the unstable ones remain large. The results also show that for over-generating cases (106 and 119), the long-term index does not give a significant difference. They may have relatively large values but still within the threshold.

The instant ISI focuses mostly on the transient behaviors during the first couple of seconds after the contingency. A larger index value refers to a more intense oscillation and transient behavior. In most cases, the contingencies with higher long term influence will have more severe transient behaviors. The instant index value may shift due to any change in the system structure or load/generation condition. The initial instant index values express a coherency between the long-term index values but the instant index could recognize over-generating cases with relatively high values. For the over-generating cases, the frequency will finally go back close to 60Hz due to the governor system however their larger transient behaviors needs more time for damping. This is also shown in the graphs. It is not safe to assume that a long-term good case is absolutely moderate in transient; these are two independent indices.

3.2.3 Curve fitting comparison and analysis

An approach to model the transient frequency oscillation of each islanding event using curve fitting program is described in this section. The fitted curve model is determined as:

$$f_{new}(t) - f_{ini} = A \cdot \sin(wt + \theta) \cdot e^{-bt} + C \quad (3.3)$$

Where:

A – the largest frequency oscillation magnitude (the magnitude of the first oscillation cycle most time);

b – the oscillation decay speed;

C – the frequency deviation after 20 seconds;

w – the oscillation natural frequency.

The values of the parameters **A**, **b** and **C** reflect the degree the frequency oscillation as well as the severity of the contingency. For a severe case, the **A** value tends to be larger and **b** smaller; while **C** could be larger in its absolute value. For the long-term stable islands in this study, the value of **C** is expected to be within (-1.5, 1.8).

Selected fitting curve samples are listed in Fig. 3.8 and 3.9:

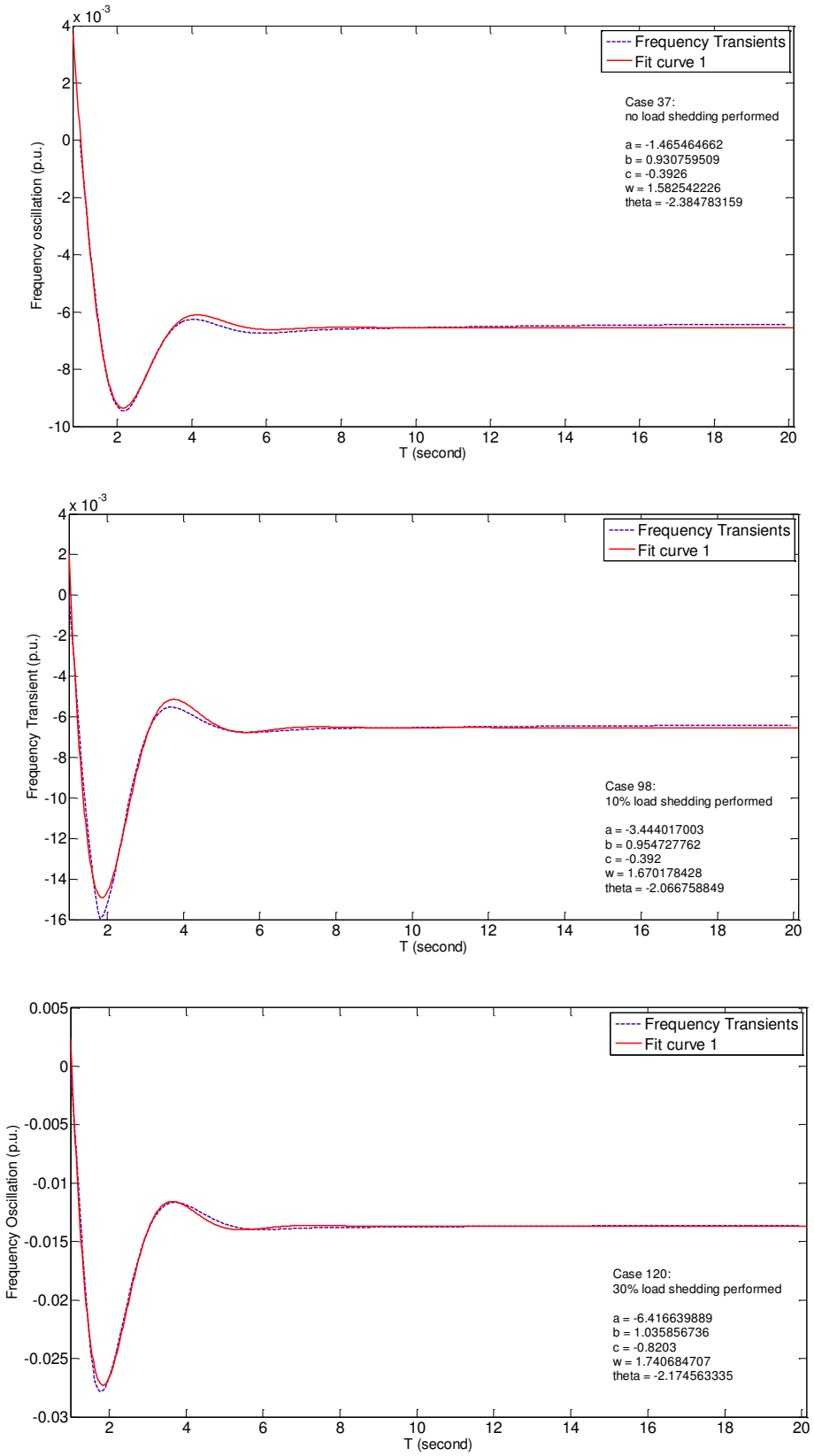

Figure 3.8: Selected fitting curve samples

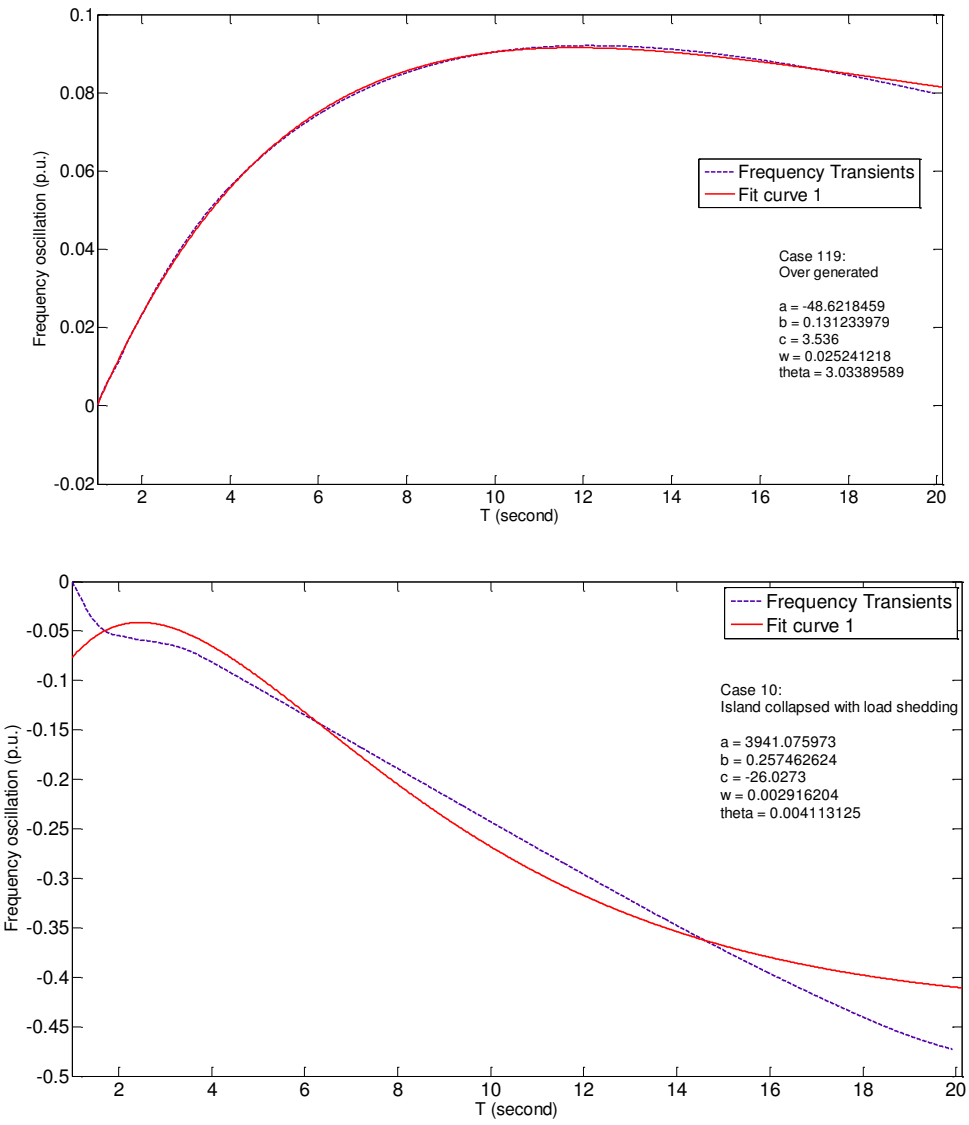

Figure 3.9: Selected fitting curve samples (cont.)

Case 37 in Fig 3.8 is stable and does not need load shedding; cases 98 needs 10% load shedding and case 120 needs 30% load shedding. Case 119 is an over-generating case stable in the long term. Case 10 is unstable and the island collapses after 20 seconds.

TABLE 3.9: ISI WITH CURVE FITTING PARAMETERS

Case #	ISI_Long(ini)	ISI_Long(post)	ISI_Instant(ini)	ISI_Instant(post)	A	b	C (in Hz)	w (in pi)
1	60.96	19.60	1.175	0.199	-6.4724	1.0086	-1.4246	1.8615
2	51.03	19.22	0.984	0.211	-5.7894	0.9864	-1.1418	1.8348
3	51.03	19.57	0.984	0.214	-5.5248	1.0205	-1.1992	1.8314
4	46.67	18.02	0.900	0.207	-5.1945	1.0043	-1.0745	1.8278
5	38.87	8.42	0.749	0.104	-4.5058	0.9962	-0.8971	1.8429
6	35.03	8.66	0.675	0.111	-4.3031	0.9742	-0.786	1.8283
7	27.23	15.83	0.525	0.200	-3.4601	0.9030	-0.5776	1.8216
8	18.95	7.87	0.365	0.110	-2.5504	0.9357	-0.5833	1.7635
9	14.00	12.46	0.270	0.174	-1.9560	0.8435	-0.4347	1.7337
10	58.25	51.60	1.123	0.401	3941.1	0.2575	-26.027	0.0029
11	48.32	48.59	0.931	0.409	14597.8	0.8184	-11.082	0.0033
12	48.32	18.11	0.931	0.205	-5.3338	1.0113	-1.1187	1.8306
13	43.96	18.59	0.847	0.217	-5.0104	0.9962	-0.998	1.8268
14	36.16	8.29	0.697	0.105	-4.2987	0.9838	-0.8192	1.8422
15	32.32	16.41	0.623	0.196	-4.0765	0.9580	-0.7113	1.8269
16	24.51	15.51	0.473	0.202	-3.1990	0.8640	-0.5028	1.8038
17	16.24	12.90	0.313	0.174	-2.2869	0.8992	-0.5012	1.7569
18	11.29	11.29	0.218	0.218	-1.8212	0.9657	-0.5068	1.6094
19	54.18	47.02	1.044	0.388	9221.4	0.8480	-9.58	0.0043
20	45.83	38.06	0.883	0.358	-10.129	1.2025	-1.7784	1.4685
21	35.90	8.72	0.692	0.110	-5.2010	0.9977	-0.7556	1.7716
22	35.90	16.77	0.692	0.193	-4.4235	0.9816	-0.8034	1.8305
23	31.54	16.32	0.608	0.196	-4.0397	0.9527	-0.6883	1.8256
24	23.74	15.40	0.458	0.203	-3.1564	0.8545	-0.4801	1.7977
25	19.90	13.58	0.384	0.174	-2.7574	0.9407	-0.6015	1.7633
26	12.10	7.67	0.233	0.118	-1.8321	0.7883	-0.3768	1.7050
27	3.82	3.82	0.074	0.074	-1.2416	0.9649	-0.2927	1.4909
28	1.13	1.13	0.022	0.022	-1.3698	1.1929	-0.1351	0.9965
29	62.81	21.51	1.211	0.211	-6.7719	0.9810	-1.4352	1.8592
30	49.06	18.38	0.946	0.206	-6.0115	1.0138	-1.1083	1.8371
31	47.43	18.19	0.914	0.207	-5.7578	1.0035	-1.0642	1.8344
32	37.50	17.52	0.723	0.219	-5.0193	0.9784	-0.7998	1.7934
33	29.15	8.66	0.562	0.118	-5.0637	1.0043	-0.5866	1.7688
34	19.22	15.26	0.370	0.211	-4.1948	0.9278	-0.3203	1.6816
35	19.22	13.73	0.370	0.177	-2.7141	0.9296	-0.5782	1.7613
36	14.86	13.51	0.286	0.184	-2.2862	0.8752	-0.454	1.7456
37	7.06	7.06	0.136	0.136	-1.4655	0.9308	-0.3926	1.5825
38	3.22	3.22	0.062	0.062	-1.2422	0.9226	-0.2775	1.4664
39	4.58	4.58	0.088	0.088	-0.3886	1.0333	-0.0597	1.4918
40	12.86	12.86	0.248	0.248	0.7113	0.2139	0.2299	0.3186
…								
93	30.02	30.02	0.579	0.579	-65.941	0.1175	-1.0713	0.0257
94	47.80	18.24	0.921	0.207	-6.5416	1.0099	-1.0233	1.7802
95	34.05	8.61	0.656	0.111	-5.0126	0.9899	-0.7273	1.8392
96	32.42	8.53	0.625	0.112	-4.7248	0.9746	-0.683	1.8308
97	22.49	15.56	0.433	0.207	-4.0524	0.9215	-0.4112	1.7363
98	14.14	8.17	0.273	0.121	-3.4440	0.9547	-0.392	1.6702
99	4.21	4.21	0.081	0.081	-1.8095	0.8451	-0.3341	1.3637
100	4.21	4.21	0.081	0.081	-1.2848	0.9092	-0.3086	1.5343
101	0.15	0.15	0.003	0.003	-1.0613	0.9633	-0.1759	1.3622
102	7.95	7.95	0.153	0.153	0.0059	0.3976	0.0157	0.9201
103	11.79	11.79	0.227	0.227	0.3813	0.2144	0.1221	0.3246
104	19.59	19.59	0.378	0.378	-2.0705	0.1991	0.7274	0.3237
105	27.87	27.87	0.537	0.537	-4.2818	0.1114	1.3733	0.2336
106	32.82	32.82	0.633	0.633	-46.501	0.1297	3.478	0.0265
107	47.80	18.23	0.921	0.207	-6.5377	1.0098	-1.0235	1.7805
108	34.05	8.60	0.656	0.111	-5.0118	0.9900	-0.7275	1.8392
109	32.42	8.53	0.625	0.112	-4.7229	0.9746	-0.6831	1.8309
110	22.49	15.56	0.433	0.207	-4.0489	0.9213	-0.4113	1.7365

111	14.14	8.16	0.273	0.121	-3.4413	0.9547	-0.3922	1.6703
112	4.21	4.21	0.081	0.081	-1.8116	0.8463	-0.3341	1.3634
113	4.21	4.21	0.081	0.081	-1.2845	0.9096	-0.3086	1.5345
114	0.15	0.15	0.003	0.003	-1.0608	0.9638	**-0.1759**	1.3624
115	7.95	7.95	0.153	0.153	**0.0067**	0.4133	**0.0157**	0.9088
116	11.79	11.79	0.227	0.227	**0.3826**	0.2146	**0.1223**	0.3245
117	19.59	19.59	0.378	0.378	-2.0715	0.1992	0.7276	0.3236
118	27.87	27.87	0.537	**0.537**	-4.2880	0.1114	1.3724	0.2334
119	32.82	**32.82**	**0.633**	**0.633**	**-48.622**	**0.1312**	**3.536**	0.0252
120	**39.81**	18.28	0.767	0.222	-6.4166	**1.0359**	-0.8203	1.7407
…								

The oscillation's curve fitting parameters demonstrate the effectiveness of the instant index. As stated before, the values of the parameters **A, b** and **C** reflect the range of the frequency oscillation as well as the severity of the contingency. Table 3.9 shows the most severe cases (10, 11 and 19) have quite large **A** values according to the fitting configuration. And so do the over-generating cases. The less severe cases have larger **b** indicating a faster damping. The least severe cases have the relatively smallest ISI values.

3.2.4 Adapted real time ISI computation and analysis

The ISI values can be computed using saved system parameters and estimated data. In other words, this index is very useful for researchers to study the islanding response of certain system. The ISI could update with real-time measurements and system status to reflect a more accurate qualification of islanding cases.

According to the Equation (2.20) in Chapter 2, the islanding severity index value has a consistency with K times the time derivative of the generator angle velocity at the isolated areas. The time derivative of the generator angle velocity of the selected station at the selected time are recorded and listed in Table 3.10.

TABLE 3.10: REAL TIME ISI COMPUTATION

Case #	ISI_Long(ini)	ISI_Long(post)	ISI_Instant(ini)	ISI_Instant(post)	2*d(theta)/d^{2}t			
					ini	Ld_shed	t = 5	t = 10
1	**60.96**	19.60	**1.175**	0.199	**11.303**	1.416	0.186	0.005
2	**51.03**	19.22	**0.984**	0.211	**9.764**	0.740	0.169	0.002
3	**51.03**	19.57	**0.984**	0.214	**9.034**	0.680	0.138	0.002
4	**46.67**	18.02	**0.900**	0.207	**8.464**	0.075	0.128	0.006
5	38.87	8.42	0.749	0.104	7.265	0.108	0.105	0.005
6	35.03	8.66	0.675	0.111	6.740	0.169	0.099	0.006
7	27.23	15.83	0.525	0.200	5.505	0.466	0.084	0.001
8	18.95	7.87	0.365	0.110	4.138	0.024	0.070	0.001
9	14.00	12.46	0.270	0.174	3.799	0.345	0.069	0.003
10	**58.25**	**51.60**	**1.123**	**0.401**	**15.792**	**5.545**	**3.226**	**3.198**
11	**48.32**	**48.59**	**0.931**	**0.409**	**13.536**	**4.180**	**1.766**	**1.681**
12	**48.32**	18.11	**0.931**	0.205	8.716	0.094	0.132	0.001
13	**43.96**	18.59	**0.847**	0.217	8.142	0.138	0.122	0.004
14	36.16	8.29	0.697	0.105	6.954	0.189	0.100	0.004
15	32.32	16.41	0.623	0.196	6.412	1.115	0.096	0.001
16	24.51	15.51	0.473	0.202	5.186	0.117	0.085	0.004
17	16.24	12.90	0.313	0.174	3.816	0.697	0.066	0.003
18	11.29	11.29	0.218	0.218	3.467		0.054	0.002
19	**54.18**	**47.02**	**1.044**	**0.388**	**14.184**	**4.574**	**1.366**	**1.336**
20	**45.83**	**38.06**	**0.883**	**0.358**	**11.870**	2.409	0.153	0.000
21	35.90	8.72	0.692	0.110	7.592	0.040	0.124	0.002
22	35.90	16.77	0.692	0.193	6.852	1.576	0.101	0.001
23	31.54	16.32	0.608	0.196	6.266	1.034	0.092	0.004
24	23.74	15.40	0.458	0.203	5.012	0.025	0.085	0.005
25	19.90	13.58	0.384	0.174	4.482	1.247	0.078	0.006
26	12.10	7.67	0.233	0.118	3.177	1.028	0.073	0.003
27	3.82	3.82	0.074	0.074	1.767		0.029	0.004
28	1.13	1.13	0.022	0.022	1.426		0.010	0.003
29	**62.81**	21.51	**1.211**	0.211	**11.303**	1.416	0.186	0.005
30	**49.06**	18.38	**0.946**	0.206	**9.764**	0.740	0.169	0.002
…								
101	0.15	0.15	0.003	0.003	2.857		0.061	0.001
102	7.95	7.95	0.153	0.153	2.138		0.042	0.004
103	11.79	11.79	0.227	0.227	1.489		0.027	0.002
104	19.59	19.59	0.378	0.378	0.151		0.000	0.000
105	27.87	27.87	0.537	**0.537**	0.363		0.001	0.037
106	32.82	**32.82**	0.633	**0.633**	1.773		0.083	0.216
107	**47.80**	18.23	**0.921**	0.207	3.271		0.508	**0.366**
108	34.05	8.60	0.656	0.111	3.647		**1.093**	0.196
109	32.42	8.53	0.625	0.112	9.994	0.209	0.178	0.005
110	22.49	15.56	0.433	0.207	7.532	0.235	0.111	0.004
111	14.14	8.16	0.273	0.121	7.138	0.389	0.109	0.005
112	4.21	4.21	0.081	0.081	5.475	0.015	0.087	0.004
113	4.21	4.21	0.081	0.081	4.618	0.827	0.066	0.003
114	0.15	0.15	0.003	0.003	2.856		0.060	0.002
115	7.95	7.95	0.153	0.153	2.137		0.042	0.002
116	11.79	11.79	0.227	0.227	1.488		0.026	0.004
117	19.59	19.59	0.378	0.378	0.150		0.001	0.000
118	27.87	27.87	0.537	**0.537**	0.364		0.001	0.036
119	32.82	**32.82**	**0.633**	**0.633**	1.774		0.082	0.214
120	**39.81**	18.28	0.767	0.222	3.272		0.508	**0.364**
…								

In the simulation, only one island is created each time and one station is involved. So the relation could be simplified as between the original instant index value and the time derivative of

the angle velocity. The test results have shown this consistency, especially at the time when the island forms. With the increase of time, the frequency oscillation decays, along with the decrease of the time derivative variable. For the unstable cases (10, 11 and 19), the time derivatives keep high even after 10 seconds, while in other cases, the values have already decayed close to 0. The time derivative could be used to compute the real-time ISI for both long-term and instantaneous indices, respectively.

3.3 Results on the Optimal PMU Placement Using BIPA

3.3.1 Optimal PMU Placement

The proposed method is tested on IEEE-14/30/39/57/118/300 BUS and WECC-128 BUS system models.

TABLE 3.11: BUS REDUCTION USING MODIFIED SCHEME

System models	Bus Reduction			
	Original scale	Virtual bus eliminated	Zero-injection bus eliminated	Final scale
IEEE-14	14×14	1	1	12×12
IEEE-30	30×30	0	2	28×28
IEEE-39	39×39	9	2	28×28
IEEE-57	57×57	0	7	50×50
IEEE-118	118×118	0	3	115×115
WECC-128	128×128	29	15	84×84
IEEE-300	300×300	24	22	254×254

Table 3.11 shows the system model scales before and after applying the modified bus reduction scheme. Due to the restrictive options, only limited number of buses is reduced.

For the purpose of monitoring the whole system's operating situation without losing information of the generations in an isolated system, placing PMUs at buses which have direct coverage of the generators is one of the priorities in the optimal PMU set determination. Converted to the Binary integer programming problem, this is solved by setting up the restrictive vectors $\mathbf{A_{EQ}}$ and $\mathbf{b_{EQ}}$. Table 3.12 shows the PMU quantity needed as modified optimal PMU placements considering islanding conditions:

TABLE 3.12: OPTIMAL PMU SETS COMPARISON

System models	Optimal PMU set				
	No Restriction	PMU at Fixed locations		PMU at all PV buses	
		Quantity	Ratio	Quantity	Ratio

IEEE-14	3	3	1.00	4	1.333
IEEE-30	8	9	1.125	11	1.375
IEEE-39	8	9	1.125	13	1.625
IEEE-57	14	14	1.00	16	1.143
IEEE-118	32	32	1.00	41	1.281
WECC-128	23	25	1.087	36	1.565
IEEE-300	74	78	1.054	97	1.311

The second column in Table 3.12 refers to the PMUs needed when the major generators (larger than 10% of the total generation) are directly monitored by PMUs. The fourth column shows when the required PMUs when all generator buses are directly observed by PMUs. From the comparison, we may see the second column is only slightly larger than the first column; when all generators are directly equipped with PMUs, the total PMU need for the system will increase for about 30%.

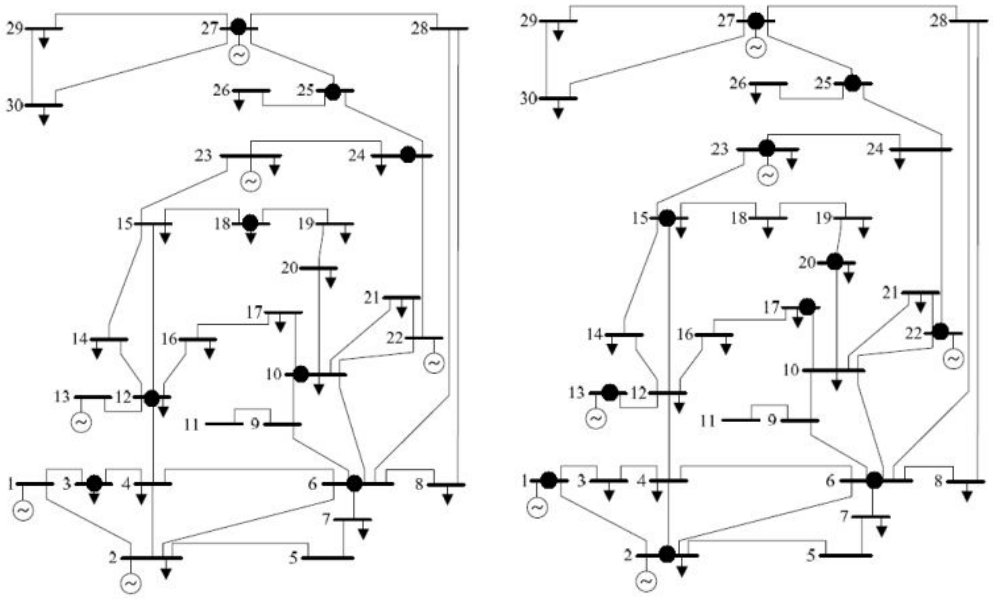

Figure 3.10: Optimal PMU sets w/wo considering islanding on IEEE-30

According to the comparison shown in Fig. 3.10, we may draw the conclusion that the modified PMU placement largely lowers the possibility of losing observability of generations when the system is split into islands. For instance, if a tornado goes through and breaks branch 4-

12, 4-6, 2-5 and 2-6, forming an island including 4 buses and 2 generators. The original optimal set will no longer offer the dynamic measurements of generator 2 during the fault, which will heavily worsen the possibility to monitor the island and to apply further protection schemes.

By using the proposed method, the modified placement needs 3 more PMUs to achieve a robust observability. The increase of PMUs is more apparent in large scale system. In such case, the restrictions can be lowered; the major plants should be considered first.

3.3.2 PMU Placement for Redundant Problem

Another important issue in PMU placement is the redundancy. According to Theorem 1 in Section 2.3.2, the redundancy can be increased in two ways. The difference is, when the redundancy is obtained by implementing multiple PMUs at the same bus, if the substation loses its power or gets isolated, all observability will be lost.

TABLE 3.13: REDUNDANCY PMU SETS COMPARISON

System models	**Observability redundancy = 2**				
	No restriction	PMU at fixed locations		PMU at all PV buses	
		Quantity	Ratio	Quantity	Ratio
IEEE-14	6	6	1.00	7	1.167
IEEE-30	16	17	1.063	18	1.125
IEEE-39	15	15	1.00	18	1.200
IEEE-57	28	28	1.00	29	1.036
IEEE-118	64	64	1.00	69	1.078
WECC-128	45	46	1.022	53	1.178
IEEE-300	148	149	1.007	165	1.115

Table 3.13 shows the PMU placements for a system observability redundancy of 2, the problem considers two PMUs at one location cases. We may find when achieving an observability redundancy of 2, PMUs are required for nearly half the number of buses, which is a considerate increase in expense.

3.3.3 The Stepwise PMU Placement Strategy & PMU Group Concept

Once the optimal set for the system is decided, it doesn't mean the system becomes observable at once. In practice the deployment may take years. PTs, CTs and the communication devices need to be installed and calibrated. Any time before all PMUs are completely installed the system is in potential danger for islanding cases and other contingencies. So we may decide a sequence for PMU implementation. For any PMU placed, the new PMU set should achieve a comprehensively larger observability of the system; at the same time the set will offer best independent observation of the generators, decreasing the chance leaving any isolated area unobserved during a contingency.

The implementation sequence of the stepwise PMU placement is determined by many aspects as the generation & loads matching, the system geographical characteristics and machine dynamic characteristics. The priority list may provide us the most beneficial PMU installation sequence in multiple-years plan.

At the same time, by studying such system priority determining aspects, the PMUs can be grouped to their geographical locations and behaviors. Thus the system could also be divided into smaller subsystems based on that. For a wide-area islanding contingency, we may easily locate the region of the isolated area and judge the exact influenced region and how severe the contingency is. New system protection strategy based on grouped PMU measurements may also be derived in the future.

CHAPTER 4: THE ISLANDING SCHEME IN DVP SYSTEM

In this chapter, the practical utilization of the decision tree algorithm based islanding scheme in the Dominion Virginia Power (DVP) system is introduced. The proposed islanding research in this dissertation is part of the PMU Measurements Application Study sponsored by the Dominion Virginia Power & the U.S. Department of Energy. For this project, an online system state monitoring and estimation protection software is being installed on the DVP server to handle real time Synchrophasor measurements from various substations located in the DVP system. The islanding module's major task is to perform an efficient online scheme, using pre-determined trigger points on critical measurements (i.e. increases in currents in transmission lines, changes in voltage phase angles of the network and unusual reactive power flows) to make islanding detection, location and qualification for such catastrophic failures.

4.1 Introduction of DVP System

Dominion Resources Inc., commonly referred to as Dominion, is a power and energy company headquartered in Richmond, Virginia that supplies electricity to parts of Virginia and North Carolina and supplies natural gas to parts of West Virginia, Ohio, Pennsylvania, and eastern North Carolina. Dominion also has generation facilities in Wisconsin, Indiana, Illinois, Connecticut and Massachusetts. The company's asset portfolio includes 27,000 MW of power generation, 6,000 miles (9,700 km) of electric transmission lines, 14,000 miles (23,000 km) of natural gas transmission, gathering and storage pipeline, and 1.2 trillion cubic feet (34 km^3) equivalent of natural gas and oil reserves [50]. One of its major electricity power distribution

companies is Dominion Virginia Power (DVP), which operates the electricity business inside Virginia.

As introduced in Section 1.2.3, the power generation and transmission system belonging to the DVP is mainly built on the Virginia Mountain territory and the operational and planning functions of Dominion's electric transmission system are provided by PJM Interconnection.

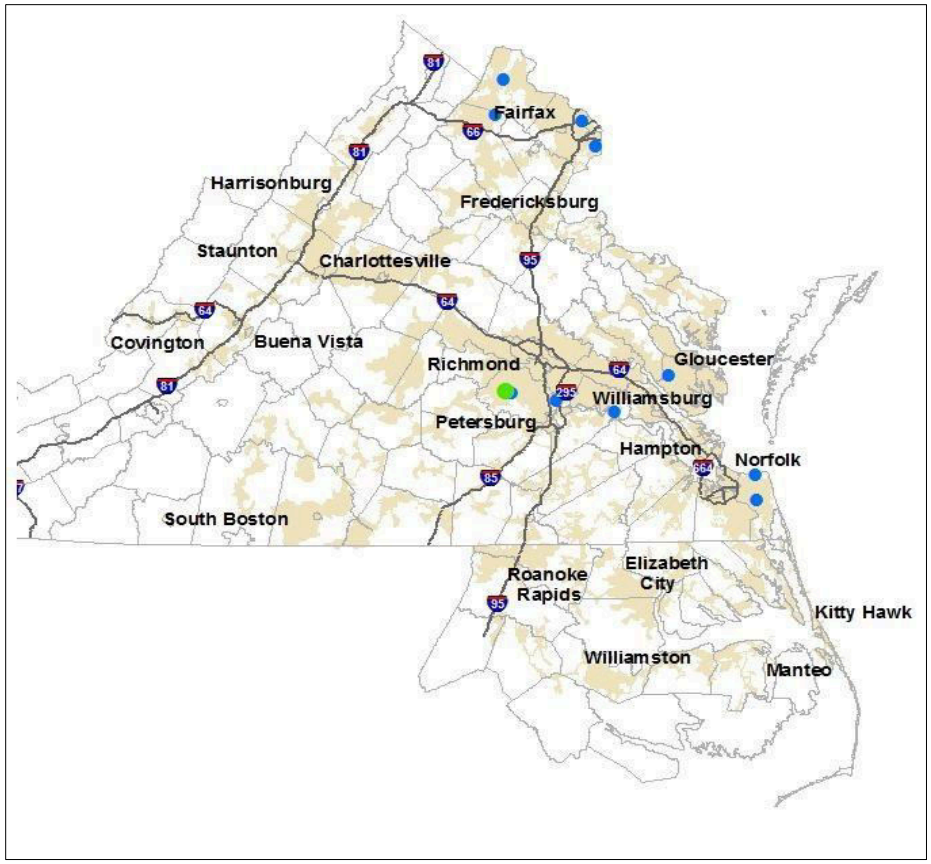

Figure 4.1: The Dominion Virginia Power Region

The DVP transmission system covers most of the Virginia and a part of the North Carolina regional territories, as shown in Fig. 4.1. It serves 2.5 million customers. The DVP system is connected with five other power utilities. They are the PJM Interconnection LLC (PJM), the Potomac Electric Power Company (PEPCO), American Electric Power (AEP), Allegheny Power (AP) and CPL Retail Energy (CPL&E). They all belong to the Eastern

Interconnection Reliability Assessment Group (ERAG). The operation regions of the DVP and its neighboring utilities are shown in Fig. 4.2.

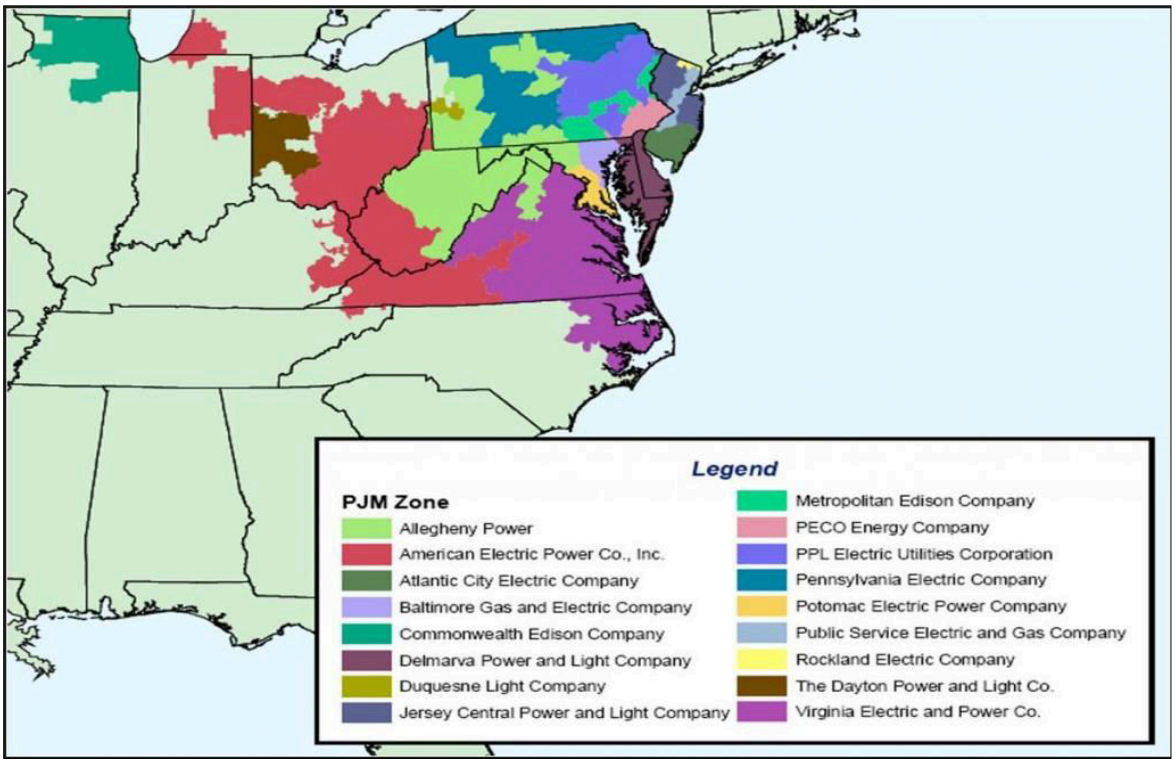

Figure 4.2: The PJM Region Zones [51]

The Dominion's generating facilities produce about 28,200 megawatts of electric power. The varieties of the generation fuel types include coal, hydro, nuclear and wind. TABLE 4.1 has listed the major stations.

TABLE 4.1: MAJOR SUBSTAIONS IN DOMINION

Station	Location	Primary Fuel Type
North Anna	Mineral, VA	Uranium
Surry	Surry, VA	Uranium
Mt. Storm	Mt. Storm, WV	Coal
Chesterfield	Chester, VA	Coal, Gas
Chesapeake	Chesapeake, VA	Coal
Clover	Clover, VA	Coal
Yorktown	Yorktown, VA	Coal, Oil
Bremo	Bremo Bluff,VA	Coal
Mecklenburg	Clarksville, VA	Coal

North Branch	Bayard, WV	Coal
Altavista	Altavista, VA	Coal
Southampton	Southampton, VA	Coal
Hopewell	Hopewell, VA	Coal
Possum Point	Dumfries, VA	Gas, Oil
Elizabeth River	Chesapeake, VA	Gas
Ladysmith	Ladysmith, VA	Gas
Bellemeade	Richmond, VA	Gas
Rosemary	Roanoke Rapids, NC	Gas
Darbytown	Richmond, VA	Gas
Bath County	Warm Springs, VA	Water
Gaston	Roanoke Rapids, NC	Water
Roanoke Rapids	Roanoke Rapids, NC	Water
Gordonsville	Gordonsville, VA	Gas

The Virginia Power system is geographically dispersed with major generation and load centers. And according to [17], there are some heavily loaded areas in the DVP system. They may become the major weak points during potential islanding conditions because these areas may face serious generation-load unbalanced situations. Besides, the Virginia Power system is located on the east coast of the United States, where is affected by windstorm and thunder storms. These severe weather conditions are major causes in tripping of heavily loaded transmission lines. One example of this vulnerability was Hurricane Irene which made its landfall over Eastern North Carolina's Outer Banks on the morning of August 27, 2011. This powerful Atlantic hurricane caused one of the major 500kV transmission lines in DVP to trip. Under certain circumstances, the heavy load situation and severe weather conditions may interact and result in additional cascading trips, forming island within the DVP areas. The decision of potential islanding areas is based on a consideration of these aspects.

In history, the DVP system was often influenced by bad weather situations: lightning, heavy winds, hurricanes, ice and snow. However no islanding situation has been experienced in the DVP. The closest case was a severe disturbance happened close to the Yorktown station.

Though no islanding has occurred, there is always a possibility and online fast-prediction to such catastrophic scenarios is essentially necessary.

4.2 Online Islanding Detection Module Schemes

4.2.1 Methodology

Figure 4.3 has illustrated the structure of the PMU application in Dominion including the islanding detection and protection strategy.

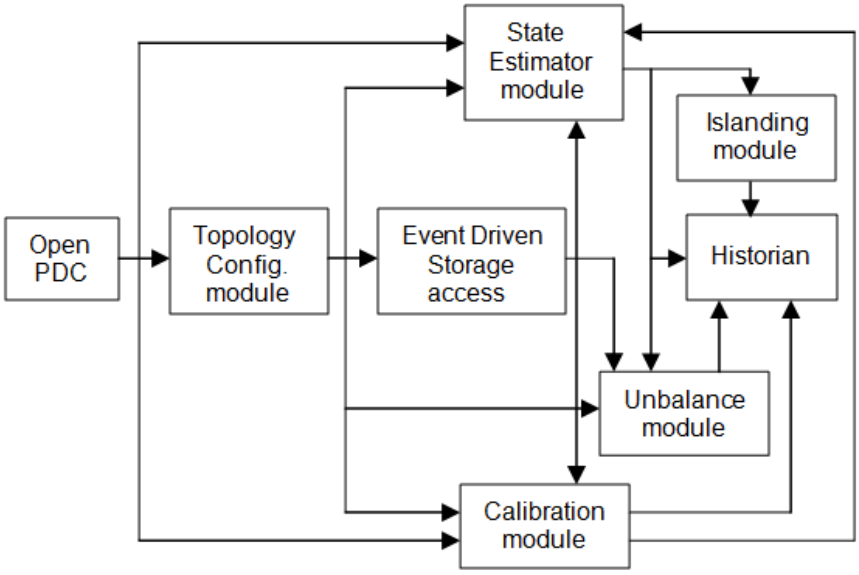

Figure 4.3: Structure of the Dominion Online System Monitoring and Protection Software

Real time PMU measurements are collected and transmitted back to the local server by an openPDC data concentrator. The raw data go through the processing stage in system topology configuration module, the calibration module and the state estimator module. The processed data are then used for islanding detection and state evaluation. The analyzed results are saved in historian module.

The proposed islanding detection methodology is part of the system monitoring and protection implementation. An investigation of possible islanding contingency cases in Dominion territory is carried out and the decision trees for islanding detection and identification are generated. However several aspects are modified subject to the practical condition in the

DVP system: 1) the determination of the potential islanding areas was primarily based on discussion and analysis of the geographical/electrical characteristics and historical cascading disturbance events in the DVP. According to the VT Power group and the Dominion group, three major areas were selected. 2) The PMU installation list and schedule for the DVP is well established and the islanding analysis focuses on this list. By the end of 2014, there will be 20 substations in the DVP system having PMUs implemented and the whole 500kV transmission network and portion of the 230/115kV network will be observable in real time. This study is primarily focused on the observed network to study the potential islanding events in the low voltage area.

Fig. 4.4 illustrates the decision tree based islanding detection and identification scheme that includes the following procedures:

1) The determination of the potential islanding locations; the DT analysis are carried out at three different regions in the DVP system. The three regions are named as Region-1: Newton station area, Region-2: Einstein and Dirac station area and Region-3: Franklin and Raphson station area.

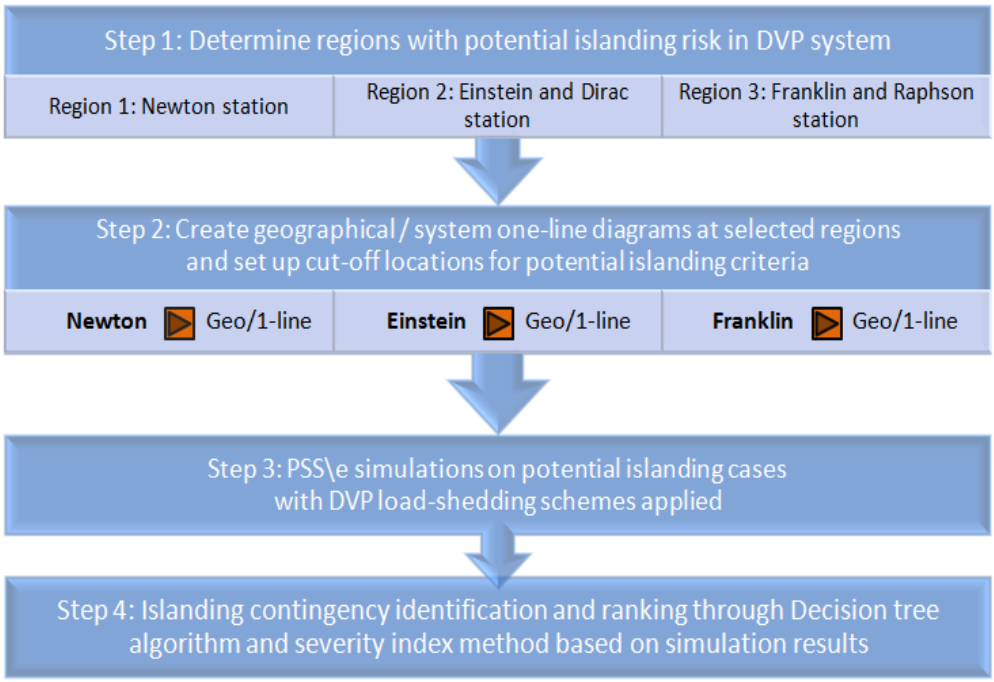

Figure 4.4: The DT Based Islanding Scheme Procedures

2) In each region, the system one line diagram and cut-off locations are created based on the geographical/electrical distribution. The detailed geographical map and islanding cut-off sections of location one can be seen in Fig. 3.6 and Fig. 3.7.

The decision of the island size is first performed based on the geographic map of Fig. 3.6. The isolated area analysis starts from the selected sub-station and radiates outwards. For each of the two directions, the transmission lines come out of the station circles with increasing radius which indicates a growth of the possible islanding area along the transmission paths. In the corresponding system one-line diagram shown in Fig. 3.7, the whole area is separated into four partitions (0-3) for a convenient load calculation. The partitioning determination is based on the system topology characteristics and load condition. The potential islanding regions are labeled by the cut-off locations using dotted lines.

3) Dynamic simulations are carried out for the three locations. When applying the simulation, the under-frequency load shedding scheme for DVP is considered. The scheme allows a maximum shedding of 30% of the total load during the protection operation. The time for communication delay and relay/breaker operation for each shedding is set to be 0.2833 sec. On the other hand, when the generation exceeds the load in an island, the intelligent generator shedding will apply, the excessive generation will be tripped if area frequency exceeds 61.8Hz for ten seconds or immediately when the frequency reaches 64.8Hz. Any island that fails to keep the area frequency beyond 58.5Hz after performing the load/generation shedding scheme is considered unstable.

4) To achieve the module's function, four decision tree sets are generated using different data sets. DT-1 is used to achieve a full area islanding detection and identification. It is also responsible for the location estimate, delivering input measurements to the correct sub-system DT for further operation. DT-2 to DT-4 are three sub-system DTs for the three locations that estimate: 1) the islanding stability condition, 2) the approximate islanded region size (isolated generation capacity). Because each tree set achieves two functions and each function requires a specific tree there are eight individual decision trees, while the trees in the same set share one common attribute dataset. Fig. 4.5 has illustrated the detailed online islanding module functions.

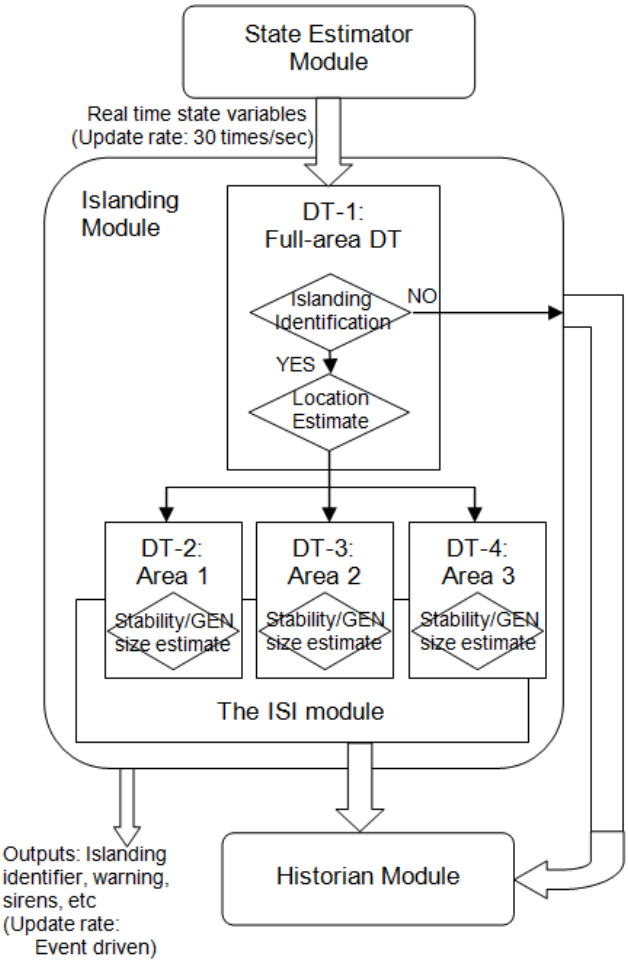

Figure 4.5: Flowchart of the Islanding Module Functions

DT-2, 3 and 4 are capable of estimating the stability condition of each event via the decision tree mechanism. Simultaneously, the updating system measurements are computed in the Islanding Severity Index module in real time and the results help make a stability judgment. The proposed module outputs include three channels: 1) one-digit identifier (0/1) for islanding contingency identification; 2) one-digit identifier (0-5) indicating estimated islanding locations (0 for non-islanding condition, 1-3 for each area, 4 for multiple area and 5 for unidentified); 3) one-digit identifier (0-5) indicating the severity estimate for the particular event; 5 indicates most severe. In the design of the visualization framework for the software, the specifically animated

flashing area signals and sirens are considered for the islanding warning purpose in the DVP full-loop geographical system diagram screen.

It is suggested to rerun the offline DT program, generating the updated DTs from modified database in the aid of the historian module. A suggested refreshing rate is no longer than once a month with minute contingencies and immediate after severe system disturbances/contingencies or significant structure changes.

4.3 Study of the Islanding Scenarios in DVP System

To initialize the database, a total of 678 islanding events were simulated and analyzed (130 cases for Area-1, 396 for Area-2 and 152 for Area-3, basing on their complexity). Together with 501 non-islanding cases (301 normal operation cases; 100 short circuit and rapid load changing fault cases and 100 line tripping cases), the size of the islanding database is 1179*87. (87 is the channel number of the simulation outputs). The attribute categories are voltage magnitudes, voltage angles and current phasors.

With the original islanding case database, it is possible to compute the prediction success for the original DTs. The specifics and prediction success are list in TABLE 4.2 and 4.3.

TABLE 4.2: DT SPECIFICS

DT name	DT1: Full DVP	DT2: Area 1	DT3: Area 2	DT4: Area 3
Total case #	1179	631	897	753
Islanding case#	678	130	396	152
Stable cases	-	126	271	84
Channel #	87	87	87	87

TABLE 4.3: DT PREDICTION SUCCESS

DT name		The DTs in Dominion			
		DT1: Full DVP	DT2: Area1	DT3: Area 2	DT4: Area 3
Islanding detection	Size	9	NA	NA	NA
	Learn	97.20			
	Test	95.67			
Location estimate	Size	13			
	Learn	99.07			
	Test	97.71			
Stability estimate	Size	NA	2	12	11
	Learn		100	93.43	89.92
	Test		100	90.40	80.92
GEN size estimate	Size		2	12	3
	Learn		100	80.56	100
	Test		100	74.24	98.68

In general, the full loop DTs achieves over 95% average success for both islanding identification and location estimate with the original data. The DT-2 achieves a high stability and GEN size estimate due to the simplicity of the area while the DT-3 performs high accuracy in stability estimate but 74% accuracy in GEN size estimate. The DT-4 has a moderate 81% stability estimate success and works well in GEN size estimate.

4.3.1 Decision Tree Analysis

A comparison has been taken among decision trees on their tree structure, composition, and diversity in this section, corresponding analysis is applied.

4.3.1.1 Decision Tree Size Analysis

The first comparison is about the tree size. DT-2 is simple in its structure and is excluded from the comparison. Fig. 4.6 indicates that all DT sets are rather similar in size. Tree-1 and Tree-2 refer to trees with different functionalities in one tree set. For DT-1, they are islanding detection and location estimate; for DT-2 to DT-4, they are stability estimate and power capacity estimate. To achieve a prediction success between 80%-100%, a tree needs to grow to around 12 nodes. This is not a bad score for decision trees. However, the simplicity (or complexity) of the tree is largely dependent on the corresponding complexity of the attribute dataset and the tree functionality. In the Dominion case, the tree size largely depends on the geographical complexity of the area and the power system diversity (i.e. the number of the plants and generators, the length and number of the transmission lines, the tie-line number of the area and the capacitor banks number, etc). Among the three locations, the area-2 has the largest power capacity and plant number, as well as the tie-line number. This is reflected in the total number for the two functional trees. The whole area tree is also respectively large in size due to the size of its dataset.

However the functions of DT-1 are different from the other trees thus the size of DT-1 is not far beyond sub-system trees.

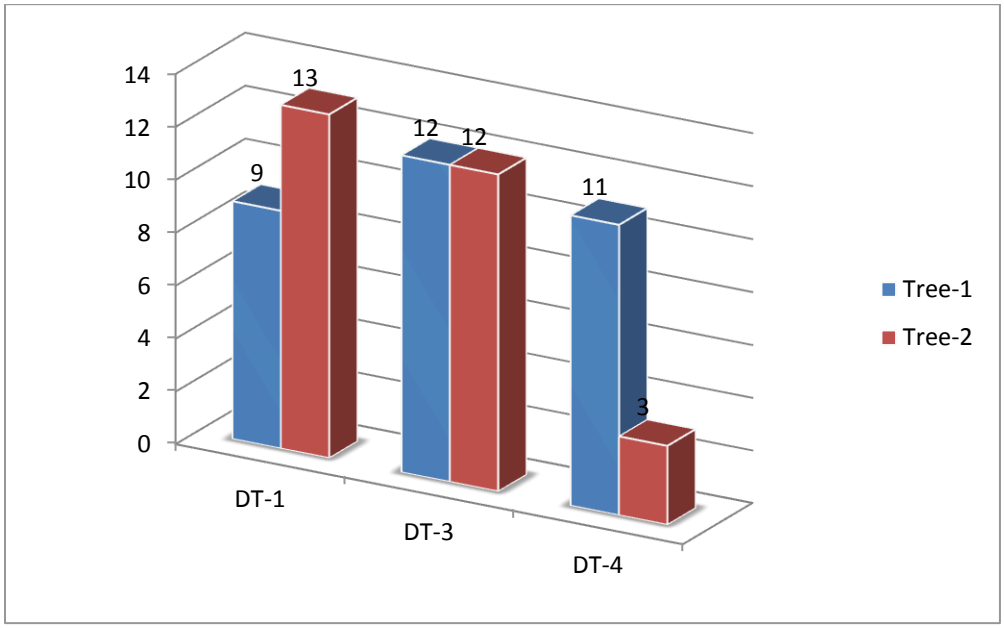

Figure 4.6: Decision Tree Size Comparison (after Prune)

In addition, the trees are manually pruned in order to achieve a balance between size and precision. Fig. 4.7 shows the original tree size comparison. It's easy to notice the Tree-2 in DT-3 and Tree-1 in DT-4 have the largest size. This indicates that CART may have difficulty generating highly converged trees using the present datasets. This is proofed by their low prediction success: 85%/75% un-pruned and 80%/74% pruned for Tree-2 in DT3, and 90.5%/82% un-pruned and 90%/82% pruned for Tree-1 in DT4. An 80% precision is still valuable for system state estimation and evaluation and could be used to implement the islanding judgment. If the system requires higher precision, two strategies can be used to modify the tree: 1) importing more cases into the dataset; 2) increase the attribute quantity. In decision tree principle, both strategies are designed to include more information about the system thus decrease the use of the twisted relationships among present attributes.

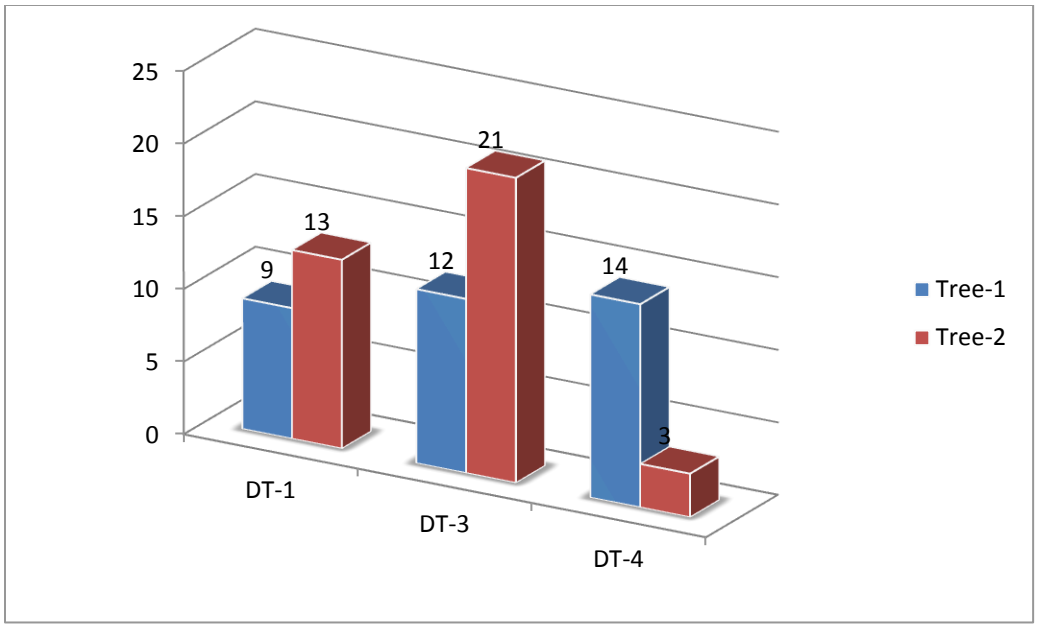

Figure 4.7: Decision Tree Size Comparison (before Prune)

4.3.1.2 Attributes Analysis

The second comparison relates the major splitting attribute types, still using the six decision trees in previous comparison. In this comparison, two calculations are performed: the major splitting attributes in formed tree and the important variables for all (including splitting points, surrogates and pruning).

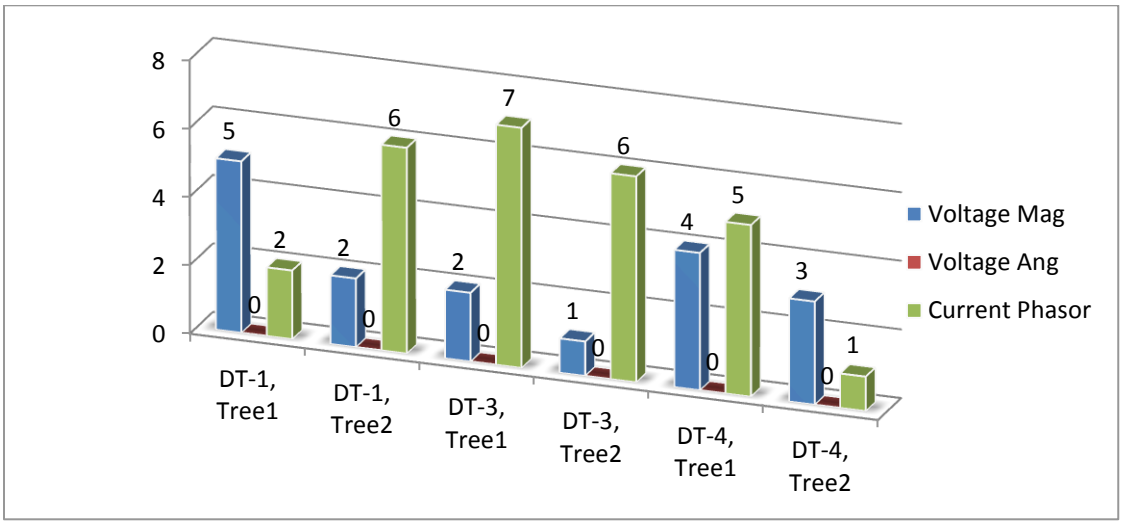

Figure 4.8: Decision Tree Attribute Type Comparison (Tree only)

The current phasor measurements exported from simulation software are complex values **X+jY**. Instead of using complex values, the current phasors are converted into single values using Fisher's method applied to phasor measurements [52] (will be discussed in Section 4.6). An analysis of the benefits using this transformation or polar form current phasors will be given in Section 4.6. The major attributes used to form the trees are voltage magnitude and current phase. By decision tree functions, the voltage magnitudes are used more than current phases in islanding detection while the current phases are most important judgments for islanding location estimate, stability estimate and power capacity estimate. The reason why voltage angles become less important is that the recorded inputs are at the 500kV network and they remain connected with the massive power system and keep stable after the initial oscillation when islanding occurs. Compared with angles, the current phasor and voltage magnitude changes are much more apparent, especially for buses near the boundaries of the isolation. CART automatically selects attributes with larger influences to build the tree, and to some extent, it has proven that the current phasor and voltage magnitudes are more important variables for islanding analytics.

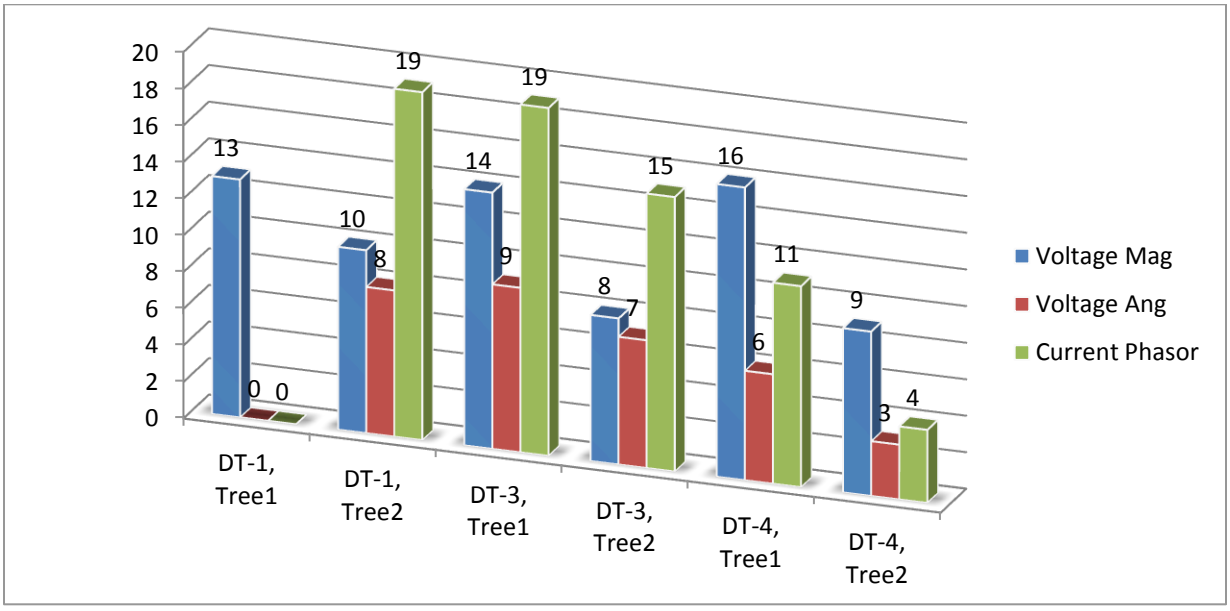

Figure 4.9: Decision Tree Attribute Type Comparison (for all)

Taking into consideration the important variables for all (including splitting points, surrogates and pruning), more attributes are involved in the tree formation. Shown in Fig. 4.9, the number of each attribute category is calculated. In such case, there are also voltage angle attributes that are selected as surrogates or back-up splitting points in the tree formation.

4.3.2 Islanding Variable Importance Analytics

With the benefit of decision trees, the appearance and importance of each Dominion's 500kV substation in the DT formation was calculated and analyzed. Shown in TABLE 4.4:

TABLE 4.4: SUBSTATION APPEARANCE IN DT FORMATION

Substation#	DT1-1	DT1-2	DT2-1	DT2-2	DT3-1	DT3-2	Rank
314900	1	1	1		1	1	A
314901					1		
314902	1	1		1	1	1	A
314903	1	1	1				C
314904	1	1	1				C
314905							
314906				1			
314907		1			1		
314908	1	1	1	1			B
314909							
314910		1					
314911		1	1	1			C
314912							
314913							
314914		1	1	1			C
314915			1				
314916		1	1				
314917			1				
314918			1	1			
314919					1		
314922						1	
314923			1				
314924			1	1	1		C
314925				1			
314926			1				
314927	1	1			1	1	B
314928	1	1	1	1	1	1	A

Among the 29 500kV substations and six decision trees, measurements from 3 locations are used by five DTs, 2 substations used four times and 5 substations used three times. The ten locations (314900, 314902, 314928, 314908, 314927, 314903, 314904, 314911, 314914 and 314924) are considered to be critical locations for Dominion Islanding detection.

Another calculation is carried out using the variable importance computation function from CART. For each variable in each tree, the software computes the relative importance of the variable and normalizes its value to the maximum variable.

TABLE 4.5: SUBSTATION IMPORTANCE IN DT FORMATION

Substation#	DT1-1	DT1-2	DT2-1	DT2-2	DT3-1	DT3-2	Total	Rank
314900	2.36	113.83	40.23		23.86		180.28	C
314901					56.24	45.76	102	C
314902	60.06	26.31		36.43	122.23		245.03	B
314903	5.36	7.49	10.93				23.78	
314904	9.6	1.33	83.02				93.95	
314905							0	
314906				16.63			16.63	
314907		2.02			73.46		75.48	
314908	5.36	66.48	73.21	100			245.05	B
314909							0	
314910		2.02					2.02	
314911		58.99	62.28	122.22			243.49	B
314912							0	
314913							0	
314914		26.31	65.79	40.56			132.66	C
314915			43.97			100	143.97	C
314916		100	40.23				140.23	C
314917			40.98				40.98	
314918			65.79	42.98			108.77	C
314919					23.86		23.86	
314922							0	
314923					42.53	100	142.53	C
314924				78.36	142.53		220.89	B
314925				12.97			12.97	
314926			40.98				40.98	
314927	104.22	89.94			91.54		285.7	B
314928	7.65	89.94	100	78.36	256.62		532.57	A

The substation importance to each tree and the total module is shown in TABLE 4.5. Based on the total value, ranks are also assign ranks to them and there are six locations reaching a value over 200%. They are 314928, 314927, 314908, 314902, 314911 and 314924. From another point of view, this calculation illustrates the order of importance for present substations in Dominion's islanding detection. This calculation counts every splitting point in the tree that if any location appears repeatedly the variable importance will also be computed repeatedly.

Both tests have demonstrated some common facts about the DT's variable importance in Dominion's islanding module.

1) Geographically, the measurements from the substations closer to the islanded area may contribute more in islanding detection and classification. Generally, during the faults, the nearby monitors are capable of collecting signals with more information and details about the voltage/current/frequency oscillation and drops than those monitor at far end. Substation 314928, 314902, 314924, and 314927 are located in places surrounded by three potential islanding regions thus they are ranked highest in DT formation.

2) Substations with tie-lines having high current transmissions may contribute more in islanding detection and classification. The sudden power drop of the isolated area causes great impact to the main power grid and those transmission lines carrying high power will mostly influenced.

4.4 Islanding Analysis with the Consideration of internal PMUs

In the future plans of the Dominion's PMU installation project, a few of 230/115kV substations/grids will have PMU installed. For islanding consideration, this indicates that a wider variety of measurements and locations can be used in the decision tree algorithms. In this section, a selected set of islanding contingency simulations with additional 230/115kV measurement outputs are run and analyzed. The modified simulations cover all three locations in the previous analysis. It should be noticed that in this section all current phasors are used in polar form.

4.4.1 DT Improvement Test: Region-1

In this test, a few internal PMUs are added at critical locations (plants, large loads, major power-flow injection buses…etc.) at lower voltage level (115KV/230KV) in Region-1. The additional PMUs measure the local bus' voltage phasors, current phasors and frequencies.

TABLE 4.6: INTERNAL PMUS IN REGION-1

Selected PMU location (Bus number)		Voltage level	Area #	Priority
Generator bus	314422	115KV	1	1
	314423	230KV		
Large load	314373	115KV	1	3
Large load	314413	230KV	1	3
Large load	314421	230KV	1	3
Large load	314398	230KV	1	3
Large load	314406	115KV	1	3
Transformer bank	314401	115KV	1	3
	314402	230KV		
Transformer bank	314406	115KV	1	3
	314407	230KV		
Transformer bank	314417	115KV	1	3
	314418	230KV		

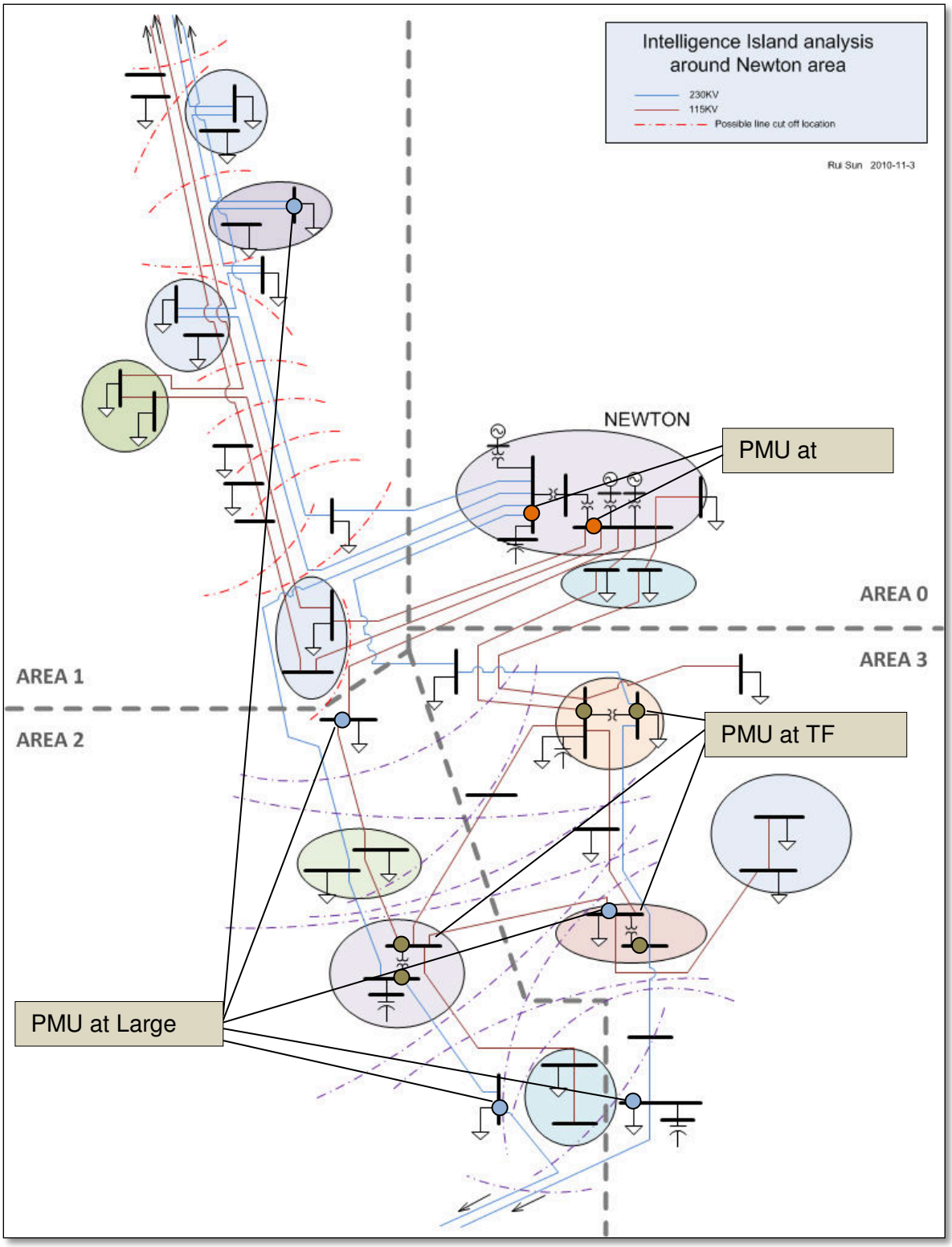

Figure 4.10: Internal PMU monitors in Region-1

A total of 9 internal locations are selected in this test due to their importance. The same islanding simulations are run and decision trees for islanding detection for Region-1 are generated using the enlarged dataset. The DT relative cost comparison is shown in Fig. 4.11.

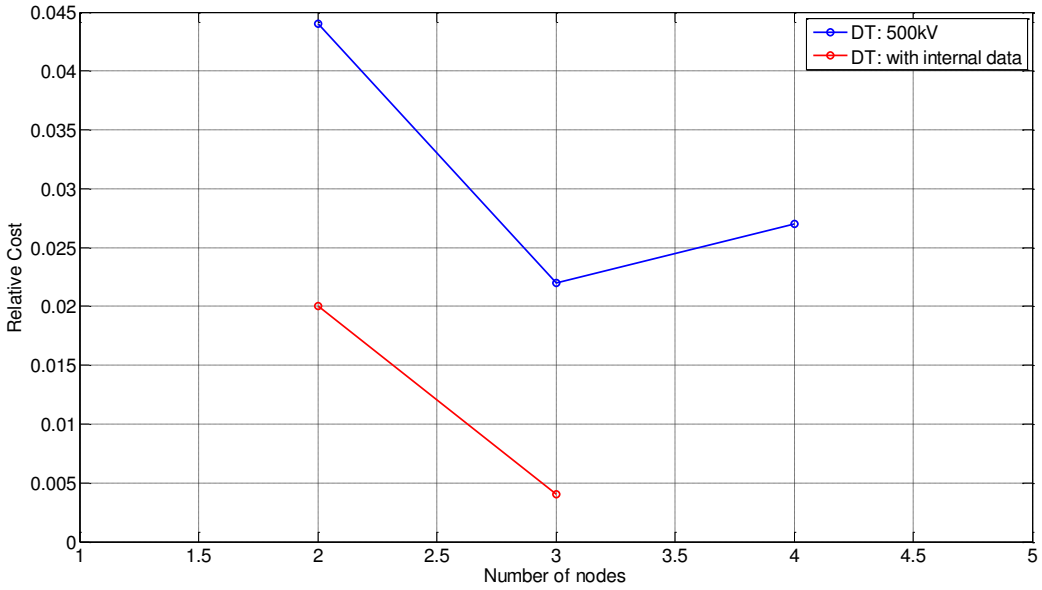

Figure 4.11: DT relative cost comparison in Region-1

With the modified dataset, the prediction success of islanding detection for Region-1 are 99.21%/98.73% for learn/test group with only 500kV measurements and 99.84%/99.68% with internal PMUs. At the same time, the tree sizes are both 3 nodes for optimal placement. This indicates both trees have high precision in islanding detection.

Another comparison is taken place on the variable importance. We can notice the internal channels are selected as variable importance when they contain more useful information.

TABLE 4.7: VARIABLE IMPORTANCE COMPARISON – REGION-1

DT with only 500kV data		**DT with lower voltage data**	
Variables	**Score**	**Variables**	**Score**
I_MAG_314923_314924	100.00	A314407	100.00
A314923	96.84	A314406	100.00
I_ANG_314915_314923	92.29	I_MAG_314923_314924	96.85
I_ANG_314902_314906	91.77	A314923	93.79

I_ANG_314904_314919	86.66	V314413	92.54
I_MAG_314911_314918	82.15	A314401	90.83
I_ANG_314914_314918	5.34	V314924	3.67
V314914	4.50	V314906	3.67
I_ANG_314900_314905	4.50	V314915	3.67
V314909	4.50	V314914	3.67
V314906	4.50	V314909	3.67
V314915	4.50	V314903	3.67

The voltage angle measurements could help in determination of the isolated area. We rank the islanding region at the Region-1 as 5 levels with respect of the load values.

TABLE 4.8: REGION-1 ISLANDING AREA RANK (A)

Islanding region rank	**Region included**	**Load condition (MW+jMVar)**
Level 1	Newton Station, K1, K2, K3, K, K5, K6, K7, K8, K9	413.2 - j54.9
Level 2	Level 1 + K10, K11, K12, K13, K14, K15	787.2 - j14.9
Level 3	Level 2 + K16, K17, K18, K19	971.8 - j66.6
Level 4	Level 3 + K20, K21, K22	1227.5 + j21.1
Level 5	Level 4 + K23, K24, K25	1466 + j73.6

And with the installation of PMUs at the local transmission network, specific locations inside the island could be monitored and the islanding level could be easily measured.

TABLE 4.9: REGION-1 ISLANDING LEVEL DETECTION (B)

Islanding region rank	**PMU Placement**						
	K25	K10	K12	K16	K17	K20	K22
Level 1	√	√	√	○	○	○	○
Level 2	√	√	√	○	○	○	○
Level 3	√	○	○	√	√	√	√
Level 4	√	○	○	○	○	√	√
Level 5	√	○	○	○	○	√	√

√ = Critical judgment; ○ = Useful judgment.

4.4.2 DT Improvement Test: Region-2

For Region-2, the major comparison is made upon the GEN size estimate, which is not very well determined by the original tree. In this test, 10 locations at lower voltage level (115KV/230KV) in Region-2 have PMU monitors implemented. The original dataset fails to offer adequate information for the DT so that the DT prediction success falls to 80%. With the internal system measurements, the new tree achieves a prediction success to 100%. It's a great leap in estimate success and the new tree only requires 5 nodes to complete the prediction.

TABLE 4.10: REGION-2 ISLANDING GEN SIZE ESTIMATE COMPARISON

	DT with only 500kV data		**DT with lower voltage data**	
	Learn	Test	Learn	Test
% Overall correct	86.62	74.24	100	100

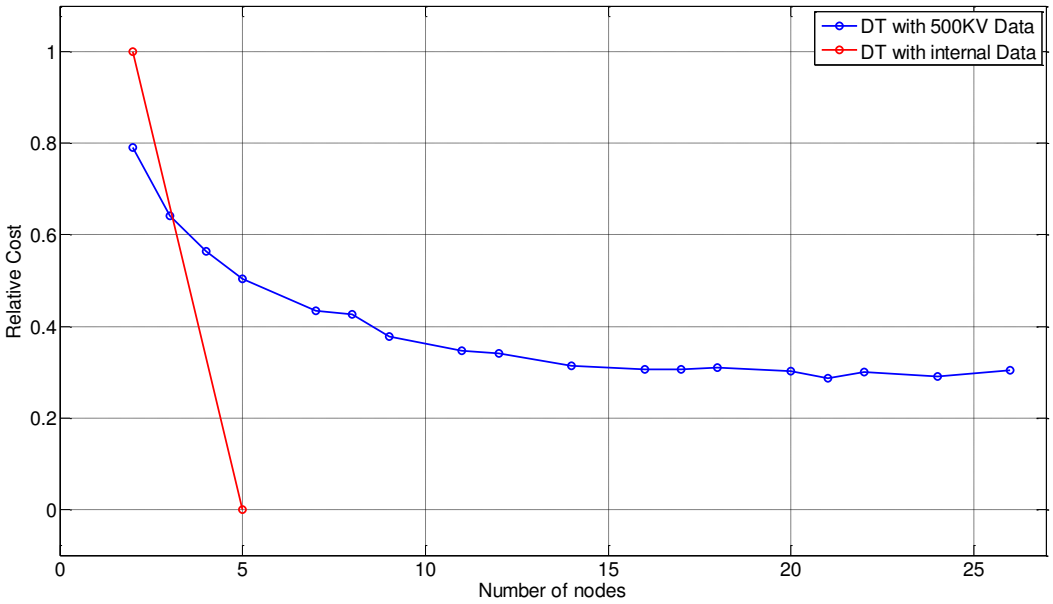

Figure 4.12: DT relative cost comparison in Region-2

The test results indicate that the local PMU measurements could offer important information of system operation behaviors during islanding scenarios. According to the analysis of system variable importance for both trees, we notice the local voltage magnitudes and angles, along with the frequency parameters are essential measurements in GEN size estimation.

TABLE 4.11: VARIABLE IMPORTANCE COMPARISON – REGION-2

DT with only 500kV data		DT with lower voltage data	
Variables	**Score**	**Variables**	**Score**
A314906	100.00	A314275	100.00
I_ANG_314924_314928	66.43	F314275	95.88
V314908	32.85	V314275	55.40
I_MAG_314908_314911	32.53	A314906	38.53
I_MAG_314909_314923	27.28	V314254	33.33
V314900	22.77	A314254	33.33
I_ANG_314902_314928	20.84	A314274	33.33
V314916	20.11	V314276	33.33
V314919	19.83	A314289	33.33
I_ANG_314914_314918	16.38	V314289	30.76
A314909	15.34	I_ANG_314924_314928	22.19
I_ANG_314923_314924	12.91	I_MAG_314909_314923	19.15
A314927	12.02	F314289	18.18
A314903	11.99	V314236	16.98
I_ANG_314911_314918	11.18	I_MAG_314919_314922	14.49
V314914	11.16		
V314902	10.57		
A314914	10.54		
I_MAG_314900_314916	10.23		
I_ANG_314915_314923	9.70		

4.4.3 DT Improvement Test: Region-3

In this test, 11 locations at lower voltage level (115KV/230KV) in Region-3 have PMU monitors implemented and the DT analysis is carried out. The original DT reached 99.8% precision in islanding detection, so the most apparent improvement comes from the stability

estimate. According to Fig. 4.13 and TABLE 4.12, with the enlarged dataset, the tree size largely decreased (from 12 nodes to 3 nodes) while the precision raises over 10% (from 80-90% to 98%).

TABLE 4.12: REGION-3 ISLANDING STABILITY ESTIMATE COMPARISON

	DT with only 500kV data		**DT with lower voltage data**	
	Learn	Test	Learn	Test
% Overall correct	94.08	78.95	100	98.03

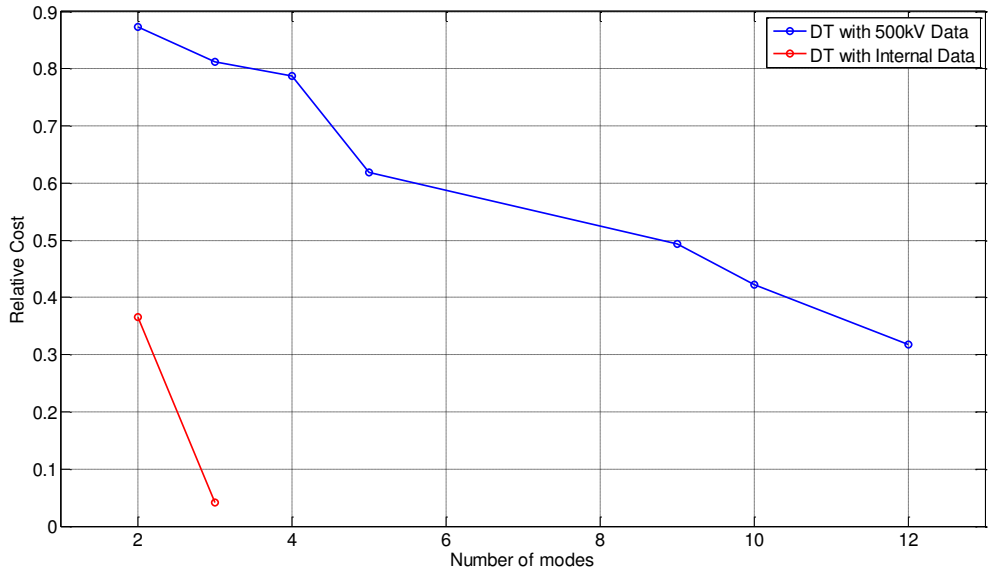

Figure 4.13: DT stability estimate comparison in Region-3

The improvement largely results from the usage of the internal frequency (phasor angle) measurements. The major variables used to form the new tree are frequency measurements for the great oscillation and phase shifts during the transients. By analysis it was proved that the internal PMUs could offer essential information for the islanding detection and qualification, especially for island stability estimation and size estimation. Yet there are other concerns that need to be solved:

1) Can the local PMU measurements help to judge the entire system's islanding situation? (i.e. an islanding occurs in other area)

2) What are the most proper locations for local PMU implementation with consideration of the entire system? (Introducing the local measurements to the whole system DT)

To solve these questions, a further investigation and analysis is needed thorough the re-simulation of the whole system.

4.5 Islanding Analysis with the Light Load Model

In this section, how the differences of the system operational conditions will contribute to the programmatic model simulation, analytics and decision tree formation in Dominion is analyzed.

In Chapter 3, the model used for DVP simulation and decision tree scheme was introduced. The major study system used is a modified MMWG 57,000 Bus Eastern Coast Power Grids model. In this model, the Dominion Transmission System operates on the edge of its power capacity. While in real world, the power generation and consumption are always dynamic. One power system has its summer and winter load peaks and tends to follow certain annual operation cycles. On the other hand, its everyday operation behavior also follows certain curve. Fig. 4.14 shows the annual load demand peaks for the DVP from 1997 to 2011.

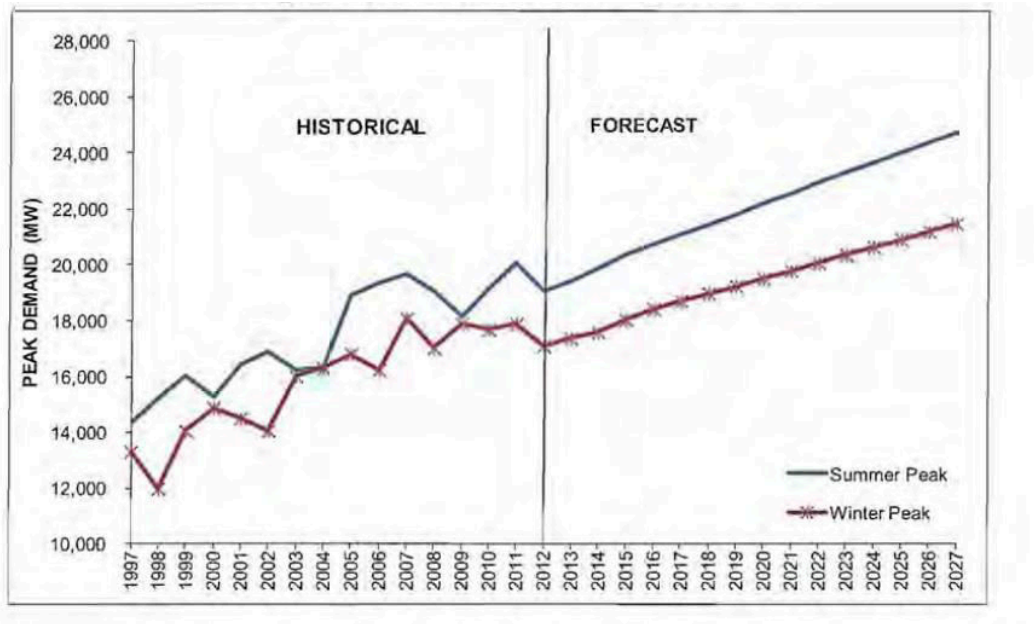

Figure 4.14: Annual Peak Load Demand for DVP [53]

The maximum load demand mostly occurs in summer whose power consumption is the highest during a one year period. The power demand in winter is relatively mild and is very different from the summer. Similarly, the daily load demand follows another curve, respectively.

Normally, this dynamic behavior is not simulated by the power flow analysis since the system load model is fixed. Thus it may be inadequate if only the fixed load model is used for the system analysis for the lack of describing system's dynamic operating conditions. In this section, the decision tree scheme in system islanding detection is studied using different load models. As introduced earlier, the model works under Dominion's "Summer Heavy load" condition. Based on the present model, a modified "summer light-load" model is created applying percentage load decrements. Certain capacitor banks, transformer taps and model dynamic parameters are tuned in order to maintain the bus voltage and angles. The light-load model operates approximately at 65% of the heavy load model.

The simulation is carried out on Region-1. The same 130 islanding contingency cases with 500 non-islanding cases are repeated in the same way as in Section 4.4.1. Two data sets are used for decision tree generation. They are the:

1) Voltage and current phasors at all external PMU locations.

2) Voltage and current phasors at all external PMU locations and voltage, current and frequency channels at internal (potential) PMU locations.

The current attributes are in polar form.

The new DTs have distinct differences from the heavy-load model DTs, yet they still share some common characteristics. For this analysis, a comparison is made among the new DTs and DTs used for Section 4.41. A total of four decision trees are compared.

TABLE 4.13: REGION-1 ISLANDING STABILITY ESTIMATE COMPARISON

		Heavy load model		Light load model	
		500kV Channel DT	DT with Internal PMUs	500kV Channel DT 1	DT with Internal PMUs
Tree Size		3	3	2	2
Variable Importance #		12	12	6	6
Direct Variable Importance #		2	2	1	1
Prediction success	Learn	99.21%	99.84%	99.68%	99.68%
	Test	98.73%	99.68%	99.37%	99.37%

According to the simplicity of Region-1, each tree has a fairly good prediction success and small tree size. However, through comparison it can be seen that the DTs formed using "light-load model" cases have higher precision and fewer nodes, which means the system parameters are more distinct for islanding detection under light load condition.

The comparison is mostly based on the variable importance of the trees.

TABLE 4.14: VARIABLE IMPORTANCE COMPARISON – REGION-1

DT with only 500kV data				DT with lower voltage data			
Heavy load		**Light load**		**Heavy load**		**Light load**	
Variables	**Score**	**Variables**	**Score**	**Variables**	**Score**	**Variables**	**Score**
I_MAG_314 923_314924	100.00	I_MAG_314 901_314926	100.00	A314407	100.00	I_MAG_314 901_314926	100.00
A314923	96.84	I_MAG_314 901_314912	99.60	A314406	100.00	I_MAG_314 901_314912	99.60
I_ANG_314 915_314923	92.29	I_MAG_314 911_314918	98.41	I_MAG_314 923_314924	96.85	I_MAG_314 911_314918	98.41
I_ANG_314 902_314906	91.77	I_MAG_314 919_314922	98.02	A314923	93.79	I_MAG_314 919_314922	98.02
I_ANG_314 904_314919	86.66	V314925	97.24	V314413	92.54	V314925	97.24
I_MAG_314 911_314918	82.15	V314916	96.85	A314401	90.83	V314916	96.85
I_ANG_314 914_314918	5.34			V314924	3.67		
V314914	4.50			V314906	3.67		
I_ANG_314 900_314905	4.50			V314915	3.67		
V314909	4.50			V314914	3.67		
V314906	4.50			V314909	3.67		
V314915	4.50			V314903	3.67		

TABLE 4.14 lists the variable importance for each decision tree formation. The two DTs for light-load condition are the same; they have the same tree structure and variables. The two DTs for heavy-load condition share several common attributes in tree formation. However, there is only a slight relation between DTs of two models. Thus the two sets of DTs are almost irrelevant.

The test results raise one important issue: will the lack of the dynamic system operational behaviors cause the DT algorithm to miss certain important system measurements in islanding detection? The answer is yes. However this issue can be greatly compensated by many aspects:

First, on the analytics side, although it is impossible to consider all system operating conditions in the simulation stage, the tests can be applied on several typical operating condition models, i.e. the summer heavy-load, summer light-load, winter heavy-load, winter light-load, and etc. Different models of different seasons indicate not only load demand changes, but also different line & generation operating schemes, protection schemes and power injection conditions. The more detailed models are used in decision tree database, the wider the range of conditions and information that can be implemented into the islanding scheme.

Second, for the utilities' practical usage, the islanding module is designed to be capable of selecting the most proper DTs depending on its operating scheme, while all DTs are pre-generated during the offline procedure using different models. The islanding module modification is also dynamic. As discussed in Section 4.2.1, the tree is suggested to be updated every month to follow certain changes on system topology and projected maintenances. While in operation, the historian module brings in database the real-world data, increasing the data's accuracy and the trees' credibility.

Last but not least, the heavy-load model is more suitable for islanding analysis than the light-load model. Taking into consideration the power system strain level, a system is easier to collapse under heavy-load condition than working in the light-load mode while facing the same amount of stress. Many islanding cases (i.e. the 1973 Gulf coast area islanding) have demonstrated that the disturbances occurred while the transmission networks were under the peak-load demands, which weakened the systems stability margin. Besides load condition, the climate condition is another consideration. Summer and winter are two hostile seasons that are easier for islanding contingencies to occur (see TABLE 4.15).

TABLE 4.15: NERC ISLANDING CASES OCCURANCE

Total case analyzed:		19
Season	Summer (6,7,8,9)	9
	Winter (11,12,1)	7
Hour	Peak hour (10-23)	10
	Off peak hour	7

4.6 Analysis of Fisher's method applied to Islanding DT Attributes

In Section 4.3, decision trees are generated and analyzed for islanding detection and identification, stability estimate and island size estimate. In Section 4.4 and 4.5, DTs using low voltage network parameters and light load model are introduced. There's a difference between them, the current attributes of the former case DTs are in single value form converted by the Fisher's method, while for the latter DTs they are in polar form. In this section, the principle and usage of the Fisher's method applied to phasor measurements in DT algorithm is discussed. The test results using the Fisher's method and polar form for attributes are compared and analyzed.

CART uses a non-parametric decision tree learning technique that is especially suited to power systems due to the complex non-linear behavior of the system. CART data is in the form of an array with rows being the events/outcomes and columns being the measurements. In its simplest form, CART picks one measurement at a time for performing binary splits. While this is very effective in handling data having invariate attributes, difficulties are observed when handling multi-modal classifications consisting of multivariate data. Traditionally, CART makes decisions based on a single attribute. However, because phasor data has two components, both must be considered simultaneously to make correct decisions. Furthermore, it has been determined that there is a need to make multi-class distinctions instead of only binary splits. Therefore, a methodology was developed that extended the use of Fisher's Linear Discriminant (FLD) to perform splits on high dimensional, multi-class data [52, 54]. In principle, while using the Fisher's method applied to the phasor measurements new attributes are formed through a linear transformation of one or multiple related phasor attribute pairs (which are directly obtained from simulations or real measuring process). The new attributes contain the characteristics of multiple existing phasor attributes and when used to form the decision trees by

replacing the existing phasor attribute pairs, they keep the tree from making decision only on single attribute from the pairs and to some extent raise the prediction success of the DTs.

In islanding analysis, along with the normal polar form current measurements, the Fisher's method is analyzed and the results are compared with the original data. TABLE 4.16 shows the comparison in both the tree prediction success and variable importance. The analysis used both Region-2 and Region-3.

TABLE 4.16: DT PREDICTION SUCCESS COMPARISON – PREDICTION SUCCESS

DT name		DT-3: Region-2		DT-4: Region-3	
		Fisher's method	Polar form phasor	Fisher's method	Polar form phasor
Stability estimate	Size	12	9	11	12
	Learn	93.43	93.43	90.13	94.08
	Test	90.40	87.88	82.24	78.95
GEN size estimate	Size	24	21	3	3
	Learn	85.35	86.62	100	100
	Test	75.51	74.24	98.68	98.68

TABLE 4.17: DT VARIABLE IMPORTANCE COMPARISON – GENSIZE

DT-3: Region-2		DT-4: Region-3	
Fisher's method	Polar form phasor	Fisher's method	Polar form phasor
I_314908_314911	A314906	I_314915_314923	A314927
I_314900_314905	I_ANG_314924_314928	I_314902_314915	A314928
I_314924_314928	V314908	V314901	I_MAG_314924_314928
V314908	I_MAG_314908_314911	V314922	I_MAG_314915_314923
I_314905_314911	I_MAG_314909_314923	V314907	I_MAG_314902_314915
I_314902_314906	V314900	V314912	A314909
I_314904_314919	I_ANG_314902_314928	V314926	I_ANG_314911_314922
I_314902_314914	V314916	A314902	I_ANG_314908_314911
I_314911_314918	V314919	A314903	A314906
V314903	I_ANG_314914_314918	V314903	I_ANG_314917_314926
I_314919_314922	A314909	V314904	A314902
I_314914_314918	I_ANG_314923_314924		I_ANG_314919_314922
A314902	A314927		
A314927	A314903		

A314909	I_ANG_314911_314918	
A314923	V314914	
A314915	V314902	
I_314915_314923	A314914	
I_314902_314915	I_MAG_314900_314916	
V314925	I_ANG_314915_314923	

TABLE 4.18: VARIABLE IMPORTANCE COMPARISON – STABILITY

DT-3: Region-2		**DT-4: Region-3**	
Fisher's method	Polar form phasor	Fisher's method	Polar form phasor
I_314902_314914	I_ANG_314902_314906	A314901	A314903
I_314924_314928	I_ANG_314903_314908	I_314924_314928	I_MAG_314902_314928
V314904	V314902	V314902	A314902
V314919	A314914	A314902	A314900
V314916	I_ANG_314902_314914	V314901	I_MAG_314907_314912
V314913	I_MAG_314914_314918	V314926	A314901
V314908	I_ANG_314917_314926	V314912	A314915
I_314923_314924	I_ANG_314923_314924	V314907	A314906
V314900	I_ANG_314907_314926	A314900	A314904
I_314914_314918	V314915	I_314927_314928	I_ANG_314902_314914
I_314908_314911	A314928	V314906	I_ANG_314903_314908
V314902	A314909	I_314902_314914	I_ANG_314924_314928
V314923	A314927	V314903	I_MAG_314901_314912
V314915	V314928	V314910	I_ANG_314914_314918
V314924	I_ANG_314900_314919	I_314902_314906	I_ANG_314907_314910
I_314917_314926	I_ANG_314907_314912	V314925	I_ANG_314919_314922
I_314900_314916	I_MAG_314902_314914	I_314903_314908	V314907
I_314902_314914	I_ANG_314901_314926	A314909	V314926
I_314924_314928	I_ANG_314907_314910	I_314902_314928	I_ANG_314902_314915
V314904	I_MAG_314909_314923	V314909	A314908

Comparison results have clearly shown that trees generated by both methods (original polar phasor attributes and single attribute generated by Fisher's method) have similar size and prediction success. Furthermore, trees of both methods share around 50% of the same most important attributes in formation. If we only consider the critical PMU locations in Dominion, the consistency could reach over 70%. The results indicate that in islanding analysis, using either method will not cause great differences in DT formation and islanding detection. The DT prediction success will not significantly improve or decrease.

Checking the precision rates in TABLE 4.16, the Fisher's method has slightly higher performance for test groups of DT-3 island size estimate, DT-3 and DT-4 stable estimate. Thus the Fisher's method is chosen for the islanding module in Dominion.

CHAPTER 5: CONCLUSION & DISCUSSION

5.1 Conclusion

In this dissertation, two major studies are concerned and presented. The first study is the power system islanding contingency detection, identification, classification and state evaluation algorithm using a decision tree algorithm and topology approach (Ch-2, 3), and its application in Dominion Virginia power system (Ch-4); the second study is the optimal PMU placement strategy using a binary integral programming algorithm (BIPA) (Ch-2, 3).

In the first study**,** the proposed power system islanding contingency detection, identification, classification and state evaluation method is composed of an intelligent decision tree scheme whose function is based on a database of the system's dynamic simulations, historical operation and contingency records, and system's geographical information.

To create the islanding contingency database, system operations and islanding contingencies are obtained through historical records of real events and program-generated simulations. In the islanding contingency simulation procedure, two schemes are used: The System Islanding Detecting Strategy (SIDS) distinguishes islanding cases from normal system operations and from other contingencies through a system incidence matrix computation. The modified enumeration method is used to select reasonable size of the islanded area with respect of the system geographical and electrical topologies. The collected data based on real world records and simulations (mostly the real-time dynamic system voltage/current/frequency state variables) are used as attributes in the intelligent decision tree formation.

The DTs are classification trees generated from the database using the CART (Classification and Regression Trees) commercial software package. They are supposed to

achieve following results: a) to distinguish an islanding scenario from other system events as short circuits, line-tripping or generator-tripping only basing on the state variables changes from outside the island; b) to estimate the stability condition of the island and locate the approximate islanded area; and c) to help determine the PMU placements for better islanding detection and identification.

In the islanding stability assessment process, besides the DT algorithm, the proposed method includes an Island Severity Index (ISI) which qualifies the long term and transient behavior of the islanded system. The transient index qualifies the instantaneous impact of the isolation from the main grid and the severity of the transient. The long term severity index determines how severely the system's operating status will vary from the normal operating criteria with all possible protection schemes carried out after a certain period of time.

In chapter three, the islanding method and decision trees are tested. The modified enumeration method is tested on the IEEE-14, 30, 54, 118 and 300 bus system models. The test results show that this method is a good substitute of the enumeration method, while applied in small scale system. When the system complexity increases, this method is more efficient in detecting and discarding unreasonable combinations and it has a faster computation time.

The decision tree algorithm has been tested on several system models including a modified MMWG 57,000 Bus Eastern Coast Power Grids model which is specially revised for this project. The selection of islanding locations is made on the system model within Dominion Virginia Power (DVP) territory. The formation of the database includes state variables from simulations of 190 islanding contingency cases and 300 non-islanding contingency and normal operating cases using Python compiled PSS\E (32.03 version). Test results from the full data set show that a full-size tree using 10-fold cross validation method can achieve 98% accuracy for

islanding detection, which is fairly good in prediction success. A successive study of the islanding characteristics is also carried out in Chapter 3. Three types of islanding categories are distinguished and analyzed.

The islanding severity index (ISI) is tested as well. The simulations were narrowed into one smaller region which is considered to be the most potential islanding location in the DVP. With the simulation of 130 islanding cases within the selected area, a curve-fitting approach is used to simulate the frequency oscillations of the isolated area to help demonstrate how the index ranks the severity of islanding events. Test results show a highly dependence relationship between index values and islanding severity for both indices (long-term and instant). Proved by the curve fitting scheme, the index values were shown to be distinct enough to identify severe islanding scenarios, especially unstable ones.

In the second study, the optimal PMU placement strategy using binary integer programming algorithm is mainly focused on system generator bus coverage and redundancy problems. In Chapter three, it is tested on IEEE-14/30/39/57/118/300 BUS and WECC-128 BUS system models under various conditions including the optimal placement, redundant problem and islanding consideration. For each condition, the BIPA method has proven its fastness, accuracy and easiness for programming features.

In the second part of the dissertation, the practical utilization of the decision tree algorithm based islanding scheme in the Dominion Virginia Power (DVP) system is introduced and analyzed. For the DVP system, an investigation of possible islanding contingency cases in Dominion territory is carried out based on the geographical information and topology distribution of the Virginia's transmission grids. The potential islanding areas are selected based on the discussion and analysis of the geographical/electrical characteristics and historical

cascading disturbance events in the DVP. The islanding contingency database was created through simulations carried out on the selected areas, with current/voltage/frequency state variables from the fixed scheduled PMU installation locations of the DVP system. The decision tree algorithm created DTs achieving functions including the full area islanding detection and identification; the location estimate which delivers input measurements to the correct sub-system DT for further operation; the islanding stability condition, and the approximate islanded region size (isolated generation capacity). A total of 678 islanding events together with 501 non-islanding cases are simulated and analyzed. The full loop DTs achieves over 95% average success for both islanding identification and location estimate with the original data. The DT-2 achieves a high stability and GEN size estimate due to the simplicity of the area while the DT-3 performs with high accuracy in stability estimate but 74% accuracy in GEN size estimate. The DT-4 has a moderate 81% stability estimate success and works well in GEN size estimate.

In Chapter four, comparisons and analysis were performed among decision trees on the tree structure, composition, and diversity. The major tree's size are compared and analyzed with respect to the complexity of the area. Tests indicate the current phasor and voltage magnitudes are the most important variables for the DTs. Analysis has also covered the critical splitting points and variable importance, using them in determining the critical locations for the islanding detection. In addition, studies about the internal PMU measurements and different load-demand situations are also introduced in Chapter four. The comparison of DT results using only external PMUs and internal measurements clearly indicate the great improvement in the DT's accuracy and structure for the latter. Tests also reflect a moderate change in DT structure, size and prediction success when different load condition models are used.

The major contributions and achievements in the researches are listed as follows:

1. The islanding algorithm:
    1) Developing and testing an Islanding detection, classification and state evaluation algorithm with the usage of Decision Tree algorithm in islanding judgment determination;
    2) Developing and testing the islanding database formation method basing on simulated islanding/non-islanding system operation cases with the usage of the islanding detecting strategy and modified depth-first method;
    3) Developing and testing an index method for islanding severity ranking.
2. The Dominion online Islanding module:
    1) Developing and adjusting a detailed load-flow/dynamic system model for Dominion basing on existed MMWG and Dominion PSS\e system models;
    2) Appropriately selecting and studying potential islanding regions in DVP system , applying dynamic islanding simulations and creating an islanding database for DVP system;
    3) Generating and testing specific Decision Trees for Dominion with the function of islanding detection, location judgment, stability estimation and size evaluation;
    4) Applying analytics on the Dominion islanding simulation results and DT module, including DT size and attributes, DT variable and Dominion PMU importance, internal PMU contribution, the influences to the DTs with variant system models, and an assessment of the Fisher's method in DT operation.
3. The optimal PMU placement method:
    1) Deriving and evaluating some theorems in PMU placement analysis;

2) Analyzing the PMU placement with the consideration of islanding issue;
3) Developing and testing a binary integer programming algorithm in optimal PMU placement with the consideration of redundancy and islanding issue.

5.2 Discussion & Future Research

In above chapters, the proposed power system islanding detection, identification, classification and evaluation scheme using the decision tree algorithm and topology approach and the optimal PMU placement strategy using binary integral programming algorithm are well introduced, analyzed and tested. During the research process, some issues related the principle of the methods or specific experimental step were raised and are worth to be discussed.

The first issue relates to the selection of the islanded area. As we can see in Chapter three, the tests of the method and in Chapter four, the DVP islanding module, two different schemes for forming the islanding contingency cases are implemented. In the former case, the islanding scenarios are generated through the System Islanding Detecting Strategy and the modified enumeration method, which are exclusively based on the system topology structure. This is an apparent and normal scheme to analyze the method for any given study system especially if it is fake. Therefore no more practical geographical/electrical information could be used or real operation/fault events could be analyzed. While in the DVP module, the islanding areas are selected basing on the geographical/electrical characteristics and historical cascading disturbance events. The second case is more reasonable for real world power grids analysis due to the complexity of the transmission system.

The second issue for discussion and future research is the state variables selection in the DT formation. The assumption that all PMU measurements located in the high voltage level is made upon the present U.S. synchrophasor device implementation status. In most utilities and ISO/RTOs, the PMUs are only installed at certain critical substations or high voltage transmission buses. The coverage of PMU monitors still remains low that no full observability is achieved in any regional level power grids. This means a shortage of real-time synchronized

phasor measurements in islanding detection. However, with the increase of synchrophasor installation and digital communication development, the observability coverage raises and some devices are also installed at lower voltage level. This will definitely benefit the islanding detection and evaluation scheme while additional system information is accessed. Furthermore, PMU measurements inside the island could be used in islanding area and severity determination and islanding restoration.

A third topic is the attribute types of the DT algorithm. The attributes presently used for analysis are mainly system voltage and current phasor measurements, and frequency measurements in certain tests. When the simulated polar form phasor measurements are used, they are exactly the same as the channel outputs from a real world PMU. However, a transform of data formats using the Fisher's method is also discussed and tested. This method is developed to be slightly better for DT application by solving the related attributes splitting problem and in the analysis, has slightly improvement in DT islanding detection.

The last and probably the most important issue is the variance of the simulated islanding cases from the real islanding scenarios. In other words, how precise could the decision trees generated from simulated islanding database behave when they are used to detect and identify real islanding disturbances? The test of different models in Chapter four indicates that the change of system load-demands and topology will largely influence the DT formation. The presently used power flow programs by utilities and ISO/RTOs can analyze the system operation behaviors at a quite precise level. However, no matter how accurate the system model is or how often the model data are updated, they cannot duplicate 100% the system and estimate its operation behaviors in transients. What need and can be done, on one side, is to ensure that the system model to be as accurate as possible and that the simulations are taken place in a correct

way with reasonable consideration of system specifics. On the other hand, for system with operation cycles, the simple analysis with static model is not enough. A correct and effective decision tree needs a thorough study of the system dynamics and transients. The real disturbances and fault cases are good supplements, the more cases and information in database, the more robust the DTs will be. However it is a little bit unrealistic for islanding analysis, because 1) there are not enough historical islanding events for analysis, 2) islanding simulations requires huge amount of research works.

In the future research the focus should include:

1) Generalization of the islanding detection and identification method to other power systems. Successive experiments may be carried out on WECC system models; as the power network that have the most islanding events in history, its specifics must be analyzed.

2) Further study of islanding disturbances under different load-demand conditions. The common behaviors of islanding scenarios on different models should be recognized, and DTs should be updated with respect of the load changing cycles.

3) Further study of the usage of low voltage PMU measurements in islanding detection, especially the frequency measurements. Look for solutions in islanding restoration procedure using the frequency measurements; broaden the functions of the islanding module for Dominion.

REFERENCES

[1] NERC Annual Disturbance Report – 1992, North America Electric Reliability Corporation.
[2] NERC Annual Disturbance Report – 1993, North America Electric Reliability Corporation.
[3] NERC Annual Disturbance Report – 1994, North America Electric Reliability Corporation.
[4] NERC Annual Disturbance Report – 1996, North America Electric Reliability Corporation.
[5] NERC Annual Disturbance Report – 1996, North America Electric Reliability Corporation.
[6] NERC Annual Disturbance Report – 1997, North America Electric Reliability Corporation.
[7] NERC Annual Disturbance Report – 1998, North America Electric Reliability Corporation.
[8] NERC Annual Disturbance Report – 1999, North America Electric Reliability Corporation.
[9] NERC Annual Disturbance Report – 2001, North America Electric Reliability Corporation.
[10] NERC Annual Disturbance Report – 2002, North America Electric Reliability Corporation.
[11] NERC Annual Disturbance Report – 2003, North America Electric Reliability Corporation.
[12] NERC Annual Disturbance Report – 2004, North America Electric Reliability Corporation.
[13] NERC Annual Disturbance Report – 2005, North America Electric Reliability Corporation.
[14] NERC Annual Disturbance Report – 2006, North America Electric Reliability Corporation.
[15] NERC Annual Disturbance Report – 2009, North America Electric Reliability Corporation.
[16] N. J. Balu; H. W. Mosteller; "Lotdys Analysis of August 1973 Gulf Coast Area Power System Disturbance", 1979 Power Industry Computer Applications Conference
[17] H.B. Ross, N. Zhu, J. Giri, B. Kindel, " An AGC Implementation for System Islanding and Restoration Conditions," IEEE Trans. on Power Systems, vol. 9, No. 3, August 1994
[18] Galvan, F.; Mandal, S.; Thomas, M.; "Phasor Measurement Units (PMU) instrumental in detecting and managing the electrical island created in the aftermath of Hurricane Gustav", Power Systems Conference and Exposition, 2009. PES '09. IEEE/PES, 15-18 March 2009 Page(s):1 – 4
[19] Kolluri, S.; Mandal, S.; Galvan, F.; Thomas, M.; "Island formation in entergy power grid during Hurricane Gustav"; Power & Energy Society General Meeting, 2009. PES '09. IEEE, 26-30 July 2009 Page(s):1 – 5
[20] Wikipedia, "Phasor Measurement Unit", http://en.wikipedia.org/wiki/Phasor_measurement_unit
[21] Yilu Liu, Lamine Mili, Jaime De La Ree, Reynaldo Francisco Nuqui, "State Estimation and Voltage Security Monitoring Using Synchronized Phasor Measurement", Research paper from work sponsored by American Electric Power, ABB Power T&D Company, and Tennessee Valley Authority (Virginia Polytechnic Institute and State University). Retrieved 2008-12-01
[22] Hashiesh, F.; Mostafa, H.E.; Mansour, M.M.; Khatib, A.-R.; Helal, I.; "Wide area transient stability prediction using on-line Artificial Neural Networks", Electric Power Conference, 2008. EPEC 2008. IEEE Canada, 6-7 Oct. 2008 Page(s):1 – 7
[23] Senroy, N. ; Heydt, G.T. ; Vittal, V. ; "Decision Tree Assisted Controlled Islanding", Power systems, IEEE Transaction on, Volume 21, Issue 4, Nov. 2006 Page(s):1709 – 1797
[24] Ruisheng Diao ; Vittal, V. ; Kai Sun ; Kolluri, S. ; Mandal, S. ; Galvan, F. ; "Decision Tree Assisted Controlled Islanding for Preventing Cascading Events" Power Systems Conference and Exposition, 2009. PSCE '09. IEEE/PES, 15-18 March 2009, Page(s): 1 – 8

[25] K. Sun, T. S. Sidhu and M. Jin, "Online Pre-Analysis and Real-Time Matching for controlled splitting of Large-Scale Power Networks", IEEE Trans. Power Syst, Vol. 18, No. 4, Nov. 2003, Page(s): 1556–1565.

[26] K. Sun, D. Z. Zheng, Q. Lu, "Splitting strategies for islanding operation of large-scale power systems using OBDD-based methods," IEEE Trans. Power Syst, Vol. 18, No. 2, May. 2003, Page(s): 912–923

[27] C. Singh and I. A. Hiskens, "Direct assessment of protection operation and non-viable transients," IEEE Trans. Power Syst., vol. 16, no. 3, pp. 427–434, Aug. 2001.

[28] T.; Yasuda, T.; Takahashi, O.; Kaminaga, M.; Imai, S.; "Islanding protection system based on synchronized phasor measurements and its operational experiences, Ohno", Power and Energy Society General Meeting - Conversion and Delivery of Electrical Energy in the 21st Century, 2008 IEEE, 20-24 July 2008 Page(s):1 – 5

[29] Rui Sun, Zhongyu Wu, Virgilio A. Centeno, "Power System islanding Detection and Identification Strategy using Topology Approach and Decision Tree", Power & Energy Society General Meeting, *2011. PES '11. IEEE, July 24*-29, 2011

[30] Rui Sun, "Voltage Stability Indices Based On Active Power Transfer Using Simulated Phasor Measurements", Master's Thesis, Clemson University, 2009

[31] Joe H. Chow; Aranya Chakrabortty; Murat Arcak; Bharat Bhargava; Armando Salazar, "Synchronized Phasor Data Based Energy Function Analysis of Dominant Power Transfer Paths in Large Power Systems", Power Systems, IEEE Transactions on Volume 22, Issue 2, May 2007 Page(s):727 – 734

[32] Yanfeng Gong; Schulz, N.; Guzman, A., "Synchrophasor-Based Real-Time Voltage Stability Index", Power Systems Conference and Exposition, 2006. PSCE '06. 2006 IEEE PES, Oct. 29 2006-Nov. 1 2006 Page(s):1029 – 1036

[33] Marek Zima, "Wide Area Monitoring System: for which purposes?", 8th International Workshop on Electric Power Control Centers, Les Diablerets, Switzerland, 5-8 June 2005

[34] Ishibashi, A.; Imai, M.; Omata, K.; Sato, S.; Takagi, T.; Nakachi, Y.; Ogawa, S.; *"New type of* islanding detection system for distributed generation based on voltage angle difference between *utility network and distributed generation site"*, Developments in Power System Protection, 2004. Eighth IEE International Conference on, Volume 2, 5-8 April 2004 Page(s):542 - 545 Vol.2

[35] Ming Zhou; Centeno, V.A.; Phadke, A.G.; Yi Hu; Novosel, D.; Volskis, H.A.R.; "A preprocessing method for effective PMU placement studies", Electric Utility Deregulation and Restructuring and Power Technologies, 2008. DRPT 2008. Third International Conference on, 6-9 April 2008 Page(s):2862 – 2867

[36] Nuqui, R.F. and A.G. Phadke, "Phasor measurement unit placement techniques for complete and incomplete observability". Power Delivery, IEEE Transactions on, 2005. **20**(4): p. 2381-2388.

[37] Classification and regression trees. 1984, Belmont, Calif: Wadsworth International Group. x, 358 p.

[38] L. Wehenkel, Automatic Learning Techniques in Power Systems. Norwell, MA: Kluwer, 1998.

[39] Mori, H. "State-of-the-art overview on data mining in power systems." Power Engineering Society General Meeting, 2006. IEEE. 2006.

[40] Emanuel E. Bernabeu, "Methodology for a Security-Dependability Adaptive Protection Scheme based on Data Mining", PhD Dissertation, Virginia Tech, 2009

[41] CART Training Manual, Salford Systems, 2001

[42] Wikipedia, "Incidence Matrix", http://en.wikipedia.org/wiki/Incidence_matrix

[43] Wang, H. ; Thorp, J.S.; "Optimal Locations for Protection System Enhancement: A Simulation of Cascading Outages", Power Delivery, IEEE Transactions on, Volume 16 , Issue 4 Oct 2001Pages(s): 528 – 533

[44] Ismail Musirin; Titik khawa Abdul Rahman, "On-Line Voltage Stability Based Contingency Ranking Using Fast Voltage Stability Index (FVSI)", Transmission and Distribution Conference and Exhibition 2002: Asia Pacific. IEEE/PES, Volume 2, 6-10 Oct. 2002 Page(s):1118 - 1123 vol.2

[45] M. Nizam; A.Mohamed; A. Hussain, "Dynamic Voltage Collapse Prediction on a Practical Power System Using Power Transfer Stability Index", Research and Development, 2007. SCOReD 2007. 5th Student Conference on, 12-11 Dec. 2007 Page(s):1 – 6

[46] Balamourougan, V.; Sidhu, T.S.; Sachdev, M.S., "Technique for online prediction of voltage collapse Generation", Transmission and Distribution, IEE Proceedings, Volume 151, Issue 4, 11 July 2004 Page(s): 453 – 460

[47] Wikipedia, "Tabu Search", http://en.wikipedia.org/wiki/Tabu_Search

[48] F. Glover and C. McMillan (1986). "The general employee scheduling problem: an integration of MS and AI". Computers and Operations Research.

[49] Wikipedia, "Genetic Algorithm", http://en.wikipedia.org/wiki/Genetic_Algorithm

[50] Wikipedia, "Dominion Resources", http://en.wikipedia.org/wiki/Dominion_Resources#Dominion_Virginia_and_North_Carolina_Power

[51] SREC, "PJM Region", http://www.srectrade.com/blog/srec-markets/new-jersey/pjm-region

[52] MaxWelling, "Fisher Linear Discriminant Analysis", http://www.cs.huji.ac.il/~csip/Fisher-LDA.pdf

[53] Dominion Annual Report, Chapter two, Load Forecast

[54] Anamitra Pal, J. S. Thorp, Taufiquar Khan, and S. Stanley Young, "Classification Trees for Complex Synchrophasor Data", submitted to Electric Power Components and Systems

[55] O. Mansour, A.A. Metwally, and F. Goderya,"Systematic Determination of Power System Network Topology", paper submitted for the 1979 Winter Power Meeting, Newo York, N.Y., Jan., 1979.

[56] F. Goderya, "Fast Detection and Identification of Islands in Power Networks", IEEE Trans. on Power Apparatus and Systems, Jan/Feb 1980, pp. 217-221.

[57] H. You, V. Vittal, and X. Wang, "Slow coherency-based islanding," IEEE Trans. Power Syst., vol. 19, no. 1, pp. 483–491, Feb. 2004.

[58] H. You, V. Vittal, and Z. Yang, "Self-healing in power systems: An approach using islanding and rate of frequency decline based load shedding,"IEEE Trans. Power Syst., vol. 18, pp. 174–181, Feb. 2003.

APPENDIX

Appendix A: Major Power System Disturbances involving Islanding

PEPCO (Washington, D.C.) Load Loss, January 6, 1992 [1.4]

This disturbance started at 17:04 P.M. EST on Monday, January 6, 1992. It caused the loss of 335 MW of customer load in downtown Washington, D.C., supplied by the Potomac River Generating Station. A shunt reactor switching device at Blue Plains Substation malfunctioned and created an external arc which blown down to an adjacent 230 kV transmission circuit and caused short circuits. This made both of the two 230 kV underground transmission circuits to trip thus disconnecting the Potomac River Generating Station and its PEPCO load to the rest of the PEPCO transmission system. "An incorrect frequency reading in the control room at the Potomac River Generating Station led the power plant personnel to respond incorrectly while trying to balance generation and load to restore 60 Hz operation. This resulted in an under-frequency condition, which caused shutdown of the generating station and loss of the load that it was serving."[1.4] The disturbance resulted in the interruption of service to approximately 18,000 customers in Washington, D.C. and it took three hours to the load. The incorrect operation was partially due to the misleading of the non well-designed alarm system. "Since over-frequency and under-frequency conditions cause the same alarm in the generating station control room, the power plant personnel did not differentiate the over-frequency indication from the under-frequency condition."[1.4]

Peninsula Florida Disturbance, March 12, 1996 [1.7]

This disturbance occurred in Peninsula Florida on March 12, 1996 that created an electrical island in west Florida and portions of central Florida. The separation was resulted from multiple conditions. Firstly, planned and forced generation outages. Although according to a review that on March 12 there were 4,793 MW of capacity reserves within Peninsula Florida available, among them over 1,585 MW of generation was on planned maintenance and 1,677 MW on forced outage or restricted output, resulting in 3,262 MW of generation unavailable in the western region. Due to the planned and forced outages in west Florida that day and unseasonably cool temperatures, electricity transfers from north and northeast Florida into west and west central Florida were higher than normal and resulted in overloads on portions of central Florida's 230 kV and 115 kV transmission system. This caused one 230 kV line tripped and the loads began to exceed limits one by one. The operators of FPC, FPL and OUC achieved several protecting operations including peaking generations, opening lines and tying units to certain lines. This successfully reduced the power intension in some extent. However these operations did not prevent the catastrophic event to happen. "The series of events described above left west Florida and portions of central Florida as an island with about 12,588 MW of demand and 9,932 MW of generation." To make things worse, the island's generation further reduced to 9,148 MW due to the loss of one plant. The island's frequency dropped to about 58.65 Hz, and under frequency relays within the island operated decrease demand. A total of 3,440 MW (27%) was shed and the system frequency within the island was restored to 59.7 Hz in six seconds. "Synchronizing relays at the Ft. White substation reclosed within 90 seconds and the island was tied back to the rest of Florida's interconnected system."

WSCC System Disturbances, July 2&3, 1996 [1.7]

A disturbance occurred at 14:24:37 MDT on July 2, 1996 that ultimately resulted in the Western Systems Coordinating Council (WSCC) system separating into five regions and in electric service interruptions to over two million customers.

Region 1 included California, Baja California, southern Nevada, Arizona, New Mexico, and El Paso Island. Within Island 1, frequency dropped to 59.1 Hz and under frequency load shedding occurred. A total of about 4,484 MW were shed affecting about 1,183,000 customers. Over 90% of the demand was restored within 30 minutes and all demand was restored within 21/2 hours. **Region 2** included Washington, Oregon, Montana, British Columbia, and Alberta. About 3,900 MW of generation was automatically removed from service in this island by over frequency relays and by the remedial action scheme that monitors the California -Oregon Intertie. Impact on customers was minimal. An estimated 7,452 customers (100 MW) were interrupted over a period ranging from minutes to about one hour. **Region 3** included Utah, Colorado, Wyoming, western Nebraska, and western South Dakota. While islanded with Arizona/California, the frequency dropped to 59.2 Hz and as much as 3,348 MW of demand was shed, mostly due to under frequency, along with over voltage and manual load shedding. After separating from Arizona/California, the frequency went as high as 61.1 Hz and 2,000 MW of generation was removed from service in the island for various reasons. The frequency remained high for about six minutes. With demand restoration, generation ramping down, and 2,000 MW of generation removed from service, the frequency again fell as low as 59.3 Hz. This drop resulted in under frequency load shedding followed by additional demand being manually shed in the island in an effort to restore proper frequency. The under frequency load shedding operated as designed and frequency recovered to 59.35. At this time, various generators under

frequency protection schemes began timing (59.4 Hz for 180 seconds). The frequency remained at 59.35 Hz for 120 seconds and leveled off at 59.5 Hz. **Region 4** was formed in southern Idaho and a small part of eastern Oregon where virtually all customer demand and generation was interrupted. About 3,368 MW of demand (425,000 customers) was interrupted. Idaho Power Company lost all customer demand in Idaho and radially served demand located in northern Nevada as well as a small part of eastern Oregon. **A fifth island** was formed in northern Nevada at 14:25:09 July 2nd. Before electric service restoration could be completed, SPP demand dropped 550 MW. Of this amount, about 418 MW was shed during the transient frequency and voltage dips, which coincided with an electricity surge going through northern Nevada toward southern Idaho.

WSCC System Disturbance, August 10, 1996 [1.7]

A major disturbance occurred in the Western Interconnection (Western Systems Coordinating Council, WSCC) at 1548 PDT, August 10, 1996 resulting in the Interconnection separating into four electrical islands. Conditions prior to the disturbance were marked by high summer temperatures (near or above 100 degrees Fahrenheit) in most of the Region, by heavy exports (well within known limits) from the Pacific Northwest into California and from Canada into the Pacific Northwest, and by the loss of several 500 kV lines in Oregon.

North Island consisted of Oregon, Washington, Idaho, Montana, Wyoming, British Columbia, Utah, Colorado, Western South Dakota, Western Nebraska, and Northern Nevada. PacifiCorp lost about 450 MW of customer demand, interrupting service to 154,000 customers in portions of southern and central Oregon, and northern California.

Northern California Island. Frequency within the Island dropped to 58.3 Hz eight minutes into the disturbance. The under frequency load shedding program within this island removed all ten blocks of customer demand, representing about 50% of the Northern California demand. The Northern California Island lost 7,937 MW of generation and 11,602 MW of demand (about 2.9 million customers). Connections to southern California were restored at 1847 when the Midway – Vincent No.1 and No.3 lines were returned to service. The Midway – Vincent No.2 line was returned to service at 1848. By 2154, 91% of the PG&E customers had electric service restored; all customers had electric service restored by 0100 on August 11.

Southern Island consisted of Southern California, Arizona, New Mexico, Southern Nevada, Northern Baja, California Mexico, and El Paso, Texas. Generation totaling 13,497 MW was removed from service, along with 15,820 MW of customer demand (about 4.2 million customers). The frequency in the Southern Island remained below 60 Hz for over an hour. As the frequency in the island began to recover and several key units in the island returned to service, system demand restoration began at 1657. The frequency returned to normal at 1655. By 2142, all the demand shed in the Southern Island was restored.

Alberta Island. At 1544, about five minutes after the Northern Island separated from the rest of WSCC, the British Columbia Hydro and Power Authority (BCHA) to Alberta interconnections (138 kV and 500 kV) opened, separating the Alberta system from the North Island. At the time of the separation, the Interconnection was supplying 1,230 MW to Alberta. Frequency in the Alberta Island dipped to 59.0 Hz. In this island, 146 MW of generation was removed from service and 968 MW of demand was shed by under frequency load shedding, affecting 192,000 customers. Alberta resynchronized with British Columbia at 1629. Electric service was restored to all customers by 1739.

Appendix B: Study System Model Introduction

IEEE-39 New England System

The IEEE 39-Bus "New England" Power System has a base unit of 100 MVA and is a 1 area system. See Figure A.1.

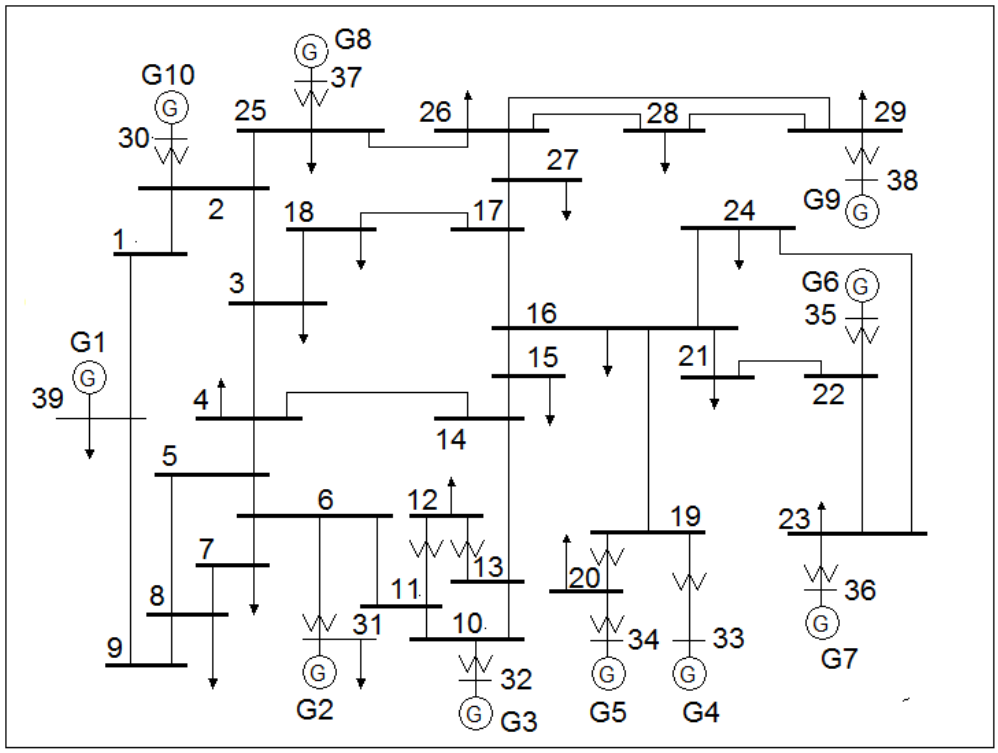

Figure A.1: IEEE 39-Bus System

B.1 Bus Data and Power data settings

All values are given based on 100 MVA. Note that generator 2; Bus No.39 is the swing node.

TABLE A.1: IEEE 39-BUS SYSTEM BUS DATA AND POWER FLOW DATA

Bus	Type	Voltage [PU]	Load		Generator		
			MW	MVar	MW	MVar	Unit No.
1	PQ	-	0.0	0.0	0.0	0.0	
2	PQ	-	0.0	0.0	0.0	0.0	
3	PQ	-	322.0	2.4	0.0	0.0	
4	PQ	-	500.0	184.0	0.0	0.0	
5	PQ	-	0.0	0.0	0.0	0.0	
6	PQ	-	0.0	0.0	0.0	0.0	
7	PQ	-	233.8	84.0	0.0	0.0	
8	PQ	-	522.0	176.0	0.0	0.0	
9	PQ	-	0.0	0.0	0.0	0.0	
10	PQ	-	0.0	0.0	0.0	0.0	
11	PQ	-	0.0	0.0	0.0	0.0	
12	PQ	-	7.5	88.0	0.0	0.0	
13	PQ	-	0.0	0.0	0.0	0.0	
14	PQ	-	0.0	0.0	0.0	0.0	
15	PQ	-	320.0	153.0	0.0	0.0	
16	PQ	-	329.0	32.3	0.0	0.0	
17	PQ	-	0.0	0.0	0.0	0.0	
18	PQ	-	158.0	30.0	0.0	0.0	
19	PQ	-	0.0	0.0	0.0	0.0	
20	PQ	-	628.0	103.0	0.0	0.0	
21	PQ	-	274.0	115.0	0.0	0.0	
22	PQ	-	0.0	0.0	0.0	0.0	
23	PQ	-	247.5	84.6	0.0	0.0	
24	PQ	-	308.6	-92.0	0.0	0.0	
25	PQ	-	224.0	47.2	0.0	0.0	
26	PQ	-	139.0	17.0	0.0	0.0	
27	PQ	-	281.0	75.5	0.0	0.0	
28	PQ	-	206.0	27.6	0.0	0.0	
29	PQ	-	283.5	26.9	0.0	0.0	
30	PV	1.0475	0.0	0.0	250.0	-	Gen10
31	SWING	0.9820	9.2	4.6	-	-	Gen2
32	PV	0.9831	0.0	0.0	650.0	-	Gen3
33	PV	0.9972	0.0	0.0	632.0	-	Gen4
34	PV	1.0123	0.0	0.0	508.0	-	Gen5
35	PV	1.0493	0.0	0.0	650.0	-	Gen6
36	PV	1.0635	0.0	0.0	560.0	-	Gen7
37	PV	1.0278	0.0	0.0	540.0	-	Gen8
38	PV	1.0265	0.0	0.0	830.0	-	Gen9
39	PV	1.0300	1104.0	250.0	1000.0	-	Gen1

B.2 Machines data settings

Parameters for the two-axis model of the synchronous machines are shown in Tables as follows. All values are given in a base of 100 MVA. And the reactive power limits are set from -500MVar to 1000MVar.

TABLE A.2: IEEE 39-BUS SYSTEM MACHINE DATA

Unit No.	H	Ra	x'd	x'q	xd	xq	T'do	T'qo	xl
1	500.0	0	0.006	0.008	0.02	0.019	7.0	0.7	0.003
2	30.3	0	0.0697	0.170	0.295	0.282	6.56	1.5	0.035
3	35.8	0	0.0531	0.0876	0.2495	0.237	5.7	1.5	0.0304
4	28.6	0	0.0436	0.166	0.262	0.258	5.69	1.5	0.0295
5	26.0	0	0.132	0.166	0.67	0.62	5.4	0.44	0.054
6	34.8	0	0.05	0.0814	0.254	0.241	7.3	0.4	0.0224
7	26.4	0	0.049	0.186	0.295	0.292	5.66	1.5	0.0322
8	24.3	0	0.057	0.0911	0.290	0.280	6.7	0.41	0.028
9	34.5	0	0.057	0.0587	0.2106	0.205	4.79	1.96	0.0298
10	42.0	0	0.031	0.008	0.1	0.069	10.2	0.0	0.0125

B.3 Branch data settings

TABLE 0.3: IEEE 39-BUS SYSTEM BRANCH DATA

Line Data		Transformer Tap				
From Bus	To Bus	R	X	B	Magnitude	Angle
1	2	0.0035	0.0411	0.6987	0.000	0.00
1	39	0.0010	0.0250	0.7500	0.000	0.00
2	3	0.0013	0.0151	0.2572	0.000	0.00
2	25	0.0070	0.0086	0.1460	0.000	0.00
3	4	0.0013	0.0213	0.2214	0.000	0.00
3	18	0.0011	0.0133	0.2138	0.000	0.00
4	5	0.0008	0.0128	0.1342	0.000	0.00
4	14	0.0008	0.0129	0.1382	0.000	0.00
5	6	0.0002	0.0026	0.0434	0.000	0.00
5	8	0.0008	0.0112	0.1476	0.000	0.00
6	7	0.0006	0.0092	0.1130	0.000	0.00
6	11	0.0007	0.0082	0.1389	0.000	0.00
7	8	0.0004	0.0046	0.0780	0.000	0.00
8	9	0.0023	0.0363	0.3804	0.000	0.00
9	39	0.0010	0.0250	1.2000	0.000	0.00

10	11	0.0004	0.0043	0.0729	0.000	0.00
10	13	0.0004	0.0043	0.0729	0.000	0.00
13	14	0.0009	0.0101	0.1723	0.000	0.00
14	15	0.0018	0.0217	0.3660	0.000	0.00
15	16	0.0009	0.0094	0.1710	0.000	0.00
16	17	0.0007	0.0089	0.1342	0.000	0.00
16	19	0.0016	0.0195	0.3040	0.000	0.00
16	21	0.0008	0.0135	0.2548	0.000	0.00
16	24	0.0003	0.0059	0.0680	0.000	0.00
17	18	0.0007	0.0082	0.1319	0.000	0.00
17	27	0.0013	0.0173	0.3216	0.000	0.00
21	22	0.0008	0.0140	0.2565	0.000	0.00
22	23	0.0006	0.0096	0.1846	0.000	0.00
23	24	0.0022	0.0350	0.3610	0.000	0.00
25	26	0.0032	0.0323	0.5130	0.000	0.00
26	27	0.0014	0.0147	0.2396	0.000	0.00
26	28	0.0043	0.0474	0.7802	0.000	0.00
26	29	0.0057	0.0625	1.0290	0.000	0.00
28	29	0.0014	0.0151	0.2490	0.000	0.00
12	11	0.0016	0.0435	0.0000	1.006	0.00
12	13	0.0016	0.0435	0.0000	1.006	0.00
6	31	0.0000	0.0250	0.0000	1.070	0.00
10	32	0.0000	0.0200	0.0000	1.070	0.00
19	33	0.0007	0.0142	0.0000	1.070	0.00
20	34	0.0009	0.0180	0.0000	1.009	0.00
22	35	0.0000	0.0143	0.0000	1.025	0.00
23	36	0.0005	0.0272	0.0000	1.000	0.00
25	37	0.0006	0.0232	0.0000	1.025	0.00
2	30	0.0000	0.0181	0.0000	1.025	0.00
29	38	0.0008	0.0156	0.0000	1.025	0.00
19	20	0.0007	0.0138	0.0000	1.060	0.00

IEEE-30 Bus System

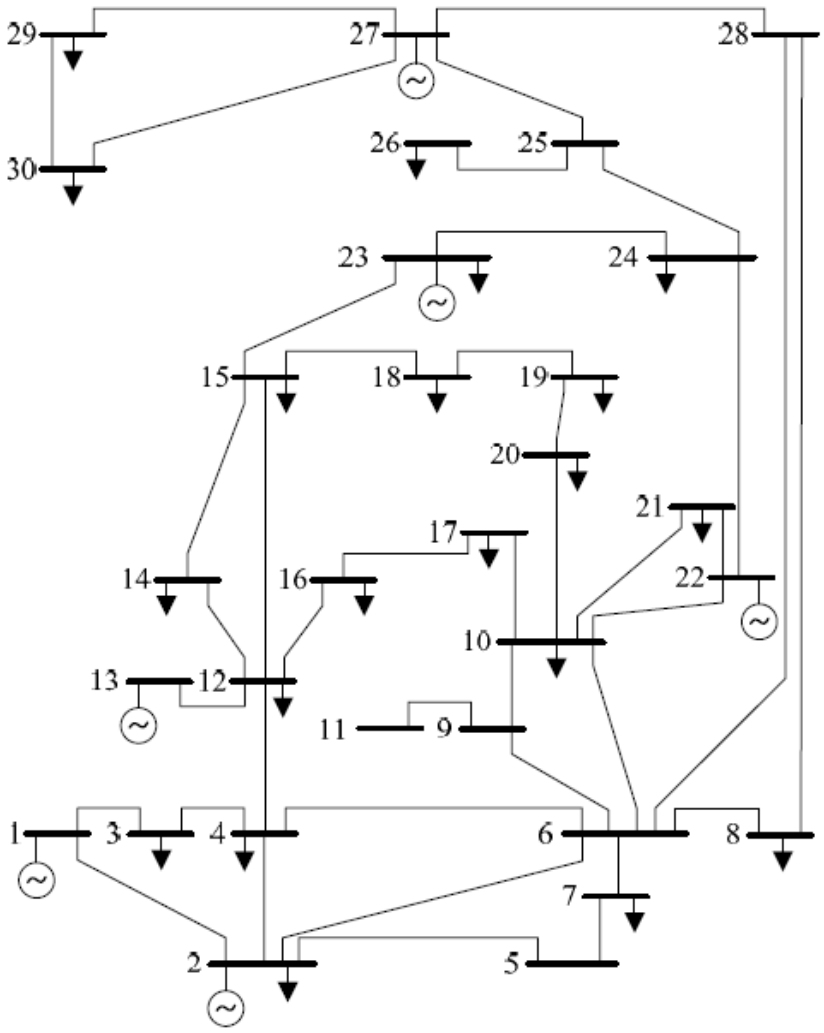

Figure A.2: IEEE 30-Bus System

TABLE A.4: IEEE 30-BUS SYSTEM MACHINE DATA

Unit	Bus	Cost coefficients			Pmax (MW)	Pmin (MW)	Min up time (h)	Min down time (h)	Ramp up (MW)	Ramp Down (MW)	Startup Ramp (MW)	Shutdown ramp (MW)
		A ($/MWh^2)	B ($/MWh)	C ($)								
G1	1	0.0200	15.00	0	80	15	2	2	25	25	70	60
G2	2	0.0175	14.75	0	80	15	2	2	25	25	70	60
G3	13	0.0250	16.00	0	50	10	3	3	15	15	70	60
G4	22	0.0625	14.00	0	50	10	4	4	15	15	70	60
G5	23	0.0250	16.00	0	30	5	3	3	10	10	70	60
G6	27	0.0083	15.25	0	55	10	4	4	15	15	70	60

TABLE A.5: IEEE 30-BUS SYSTEM BRANCH DATA

Line No.	From	To	X (p.u.)	Flow limit (MW)	Failure rate	Repair rate
1	1	2	0.06	130	0.9783	0.0217
2	1	3	0.19	130	0.9841	0.0159
3	2	4	0.17	65	0.9532	0.0468
4	3	4	0.04	130	0.9172	0.0828
5	2	5	0.20	130	0.9786	0.0214
6	2	6	0.18	65	0.9497	0.0503
7	4	6	0.04	90	0.9828	0.0172
8	5	7	0.12	70	0.9760	0.0240
9	6	7	0.08	130	0.9211	0.0789
10	6	8	0.04	32	0.9494	0.0506
11	6	9	0.21	65	0.9494	0.0506
12	6	10	0.56	32	0.9211	0.0789
13	9	11	0.21	65	0.9535	0.0465
14	9	10	0.11	65	0.9509	0.0491
15	4	12	0.26	65	0.9660	0.0340
16	12	13	0.14	65	0.9838	0.0162
17	12	14	0.26	32	0.9754	0.0246
18	12	15	0.13	32	0.9598	0.0402
19	12	16	0.20	32	0.9510	0.0490
20	14	15	0.20	16	0.9494	0.0506
21	16	17	0.19	16	0.9494	0.0506
22	15	18	0.22	16	0.9236	0.0764
23	18	19	0.13	16	0.9514	0.0486
24	19	20	0.07	32	0.9509	0.0491
25	10	20	0.21	32	0.9666	0.0334
26	10	17	0.08	32	0.9824	0.0176
27	10	21	0.07	32	0.9786	0.0214
28	10	22	0.15	32	0.9612	0.0388
29	21	22	0.02	32	0.9462	0.0538
30	15	23	0.20	16	0.9498	0.0502
31	22	24	0.18	16	0.9506	0.0494
32	23	24	0.27	16	0.9181	0.0819
33	24	25	0.33	16	0.9483	0.0517
34	25	26	0.38	16	0.9537	0.0463
35	25	27	0.21	16	0.9733	0.0267
36	28	27	0.40	65	0.9818	0.0182
37	27	29	0.42	16	0.9808	0.0192
38	27	30	0.60	16	0.9564	0.0436
39	29	30	0.45	16	0.9537	0.0463
40	8	28	0.20	32	0.9537	0.0463
41	6	28	0.06	32	0.9536	0.0464

IEEE-57 Bus System

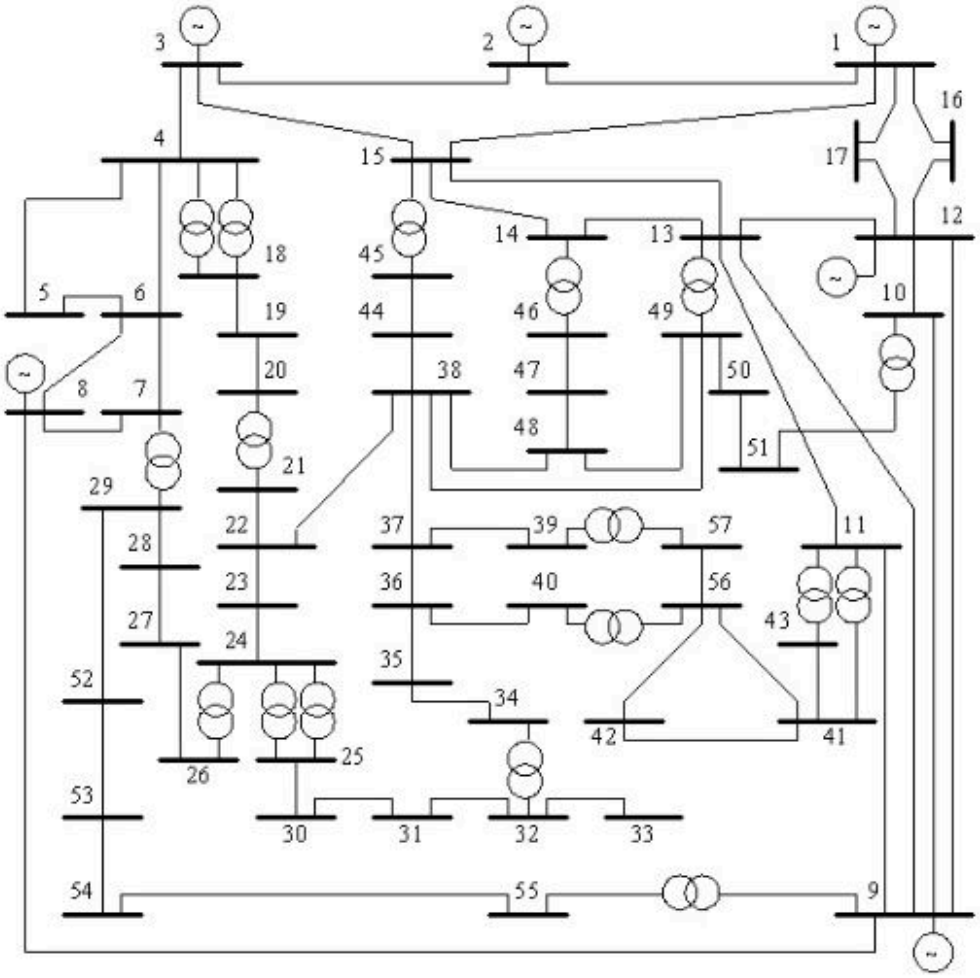

Figure A.3: IEEE 57-Bus System

IEEE-300 Bus System

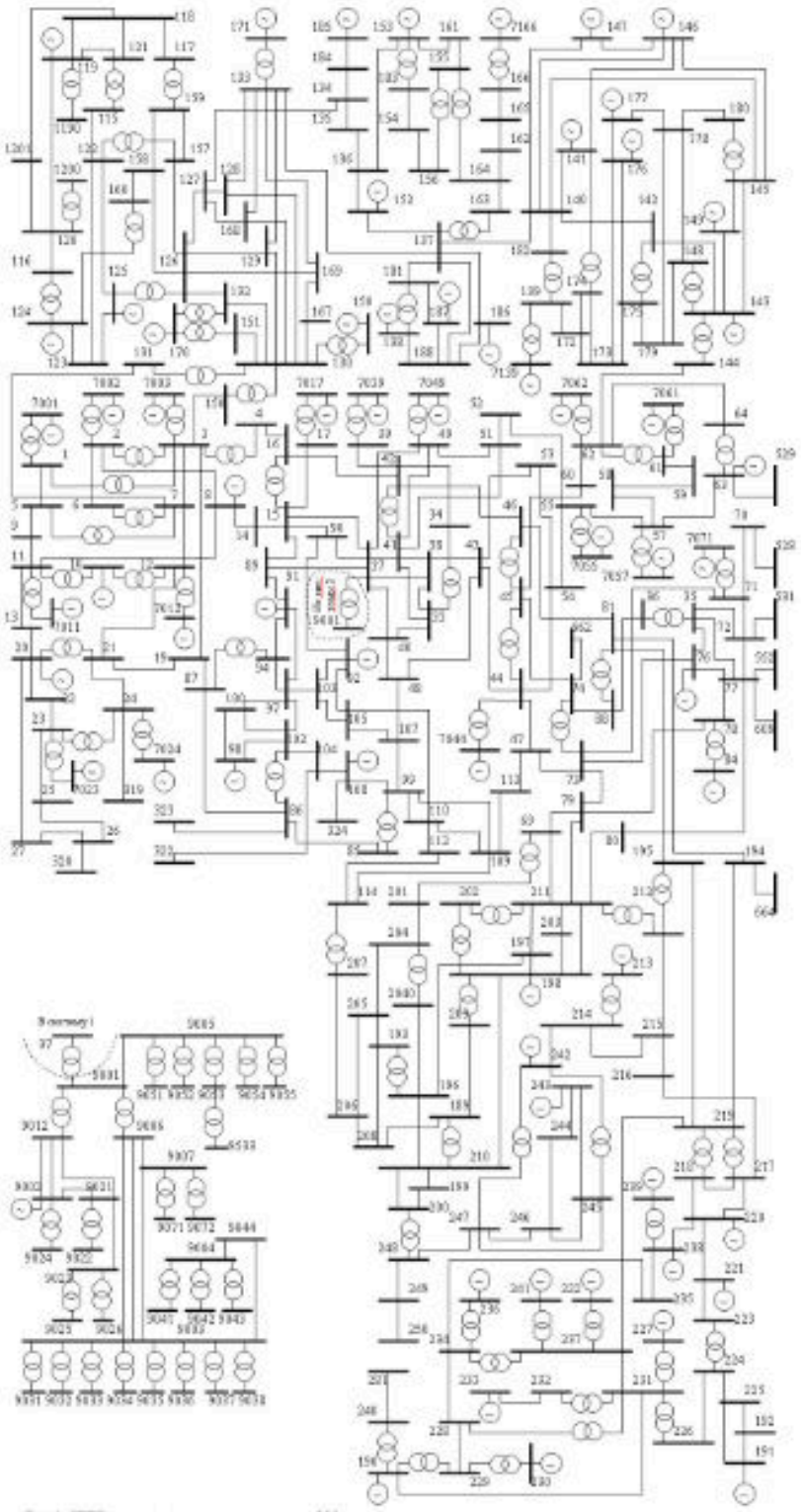

Figure A.4: IEEE 300-Bus System

Appendix C: Matlab Codes for Some of the Algorithms

Islanding Database Initialization

```
%Main
clear;
clc;
[G,A,Q] = CreateInciM;

%%
BusNum = length(A(1,:));
LineNum = (sum(sum(A))-BusNum)/2;
LineMatrix = zeros(LineNum,2);

t1 = 1;
for k1 = 1:BusNum-1
   for k2 = k1+1:BusNum
      if(A(k1,k2)==1)
         LineMatrix(t1,:) = [k1,k2];
         t1 = t1+1;
      end
   end
end

fprintf('Islanding Analysis')
fprintf('\n')
fprintf('Bus number: ')
fprintf('%3d',BusNum)
fprintf('\n')
fprintf('Line number: ')
fprintf('%3d',LineNum)
fprintf('\n')

%%
MaxTriLine = 2;        %Define maximum lines tripped here
%MaxTriLine = LineNum/3;

ObservDepth = 2;
SysObsMat = Nto1(A^ObservDepth,BusNum);

ObsvMatLineNum = (sum(sum(SysObsMat))-BusNum)/2;
ObsvMatLineMatrix = zeros(ObsvMatLineNum,2);

t2 = 1;
for k46 = 1:BusNum-1
   for k47 = k46+1:BusNum
      if(SysObsMat(k46,k47)==1)
         ObsvMatLineMatrix(t2,:) = [k46,k47];
         t2 = t2+1;
      end
   end
end

GLAN = 100;
```

```
Tab1 = zeros(1,MaxTriLine);
Tab2 = zeros(1,BusNum+MaxTriLine+4+GLAN);

fprintf('Islanding Creation & Computation')
fprintf('\n')

T = eye(length(A(:,1)));
for k6 = 1:length(A(:,1))
   for k7 = 1:length(A(:,1))
      T(k6,k7) = 1;
   end
end

count1 = 1;

for k3 = 1:MaxTriLine

   fprintf('Trip ')
   fprintf('%2d',k3)
   fprintf(' line(s)')
   fprintf('\n')

   if(k3==1)
      %Selection = nchoosek(1:LineNum,k3);
      for k4 = 1:LineNum%length(Selection(:,1))
         C = A;
         %for k5 = 1:k3
            a1(1,:) = LineMatrix(k4,:);
            C(a1(1,1),a1(1,2)) = 0;
            C(a1(1,2),a1(1,1)) = 0;
         %end
k4
         if(mod(count1,100)==0)
            count1;
         end
         [Tab1,Tab2] = IslandComp(BusNum,C,G,T,a1,Tab1,Tab2,MaxTriLine);
         count1 = count1+1;
      end
   else if(k3>1)
         ListforT = zeros(1:2);
         ListforTset = 1;
         for k45 = 901:1100%LineNum
            Buss1 = LineMatrix(k45,1);
            Buss2 = LineMatrix(k45,2);
            SavAslct = zeros(1,2);
            savA1 = 1;
            PropBus = [Buss1 Buss2];
            prpset = 3;
            for k48 = 1:ObsvMatLineNum
               if(ObsvMatLineMatrix(k48,1)==Buss1||ObsvMatLineMatrix(k48,1)==Buss2)
                  PropBus(prpset) = ObsvMatLineMatrix(k48,2);
                  prpset = prpset+1;
               else if(ObsvMatLineMatrix(k48,2)==Buss1||ObsvMatLineMatrix(k48,2)==Buss2)
                     PropBus(prpset) = ObsvMatLineMatrix(k48,1);
                     prpset = prpset+1;
                  end
```

```
            end
        end
        for k52 = 1:LineNum
            if(ismember(LineMatrix(k52,:),PropBus))
                SavAslct(savA1,:) = LineMatrix(k52,:);
                savA1 = savA1+1;
            end
        end

        m = length(SavAslct(:,1));
        for k63 = 1:m
            if(isequal([Buss1 Buss2],SavAslct(k63,:)))
                SavAslct(k63:m-1,:) = SavAslct(k63+1:m,:);
                break;
            end
        end
k45
Selection = nchoosek(1:m-1,k3-1);
length(Selection(:,1))

        for k51 = 1:length(Selection(:,1))
            a1(1,:) = [Buss1 Buss2];
            C = A;
            C(a1(1,1),a1(1,2)) = 0;
            C(a1(1,2),a1(1,1)) = 0;
            for k53 = 1:k3-1
                a1(k53+1,:) = SavAslct(Selection(k51,k53),:);
                C(a1(k53+1,1),a1(k53+1,2)) = 0;
                C(a1(k53+1,2),a1(k53+1,1)) = 0;
            end
            a1 = sortrows(a1);
            Duplcotl = 1;
k51
            if(ListforTset==1)
                ListforT(ListforTset:ListforTset+k3-1,:) = a1;
                ListforTset = ListforTset+k3;
                [Tab1,Tab2] = IslandComp(BusNum,C,G,T,a1,Tab1,Tab2,MaxTriLine);
                count1 = count1+1;
            else for k54 = 1:k3:length(ListforT(:,1))
                    if(isequal(ListforT(k54:k54+k3-1,:),a1))
                        Duplcotl = 0;
                        break;
                    end
                end
                if(Duplcotl==1)
                    ListforT(ListforTset:ListforTset+k3-1,:) = a1;
                    ListforTset = ListforTset+k3;
                   if(mod(count1,100)==0)
                      count1
                   end
                    [Tab1,Tab2] = IslandComp(BusNum,C,G,T,a1,Tab1,Tab2,MaxTriLine);
                    count1 = count1+1;
                end
            end
        end
```

```
        end
    end

end

fprintf('----------------')
fprintf('\n')

for k24 = 1:MaxTriLine
    fprintf('%1d',k24+1)
    fprintf('Islands cases number: ')
    fprintf('%3d',Tab1(k24))
    fprintf('\n')
end

fprintf('----------------')
fprintf('\n')

fprintf('Different Islands combo: ')
fprintf('%3d',length(Tab2(:,1)))
fprintf('\n')
fprintf('----------------')
fprintf('\n')
for k25 = 1:length(Tab2(:,1))
    fprintf('Islands created:')
    fprintf('%2d',Tab2(k25,1))
    fprintf(' [')
    for k26 = 2:MaxTriLine+BusNum+6
        if(Tab2(k25,k26)>0)
            fprintf('%2d',Tab2(k25,k26))
            fprintf(',')
        else if(Tab2(k25,k26)==-1&&Tab2(k25,k26+1)~=0)
                fprintf(']and[')
            else if(Tab2(k25,k26)==-1&&Tab2(k25,k26+1)==0)
                    fprintf(']')
                    break;
                end
            end
        end
    end
    fprintf('\n')
    fprintf('Tri_line combo number:')
    fprintf('%3d',Tab2(k25,MaxTriLine+BusNum+5))
    fprintf('   Base combo:(')
    for k27 = MaxTriLine+BusNum+6:2:length(Tab2(1,:))
        if(Tab2(k25,k27)>0)
            fprintf('%2d',Tab2(k25,k27))
            fprintf(' -')
            fprintf('%2d',Tab2(k25,k27+1))
            fprintf(',')
            else if(Tab2(k25,k27)==-1&&Tab2(k25,k27+1)==-1)
                fprintf(')')
                break;
            end

%         else if(Tab2(k25,k27)==-1&&Tab2(k25,k27+2)~=0)
```

```
%                fprintf(')and(')
%            else if(Tab2(k25,k27)==-1&&Tab2(k25,k27+2)==0)
%                fprintf(')')
%                break;
%            end
%        end
      end
   end
   fprintf('\n')
   fprintf('\n')
end
```

Incidence Matrix Creation – IEEE-14 Bus System Example

```
function[G,A,Q] =  CreateInciM()
% IEEE-14

 Branch14 = [
 1 2 0.01938 0.05917 0.0528
 1 5 0.05403 0.22304 0.0492
 2 3 0.04699 0.19797 0.0438
 2 4 0.05811 0.17632 0.0374
 2 5 0.05695 0.17388 0.034
 3 4 0.06701 0.17103 0.0346
 4 5 0.01335 0.04211 0.0128
 4 7 0 0.20912 0
 4 9 0 0.55618 0
 5 6 0 0.25202 0
 6 11 0.09498 0.1989 0
 6 12 0.12291 0.25581 0
 6 13 0.06615 0.13027 0
 7 8 0 0.17615 0
 7 9 0 0.11001 0
 9 10 0.03181 0.0845 0
 9 14 0.12711 0.27038 0
 10 11 0.08205 0.19207 0
 12 13 0.22092 0.19988 0
 13 14 0.17093 0.34802 0
 ];

 A = eye(14);
 for l1 = 1:length(Branch14(:,1))
    A(Branch14(l1,1),Branch14(l1,2)) = 1;
    A(Branch14(l1,2),Branch14(l1,1)) = 1;
 end

 Ld14 = [
 1 3 0 0 0 0
 2 2 21.7 12.7 0 0
 3 2 94.2 19 0 0
 4 1 47.8 -3.9 0 0
 5 1 7.6 1.6 0 0
 6 2 11.2 7.5 0 0
 7 1 0 0 0 0
```

```
8 2 0 0 0 0
9 1 29.5 16.6 0 19
10 1 9 5.8 0 0
11 1 3.5 1.8 0 0
12 1 6.1 1.6 0 0
13 1 13.5 5.8 0 0
14 1 14.9 5 0 0
];

Gen14 = [
1 232.4 -16.9 10 0 1.06 332.4 0
2 40 42.4 50 -40 1.045 140 0
3 0 23.4 40 0 1.01 100 0
6 0 12.2 24 -6 1.07 100 0
8 0 17.4 24 -6 1.09 100 0
];

for l1 = 1:length(Gen14(:,1))
   G(1,l1) = Gen14(l1,1);
end

Q = 10;
```

Islanding Contingency Detecting Stratgy

```
function [Tab1,Tab2] = IslandComp(BusNum,C,G,T,a1,Tab1,Tab2,MaxTriLine)

Cb = C;
for iteration = 2:BusNum

   C1 = C;
   C = Nto1(C*Cb,BusNum);

   if(isequal(C,T))
      Tab1 = Tab1;
      Tab2 = Tab2;
      return;
   end

   if(isequal(C1,C))

      Islandgroup = zeros(length(a1(:,1))+1,BusNum);
      Islandgroup(1,1) = 1;
      GroupNum = 1;
      Grouplength = zeros(length(a1(:,1))+1,1);
      Grouplength(1,1) = 1;

      for k8 = 2:BusNum
         set = 1;
         for k9 = 1:GroupNum
            for k10 = 1:Grouplength(k9,1)
               if(C(Islandgroup(k9,k10),k8)==1)
                  Grouplength(k9,1) = Grouplength(k9,1)+1;
                  Islandgroup(k9,Grouplength(k9,1)) = k8;
```

```
            set = 0;
            break;
        end
    end
    if(set==0)
        break;
    end
  end
  if(set==1)
    GroupNum = GroupNum+1;
    Grouplength(GroupNum,1) = Grouplength(GroupNum,1)+1;
    Islandgroup(GroupNum,1) = k8;
  end
end

IslandNum = GroupNum;
sign = 1;
badpart = 0;

for k14 = 1:GroupNum
  test = 1;
  for k15 = 1:Grouplength(k14,1)
    for k16 = 1:length(G)
      if(G(k16)==Islandgroup(k14,k15))
        test = 0;
        break;
      end
    end
    if(test==0)
      break;
    end
  end
  if(test==1)
    IslandNum = IslandNum-1;
    badpart(sign) = k14;
    sign = sign+1;
  end
end

if(IslandNum>1)
  Islandgroup_2 = Islandgroup;
  if(IslandNum<GroupNum)
    for k18 = 1:length(badpart)
      Islandgroup_2(badpart(k18):length(a1(:,1)),:) = Islandgroup_2(badpart(k18)+1:length(a1(:,1))+1,:);
    end
    Islandgroup_2(length(a1(:,1))+2-length(badpart):length(a1(:,1))+1,:) = 0;
  end

  zhizhen1 = 1;
  Save = zeros(1,BusNum+MaxTriLine+1);
  for k19 = 1:IslandNum
    for k20 = 1:BusNum
      if(Islandgroup_2(k19,k20)~=0)
        Save(zhizhen1) = Islandgroup_2(k19,k20);
        zhizhen1 = zhizhen1+1;
      end
```

```
            end
            Save(zhizhen1) = -1;
            zhizhen1 = zhizhen1+1;
        end

        zhizhen2 = 1;
        for k21 = 1:length(a1(:,1))
            Save2(1,zhizhen2:zhizhen2+1) = a1(k21,:);
            zhizhen2 = zhizhen2+2;
        end
        Save2(1,zhizhen2:zhizhen2+1) = [-1,-1];

        Tab1(1,IslandNum-1) = Tab1(1,IslandNum-1)+1;
        if(Tab2(1,1)==0)
            Tab2(1,1) = IslandNum;
            Tab2(1,2:MaxTriLine+BusNum+2) = Save;
            Tab2(1,MaxTriLine+BusNum+5) = 1;
            Tab2(1,MaxTriLine+BusNum+6:MaxTriLine+BusNum+5+length(Save2)) = Save2(1,:);
        else
            judge2 = 1;
            for k22 = 1:length(Tab2(:,1))
                if(Tab2(k22,1)~=0)
                    if(isequal(Save,Tab2(k22,2:MaxTriLine+BusNum+2)))
                        Tab2(k22,MaxTriLine+BusNum+5) = Tab2(k22,MaxTriLine+BusNum+5)+1;
                        for k23 = MaxTriLine+BusNum+6:length(Tab2(1,:))
                            if(Tab2(k22,k23-1)==-1&&Tab2(k22,k23)==0)
                                Tab2(k22,k23:k23+length(Save2)-1) = Save2(1,:);
                                Tab2(k22,length(Tab2(k22,:))+1) = 0;
                                judge2 = 0;
                                break;
                            end
                        end
                    end
                    if(judge2==0)
                        break;
                    end
                end
            end
            if(judge2==1)
                Tab2(length(Tab2(:,1))+1,1) = IslandNum;
                Tab2(length(Tab2(:,1)),2:MaxTriLine+BusNum+2) = Save;
                Tab2(length(Tab2(:,1)),MaxTriLine+BusNum+5) = 1;
                Tab2(length(Tab2(:,1)),MaxTriLine+BusNum+6:MaxTriLine+BusNum+5+length(Save2)) = Save2(1,:);
            end
        end

    end
    return;
  end

end
```

Boolean Conversion

```
function [A] = Nto1(A,BusNum)
 for i = 1:BusNum
    for j = 1:BusNum
       if(A(i,j)~=0)
          A(i,j) = 1;
       end
    end
 end
```

Non-Islanding Cases Generation

```
BUS138_115 = [
….
];

t1 = randperm(length(BUS138_115));
t1 = t1(1,1:100);

for i = 1:100
   RdmFltBus(i,:) = BUS138_115(t1(i),:);
end

------

Triporder = [
 ……
     ];

Trip_havingLD = [
……
];

T = length(Trip_havingLD(:,1));
T2 = length(Triporder(:,1));
flag1 = 1;
for r1 = 1:T
   for r2 = 1:T2
      if(Trip_havingLD(r1,:)==Triporder(r2,1:4))
         KeepTrip(flag1,1) = r2;
         flag1 = flag1+1;
      end
   end
end

KeepTrip = sort(KeepTrip);
```

Curve Fitting for ISI

```
%% Islanding curve fitting
AA = [
…..
];

for num = 10:10
   BB = Islandingcurvefitting(:,num);
   [a1,b1] = Curvefitting1(AA,BB);
   A(num,1) = a1.a;
   B(num,1) = a1.b;
   C(num,1) = a1.c;
   D(num,1) = a1.d;
   E(num,1) = a1.e;
end
```